ABSTRACT

TERRY, STEPHEN DOUGLAS. On Flame Stability In The Hysteresis Regime In Co-Flow. (Under the direction of Kevin M. Lyons).

This study documents experiments performed on lifted turbulent diffusion flames in the hysteresis regime with air co-flow. Undiluted methane, ethylene, and propane were used as fuels and two nozzle sizes were used. The results confirm the non-linearity of the lift-off height with nozzle velocity, showing a previously undocumented region where lifted flame height increases as fuel velocity is decreased and that reattachment nozzle velocity varies linearly with co-flow. Using jet relations from Tieszen, the local excess jet velocity was computed and found to vary linearly for flames lifted well above the nozzle. The effect of co-flow was captured using an effective local excess jet velocity, similar to the effective nozzle jet velocity proposed by Montgomery used in conjunction with the results of Khalghatgi. Local excess jet velocities at the reattachment point were also compared for varying co-flow and found to be consistent between co-flow cases. This threshold velocity was found to vary with the inverse of the laminar burning velocity of the fuel squared. Relations for reattachment nozzle velocity and flame lift-off height at reattachment were also determined. The results extend the work of Khalghatgi into the hysteresis regime and complement the work of Gollahalli in determining the mechanisms that support flame stability in the hysteresis regime. Any comprehensive theory for flame stability will have to explain some of the unexpected results seen in the hysteresis regime and incorporate the findings of this study.

ON FLAME STABILITY IN THE HYSTERESIS REGIME IN CO-FLOW

By

Stephen Douglas Terry

A dissertation submitted to the Graduate Faculty of
North Carolina State University
in partial fulfillment of the
requirements for the Degree of
Doctor of Philosophy

MECHANICAL ENGINEERING

Raleigh, N.C.
2005

APPROVED BY:

Dr. Kevin Lyons, Chair of Advisory Committee Department of Mechanical & Aerospace Engineering	Date
Dr. Herbert Eckerlin Department of Mechanical & Aerospace Engineering	Date
Dr. Richard Johnson Department of Mechanical & Aerospace Engineering	Date
Dr. William Roberts Department of Mechanical & Aerospace Engineering	Date

Biography

Stephen Terry is a native of Raleigh, NC, but grew up in nearby Chapel Hill. He graduated from Chapel Hill High School in 1987, and attended North Carolina State University studying Mechanical Engineering. Upon graduation with a Bachelor of Science in May 1992, he started graduate school at NCSU. At that time, Dr. Jim Leach and Dr. Herb Eckerlin began the Industrial Assessment Center, a U.S. Department of Energy program that helps small and medium manufacturers reduce energy costs and trains the next generation of energy managers. Stephen was the first student hired and continued as a graduate research student until earning his Masters Degree in December 1994. Early the next year, Stephen was hired full-time as an Extension Specialist, also beginning his Ph.D. studies. After briefly switching his focus to Environmental Engineering, Stephen began working with Dr. Kevin Lyons studying flame stability. Stephen now resides in Garner with his wife Susan, and his three-year-old son Andrew.

Table of Contents

Table of Contents - continued

List of Tables

List of Figures

List of Figures, continued

List of Symbols Used

C_n	-	Constants used in derivations
d	-	Nozzle diameter
f	-	Fuel mixture fraction
D_{AB}	-	Binary diffusion coefficient
H_L	-	Lifted flame height
$H_{L,RA}$	-	Lifted flame height just prior to reattachment
I_f	-	Jet mass invariant (fuel mass flow)
J	-	Jet momentum invariant (initial jet momentum)
Pr	-	Prandtl number
r	-	Radial coordinate
r_o	-	Radius of nozzle
Re	-	Reynolds number
Sc	-	Schmidt number
S_{tri}	-	Tribrachial flame speed
S_L	-	Laminar burning velocity
u	-	Velocity in the x-direction
u_{LO}	-	Liftoff velocity
U_o	-	Initial fuel nozzle exit velocity
U_∞	-	Co-flow velocity
u'	-	Axial velocity fluctuation
u_{RA}	-	Reattachment fuel velocity
v	-	Radial velocity
V_{CO}	-	Co-flow velocity
x, z	-	Axial coordinate, i.e., vertical distance from nozzle exit
Y_F	-	Fuel mass fraction
$Y_{F, st}$	-	Fuel mass fraction at stoichiometric conditions
$Y_{F,o}$	-	Fuel mass fraction of initial fuel jet
α	-	Thermal diffusivity
η	-	Similarity variable
ρ	-	Density
ρ_∞	-	Density of co-flow fluid (air)
υ	-	Kinematic viscosity
ξ	-	Similarity variable
Φ	-	Momentum radius
Ψ	-	Stream function

1. Introduction and Literature Review

1.1 Scope of Work

Turbulent diffusion flames are an important part of many practical industrial combustion devices, with applications ranging from small boilers and water heaters to large gas turbines. Working with the Industrial Assessment Center has allowed this author a perspective on the macroscopic behavior of flames, particularly in boilers and direct fired ovens. Measurements such as excess oxygen concentration, carbon monoxide concentration, and stack gas temperature provide basic indicators of overall combustion performance for these types of devices. Analysis of the macroscopic results permits computation of savings that may occur from improving the measured combustion indicators.

One major issue affecting combustion devices is turndown. Low fire on a steam boiler may be 30% of full load. When demand for steam is less than the minimum burner firing rate, the boiler must cycle between low fire and no fire conditions (i.e., not any firing fuel). Before a flame is reestablished, there is a purge cycle that blows cold outside air through the combustion chamber and heat transfer surfaces to purge any remaining combustible gases. This cycle and the natural convection that occurs during shutdown represent significant heat loss and thermal cycling of the materials. The efficiency of a boiler operating below low fire condition is therefore quite low.

Flames in combustion devices that are near the turndown limit are also susceptible to blowout due to variation of air currents in the combustion zone. This can become a safety issue, if proper flame detection equipment is not employed to either re-light the flame or to turn off the flow of fuel.

One barrier to making turndown on burners even lower is the issue of flame stability. This is a topic that is not completely understood, especially at low firing rates. Therefore, this study is an attempt to describe some of the behaviors of a turbulent jet diffusion flame at low Reynolds Number, when flame stability issues are critical. Any complete theory of flame stability must include some of the unexpected flame behavior at low (but still turbulent) Reynolds number, especially in co-flow.

What makes this study unique is the use of varying co-flow for flames in the hysteresis regime. Although several studies in the past have attempted to describe flame behavior in the hysteresis regime, none have used co-flow as a tool to illustrate how certain parameters affect flame lift-off height and stability. The behavior described below in the results section have not been reported in the literature, to this author's knowledge. Using turbulent jet theory, relations from previous researchers describing flame stability, and the results from these experiments, this work sheds light on the developing theory of flame stability.

Early studies of turbulent jet diffusion flames were reported in the Garside and Scholenfield paper in 1949 [1]. Here, many of the more familiar characteristics of the flames were discussed, including the phenomenon of flame hysteresis. They speculated that turbulent jet flow must occur before a flame will lift off the burner, a supposition that has since been disproven. The work forms the basis for combustion research, though some of the ideas are outdated. Since then, many studies have been performed to determine the underlying physics of flames and stability criteria, to improve understanding and aid in the design of practical combustion devices.

1.2 Hysteresis Regime

The hysteresis regime refers the situation where the jet flame has dual positions favorable to flame stabilization: attached and lifted. Figure 1.1 below illustrates how the flame lift-off height changes as the fuel velocity is changed. Flames may exhibit one of two stable flame states. One case is for the flame to be attached (Figure 1.2) and the other case is for the flame to be lifted some distance above the nozzle (Figure 1.3). When the flame is ignited at relatively low fuel velocities, the flame is always attached to the burner. As the fuel velocity is increased, it reaches a threshold value in which the flame spontaneously lifts above the nozzle some distance. This is referred to as the lift-off velocity. Fuel velocities greater than the lift-off velocity only results in one stable flame position – lifted above the nozzle. As the fuel velocity is lowered to below the lift-off velocity, the lifted flame remains lifted. The flame will spontaneously reattach to the burner nozzle when the fuel velocity is reduced to a value well below the original lift-off velocity. This is referred to as the reattachment velocity. The hysteresis regime is comprised of the set of fuel velocities between the liftoff velocity and the reattachment velocities. Flame position in the hysteresis regime therefore depends on the previous state – whether it was previously lifted, or previously attached. For the experiments in this work, the flames will be ignited at a low velocity, where the flame is attached, lifted by increasing the fuel velocity to above the lift-off velocity, and then the hysteresis regime achieved by reducing the fuel velocity to below the lift-off height.

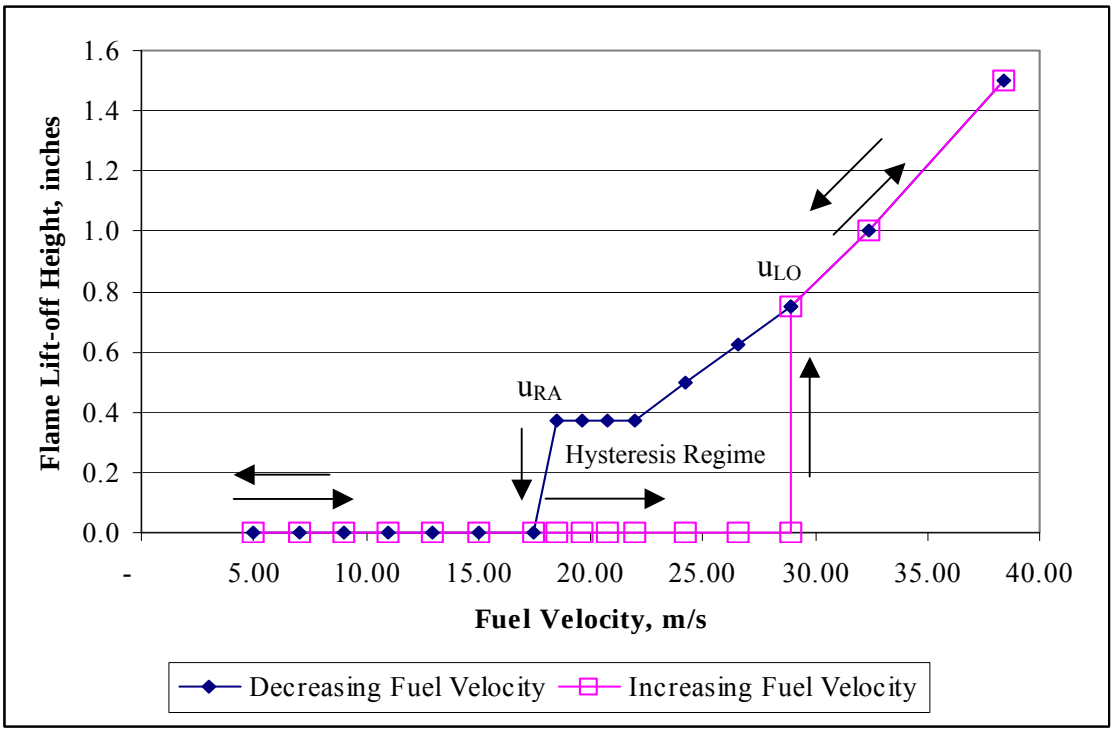

Figure 1.1 – Graphical Representation of the Hysteresis Regime

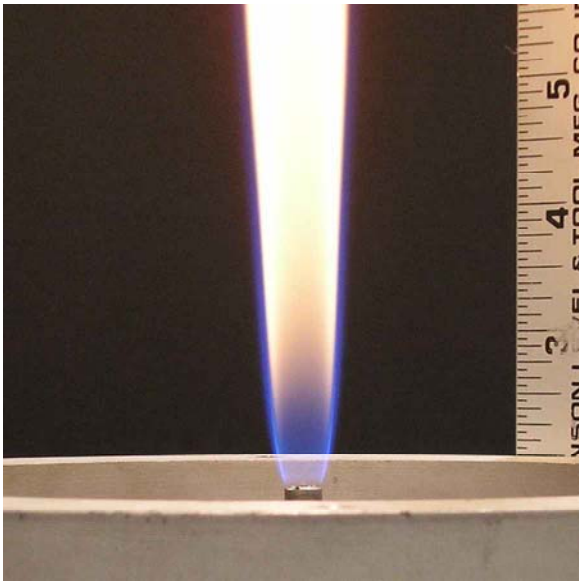

Figure 1.2 – Attached Flame

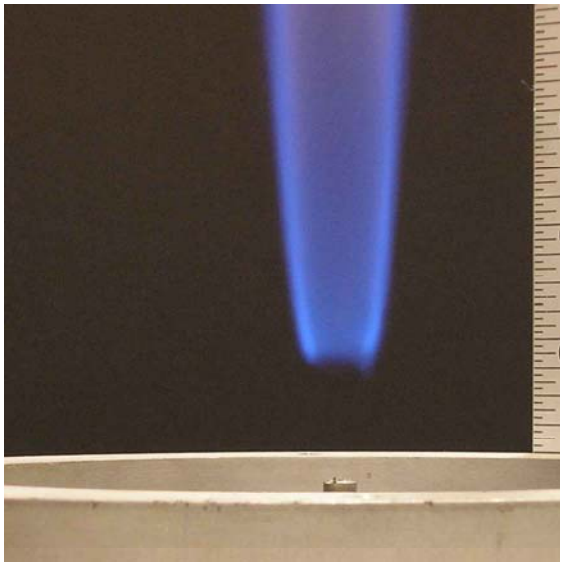

Figure 1.3 – Lifted Flame

1.3 Turbulent Burning Velocity

Vanquickenborne and van Tieggelen [2] proposed that at the base of turbulent flames, the conditions are completely premixed and the flames propagate at some characteristic turbulent burning velocity, depending on the fuel and other parameters. Eickhoff et al. [3] support this notion in a study of the amount of premixing that occurs in turbulent jet flames. They found that about 40-50% of the fuel has mixed into the area around the flame base, which reacts very quickly. Therefore the study concludes that the assumption of a premixed flame has some merit.

Kalghatgi [4] performed experiments relating the turbulent flame heights of several fuels of varying properties (density, laminar burning velocities, diffusion coefficients) with fuel velocity and other parameters. He took the ideas of Vanquickenborne and van Tieggelen [2] and proposed a turbulent burning velocity, which is related to the laminar burning velocity. This turbulent burning velocity is the speed at which the flame propagates back to the burner and is related to the square root of the local axial velocity fluctuations, u'.

The flame lift-off height (h) and the local axial jet velocity (U_m) were shown to be related for flames above the hysteresis regime. The result is the relation:

$$\left(\frac{hS_L}{\upsilon_f}\right) = C_1\left(\frac{U_m}{S_L}\right)\left(\frac{\rho_o}{\rho_\infty}\right)^{3/2} \tag{1.1}$$

where C_1 is constant that must be determined experimentally. Simplifying this for a given fuel, the flame height is:

$$h = \frac{C_2 U_m}{S_L^2 / \alpha} \tag{1.2}$$

where C_2 includes the constant C_1 and the density ratio term. The kinematic viscosity term has been replaced with the thermal diffusivity. The flame height is thus a function of the characteristic chemical reaction rate, expressed as S_L^2/α, and the initial jet velocity, U_m from the nozzle. Khalghatgi's experiments confirmed that lift-off heights were linear with respect to fuel velocity.

Tieszen et al. [5] described the turbulent velocity profiles of one fluid (fuel) from a nozzle into a second co-flowing fluid (air):

$$\frac{\overline{U}}{U_o} = 11.8\left(\frac{\rho_o}{\rho_\infty}\right)^{1/2}\left(\frac{r_o}{z}\right)e^{-93.7(r/z)^2} \tag{1.3}$$

where $\overline{U}$ is the excess jet velocity (i.e., the velocity of the fluid relative to the co-flow). The mass fraction of fuel into the air (without co-flow) is given by [5]:

$$Y = 10\left(\frac{\rho_o}{\rho_\infty}\right)^{1/2}\left(\frac{r_o}{z}\right)e^{-57(r/z)^2} \tag{1.4}$$

Note the similarity to the relation for velocity, in that the density ratio is taken to the one-half power and the exponential of a negative constant multiplied by the ratio r/z squared. These results are valid for the similarity region, which is postulated to begin about 20 nozzle diameters downstream (in this study about 40-80 mm or 1.6-3.2 inches).

Brown, Watson, and Lyons [6] provided a parametric analysis of lifted flames in co-flow. Lift-off heights were plotted against fuel velocity and co-flow velocity. The analysis included the use of methane, propane, and ethylene using an axisymmetric jet flame in co-flow. The study correlated flame properties to an analytical relation for the turbulent burning velocity. The ideas of Kalghatgi [4] were used to numerically determine the turbulent flame

speed and then compared to the computed local axial jet velocities at the flame height using a relation from Tieszen [5]. For flames near blowout it was determined that the turbulent burning velocity is a good indicator of where the flame will stabilize. However, for flames in the near field, three times the laminar burning velocity is argued to be a more suitable guideline.

This guideline is further emphasized by Watson et al. [7]. CH and velocity measurements of lifted methane flames are made using CH PLIF and PIV techniques. Their conclusion is that the flame, as determined by peak CH concentration, sits in a premixed region of relatively low axial velocity, about 1.18 m/s. This is about 3 times the laminar burning velocity for methane.

Montgomery et al. [8] extended Kalghatgi's analysis to include turbulent flames in co-flow. Their analysis included modeling and experimental work. They argue that an effective jet velocity can be determined using the original nozzle velocity, the co-flow velocity and considering the densities of the two fluid streams. The effective velocity, V_{eff}, is given as:

$$V_{eff} = V_{jet} + C\sqrt{\frac{\rho_{coflow}}{\rho_{jet}}}V_{coflow} \qquad (1.5)$$

The authors suggest a value of 5.2 for the constant C for methane. Using this in place of the jet (nozzle) velocity results in a linear lift-off height as the nozzle velocity is varied. Their results included methane with nozzle velocities between 20 and 50 m/s and with co-flows of between zero and 1.5 m/s. The nozzle size used in experiments was 10 mm, much larger

than for the subject of our analysis. These experiments were conducted for fuel nozzle velocities in excess of the lift-off velocity (i.e., outside the hysteresis regime).

Their results also determined that inner shear layer vortices form further downstream and the jet spreads less as co-flow velocity is increased. The scalar dissipation rate was found to decrease sharply at the flame lift-off height.

1.4 Large Scale Structures and Scalar Dissipation Rate

The proposition that the flame exists in a region where the fuel and air are completely premixed was challenged in a paper authored by Peters and Williams [9]. The results of Peters and Williams were expanded upon by Broadwell et al. [10], Miake-Lye and Hammer [11], Dahm and Dibble [12], and Pitts [13]. Vortical structures were theorized to entrain hot combustion products into unburned fuel and air. These structures scale with the local jet diameter. At a time t_d, the vortical structures have cascaded down to the Kolmogorov scale, where molecular diffusion homogenizes the mixture. Reactions occur in the interface between fuel and air, which are argued to be strained laminar flame sheets. As the scalar dissipation rate increases (with the flame burning upstream), the flame is quenched as it becomes more fuel rich and it cools due to high gradients.

For non-co-flowing flames a critical stability parameter was identified, defined as the ratio of the local mixing time to the chemical reaction time:

$$\varepsilon = \frac{t_{mixing}}{t_{chemical}} = \frac{\delta / u}{k / S_L^2} \tag{1.6}$$

where, k is the thermal conductivity and δ is the width of the jet at the location of the flame. The threshold value for blowout was found by Dahm and Dibble to be about 4.3, and between 3.9 and 5.6 for various fuels, according to Broadwell et al. This ratio is similar to Damkohler Number, which is the ratio of characteristic reaction time to the characteristic time of diffusion.

For co-flowing jets, Dahm and Dibble suggested several scaling arguments be made to derive a new relation for ε for co-flowing jets.

$$\varepsilon = \Phi \frac{S_L^2}{U_\infty k} f_1(x/\Phi) f_2(x/\Phi) \qquad (1.7)$$

where,

$\Phi^2 = \dfrac{J}{\pi \rho_\infty U_\infty^2}$ is the momentum radius of the flow

$f_1(x/\Phi) \propto \left(\delta/\Phi\right)$

$f_2(x/\Phi) \propto \left(u/U_\infty\right)^{-1}$

The critical value for the new formulation of ε is still about 4.3. Dahm and Dibble note that even a small co-flow causes significant changes in blowout points. They conclude that "local molecular mixing rate in the flow may be the underlying mechanism controlling blowout in turbulent diffusion flames." This is similar to what this study concludes for lift-off and reattachment points.

Savas and Gollahalli [14] provide some photographic evidence of large-scale structures in propane flames. The flow structures for cold jets, lifted flames, and attached

flames are visualized using Schlieren photographs. The cold jet and lifted flame cases appear nearly identical. The presence of the attached flame dramatically reduces the size of the vortical structures in the near-field of the flame. The nozzle used in this analysis was 8.74 mm, about twice that used in our study, and Reynolds numbers varied from 30,700 at lift-off down to 8,600 at reattachment.

In 1986, Gollahalli, et al. [15] published results of a study of hysteresis behavior using several different nozzle size and fuels. Nozzles ranged in size from 5.5 to 12.4 mm, comparable to those used in this study. Gollahalli utilized un-diluted methane and propane fuels, and propane diluted to varying degrees with nitrogen or carbon dioxide. Both diluents were chosen to be non-contributors to the overall reaction, but capable of removing heat from the reaction zone through thermal mass and radiation. The study concluded that dilution of the fuel and increasing the burner size reduces the initial lift-off velocity. Increasing the burner size also decreases the reattachment velocity, but interestingly, the type of fuel used or dilution of the fuel with nitrogen or carbon dioxide does not significantly change the reattachment velocity. This suggests that reattachment is "governed by the dynamics of organized structures rather than molecular properties of [the] fuel". Their work also includes Schlieren photographs of cold flows, attached flames, and lifted flames, but did not address the effect of air co-flow to any detailed level.

Lin, Jeng, and Chao [16] performed a study of stability mechanisms of flames in the hysteresis region using acoustic excitation. The turbulent jet was likened to an amplifier of disturbances. If the frequency of the acoustic excitation were changed, then vortical structures would pass at different rates. The most significant effect was found around the

fundamental frequency of the vortex. The most probable locations for the lifted flame to exist were found to be at roll-up and at the first and second pairing of the vortices.

Demare and Baillot [17] also noted a dependence of lift-off properties with acoustic excitation. Their analysis also included flow velocity mapping and a discussion of how Kelvin-Helmholtz vortices and filaments appear to affect flame location.

Turbulent burning velocity and large-scale structures represent two mechanisms that researchers believe are responsible for the stability of flames. There is still much controversy over which mechanism is responsible for the behavior of lifted turbulent diffusion flames. Although each theory explains some phenomena well, neither theory completely describes what researchers observe. It is the intent of this work to study flames near their lower stability limit (the hysteresis regime) in co-flow to shed light on the merits of each idea.

1.5 Turbulent Triple Flames

In Muniz and Mungal's work [18], turbulent jet diffusion flames, similar to those in our study, are analyzed in co-flow. Much of the experimental procedure used, such as the relative size of the nozzles and the range of co-flows used are consistent between our work and the work done by Muniz and Mungal. However, Muniz and Mungal analyzed flames from initial lift-off velocity up to blowout, while our study presents data from initial liftoff fuel velocity down to reattachment. Muniz and Mungal's results show that the measured jet velocity at the flame base "must be near the premixed laminar flame speed and not exceed 3 S_L." This finding leads Muniz and Mungal to conclude that small co-flows can have such a big effect on flame stability and that the maximum sustainable co-flow will be approximately

3 S_L. This result was confirmed for methane (3 S_L = 1.15 m/s), but could not be confirmed for ethylene, since their experimental apparatus could not attain co-flows in excess of 1.85 m/s (3 S_L = 2.1 m/s).

Muniz and Mungal also conclude that the assertions of Kalghatgi that a turbulent flame velocity is responsible for flame stabilization cannot be substantiated. The turbulent flame velocity was theorized to be related to the laminar burning velocity, multiplied by the local turbulence Reynolds number, which is in turn dependent on the turbulent axial velocity fluctuations (u'), the integral length scale, and the kinematic viscosity at the flame base. Using Kalghatgi's model, the flame would stabilize at positions where the turbulent burning velocity is between 3 and 8 times the laminar burning velocity. This is in contrast to the findings of Muniz and Mungal, which report that the local jet velocity at the flame base is about three times the laminar burning velocity, as measured by PIV methods. Their results appear valid for Reynolds Numbers between 3,800 and 22,000 and for both methane and ethylene fuels.

Another conclusion of Muniz and Mungal is that a modified triple flame is setup for turbulent flames. For laminar flames, a classic triple flame with lean and rich branches and a trailing diffusion flame are easily observed. For turbulent flames, some of the same observations can be made, but not all three flame parts can be seen. Muniz and Mungal conclude that vortical structures warp the rich and lean branches. Several researchers have dubbed these flames as leading edge flames, to distinguish them from the classic laminar triple flame. These results are also supported by Su et al. [19].

In a later study, Han and Mungal [20] investigated entrainment rates of air into fuel for turbulent jets in co-flow. Both reacting and non-reacting cases were analyzed. They concluded that co-flow decreases the rate of entrainment, and heat release dramatically decreases the rate of entrainment (by a factor of 2.5 in some cases) - but buoyancy offsets the decrease in entrainment caused by heat release in the reacting jet.

In a study by Watson et al. [21] the scalar dissipation rates of various flames are measured. The flame velocity relative to the flow is approximately constant and that "scalar dissipation rates do not reach levels thought to cause extinction of the leading edge flames based on comparisons with extinction data for counterflow diffusion flames". Therefore, the authors conclude that the concepts of partially premixed flame propagation are likely more relevant to flame stabilization.

Upatnieks et al. [22] used cinema PIV to observe turbulent flames with relatively low Reynolds numbers (Re<8500). The study also concluded that many of the current theories do not address the actual cause of flame stabilization. Turbulence intensity, u', was not found to be correlated with the speed of the flame base, as was concluded by Muniz and Mungal. Instead, Upatnieks et al. conclude that low Reynolds number turbulent flames seem to stabilize due to streamline divergence caused by the heat release of the edge flame. The heat release was correlated to S_L^2 / α, which is a part of Kalghati's relation for flame height that describes the characteristic chemical reaction time (see equation 1.1 above).

In Lyons and Watson [23], there is evidence for three burning regimes for flames that are ignited well above the stable flame lift-off height. The first regime is a completely premixed fuel and air region where the classic blue flame brush is seen, indicative of

premixed combustion. Because the flame burning velocity is higher relative to the jet velocity, the flame will burn down into a region where partially premixed combustion effects dominate. This second partially premixed regime is seen for most turbulent jet flames, including the flames in this study for the small nozzle-methane fuel, the large nozzle-methane fuel with large co-flow, and the ethylene cases.

The third regime of burning is when the flame approaches the nozzle, where it can be treated as the edge of a diffusion flame. The amount of premixing that can be accomplished in the short distance between the burner edge and the flame base is limited. For small distances above the nozzle, the gradient of mass fraction of the fuel is quite steep and flammability conditions are only for a very few radii close to the flame location. Therefore, it would be expected that diffusion effects would dominate such flames and chemical reactions could be considered to be instantaneous (i.e., infinite Damkohler number).

1.6 Laminar Flames

Savas and Gollahalli [24] in 1986 studied the stability of laminar lifted flames issuing from round nozzles. Exact solutions of the velocity and concentration fields were derived for a variety of fuel Schmidt numbers. Savas and Gollahalli concluded that the fuel concentration at blowout is between the lean limit and the concentration at which the flame speed is maximum. The Reynolds number at blowout was found to be directly proportional to the nozzle diameter.

Chung, Lee and co-workers published a comprehensive series of papers correlating analytical solutions with experimental data for laminar flames using propane fuel and very

small nozzles [25-30]. The main assumption is the use of similarity solutions, which work well for fully-developed laminar cold flows. The similarity solution is presented in the next section. These authors have correlated measurable flame parameters such as lift-off height, reattachment velocities, and blowout velocities to the fuel properties through the Schmidt number and fuel velocity. Importantly, the analytical results concluded that lifted laminar diffusion flames of fuel with Schmidt numbers of between 0.5 and 1.0 (e.g., methane, Sc = 0.7) were not stable, but flames were stable for other Schmidt number fuels (e.g. propane, Sc = 1.4). These results were experimentally verified.

The flames in their analysis were determined to be triple flames, propagating at a tribrachial flame speed of about twice the laminar burning velocity. Using similarity solutions, the flame lift-off height is given to be:

$$\frac{H_L}{d^2}\frac{\upsilon}{S_{tri}} = \left(\frac{3}{32}\frac{3}{2Sc+1}\frac{Y_{F,st}}{Y_{F,o}}\right)^{\frac{1}{Sc-1}}\left(\frac{u_o}{S_{tri}}\right)^{\frac{2Sc-1}{Sc-1}} \tag{1.8}$$

The term $Y_{F,o}$ refers to the mass fraction of fuel in the nozzle initially (accounting for partially premixed fuel) and $Y_{F,st}$ refers to the stoichiometric fuel mass fraction. The Schmidt number, Sc, is the ratio of momentum diffusivity to molecular diffusivity, as measured by the kinematic viscosity and the binary diffusion coefficient [31].

$$Sc = \frac{\upsilon}{D_{AB}} \tag{1.9}$$

Schmidt numbers of unity are obviously a problem, since it would make both exponents infinite. Schmidt numbers less than 0.5 will result in the numerator of the second exponent becoming negative. Interestingly, for a Schmidt number of 0.5, the lift-off height

becomes a linear function of u_o and related to the laminar burning velocity (by means of the tribrachial flame speed) squared. This is similar to the result for turbulent flames. However, studies have shown that turbulent Schmidt Numbers are generally closer to unity [32]. Also apparent in this analysis is the dependence of the lift-off height on the nozzle diameter squared.

Ghosal and Vervisch [33] extended the results of Lee, Chung, and co-workers to include the effects of flame curvature and the effect of heat release on the flow. They concluded that the heat release effect on the upstream flow, reduced by a small flame curvature, would account for the difference between the laminar flame speed and the observed tribrachial flame speed. An interesting consequence of including the flame curvature in the analysis is that lifted laminar flames with a Schmidt number less than unity can exist, though would probably oscillate between the attached and lifted conditions. This observation was not confirmed experimentally.

Boulanger et al. [34], further the work of Ghosal and Vervisch in that the effects of the heat release and flame curvature are quantified. They note that the flame sits at a location where the local flow velocity, as seen by the flame, is the laminar burning velocity at the stoichiometric mixture fraction. Instead of using a tribrachial flame speed that is assumed to be twice the laminar burning velocity, a new relation for the tribrachial flame speed is derived based on flame curvature and heat release.

$$U_{flamebase} = S_L(1+\alpha) - F(\chi_s) \tag{1.10}$$

where α is the heat release parameter defined as:

$$\alpha = \frac{T_{stoichiometric} - T_o}{T_{stoichiometric}} \tag{1.11}$$

A typical value for α is about 0.8. The function $F(\chi_s)$ accounts for the effects of flame curvature, also modified by the heat release. The results of the analysis did accurately predict how flames react to changes in nozzle flow rate, but did not accurately predict the magnitude of the lifted flame height. The authors theorize that the heat release also affects the shape of the stoichiometric mixture fraction surface, such that the flame can exist upstream of where cold flow solutions would predict. The effect is more pronounced for higher Reynolds numbers and the authors predict that this effect would likely continue into the turbulent regime.

Lee and Chung [35] also analyzed flames in co-flow, developing a series of relations for lift-off height and reattachment velocity in a co-flow. The relation for the axial velocity, u (equation 1.24 in the next section) is modified by subtracting the co-flow velocity. This is similar to considering the excess jet velocity.

$$u - V_{co} = \frac{3}{8\pi\nu_\infty x}\frac{J}{\rho_\infty}\frac{1}{\left(1+\eta^2/8\right)^2} \tag{1.12}$$

where η is a similarity variable. The fuel mass fraction is given, as in the case of zero co-flow, as:

$$Y_F = \frac{3}{8\pi\upsilon_\infty x}\frac{J}{\rho_\infty}\frac{1}{\left(1+\eta^2/8\right)^{2Sc}} \tag{1.13}$$

Solving these relations, the relation for lift-off height is:

$$\frac{H_L}{d^2}\left(S_{tri} - V_{co}\right)^{\frac{Sc}{Sc-1}} = const. \times u_o^{\frac{2Sc-1}{Sc-1}} \quad (1.14)$$

The lift-off height is related to the excess jet velocity to a power. For propane, the exponent is about 3.5 ($Sc_{propane}$ = 1.4). The lift-off height is definitely non-linear, unlike with turbulent flames.

The co-flow velocity modifies the tribrachial flame speed. Since the tribrachial flame speed is about twice the laminar flame speed ($S_{L,\ propane}$ = 0.4 m/s and therefore $S_{tri,\ propane}$ = 0.8 m/s [35]), a small co-flow can make a big difference. The flame lift-off height is still a function of the nozzle fuel velocity to the same power as without co-flow. Thus, for laminar flames the burning speed is the only significant term modified by co-flow. It would also suggest that the co-flow velocity could not exceed the tribrachial flame speed (else the term becomes negative). Another conclusion of Lee and Chung's work is the linearity of the reattachment velocity, the lift-off velocity and the blowout velocity with co-flow for laminar flames.

1.7 Derivation of Laminar Jet Relations

The velocity profile for a laminar jet with a top-hat velocity profile can be derived from basic relations with the following assumptions [36]:

1. The surrounding air far from the nozzle is quiescent
2. No chemical reactions (cold flow)
3. Uniform gas properties and pressure in the fluid
4. Steady axisymmetric flow (no θ component)
5. Buoyancy forces are negligible compared to jet
6. Mass diffusion, heat transfer, and viscous forces act radially only and not axially
7. Sc = Pr = 1, diffusion of momentum, temperature, and concentrations behave similarly. This is equivalent to assuming that Le = 1

Conservation of mass in the r, x direction can be written as:

$$\frac{\partial}{\partial x}(\rho u r) + \frac{\partial}{\partial r}(\rho v r) = 0 \tag{1.15}$$

Since density is assumed constant, the density term can be eliminated.

$$\frac{\partial}{\partial x}(u r) + \frac{\partial}{\partial r}(v r) = 0 \tag{1.16}$$

Breaking out the derivatives of the products using the product rule,

$$r\frac{\partial u}{\partial x} + u\frac{\partial r}{\partial x} + \frac{\partial v}{\partial r} + v\frac{\partial r}{\partial r} = 0 \tag{1.17}$$

Simplifying the equation by dividing by r yields

$$\frac{\partial u}{\partial x} + \frac{\partial v}{\partial r} + \frac{v}{r} = 0 \qquad \leftarrow \text{Conservation of mass relation} \tag{1.18}$$

The x-momentum relation is for constant properties, neglecting terms and derivatives in the theta direction and time dependencies is:

$$\rho u\frac{\partial}{\partial x}(u) + \rho v\frac{\partial}{\partial r}(u) = \frac{1}{r}\mu\frac{\partial}{\partial r}\left(r\frac{\partial u}{\partial r}\right) \tag{1.19}$$

or, after combining density and viscosity,

$$u\frac{\partial u}{\partial x} + v\frac{\partial u}{\partial r} = \frac{v}{r}\frac{\partial}{\partial r}\left(r\frac{\partial u}{\partial r}\right) \tag{1.20}$$

The fuel species can be expressed in terms of the mixture fraction, f. It has a similar form to the momentum relation above.

$$u\frac{\partial f}{\partial x} + v\frac{\partial f}{\partial r} = \frac{v}{r}\frac{\partial}{\partial r}\left(r\frac{\partial f}{\partial r}\right) \tag{1.21}$$

The boundary conditions at x=0 (exit of the nozzle)

$x = 0$ and $r \le r_o$	$u = u_o$	(uniform exit profile)
	$f = 1$	(all fuel)
$x = 0$ and $r > r_o$	$u = 0$	(no flow of air)
	$f = 0$	(all air, no fuel)

and,

$x \rightarrow \infty$	$u = 0$	(quiescent flow)
	$f = 0$	(no fuel)

There are two jet invariants, which are based on conservation of momentum and species. These invariants are, as their name implies, constants that are determined by summing the momentum or mass fraction at any x from the jet axis to infinity. Momentum and mass can diffuse away from the jet axis in the radial direction, but total momentum and mass provided by the jet must be conserved.

$$J = \frac{1}{\nu}\int_0^\infty u^2 r dr = \frac{1}{2\nu}\left(u_o^2 r_o^2\right) \qquad \text{and} \qquad (1.22a)$$

$$I_f = \frac{1}{\nu}\int_0^\infty ufr dr = \frac{1}{2\nu}\left(u_o r_o^2\right) \qquad (1.22b)$$

The partial differential equations can be solved using similarity analysis. Spalding [37] and Schlichting [38] determined the following solutions.

$$u = \frac{3}{4}\frac{J}{x}\left(1+\frac{\xi^2}{4}\right)^{-2} \qquad (1.23a)$$

$$v = \left(\frac{3J\nu}{8}\right)^{1/2}\frac{\xi}{x}\left(1-\frac{\xi^2}{4}\right)\left(1+\frac{\xi^2}{4}\right)^{-2} \qquad (1.23b)$$

and

$$f = \frac{3}{4}\frac{I_f}{x}\left(1+\frac{\xi^2}{4}\right)^{-2} \qquad (1.23c)$$

where,

$$\xi = \left(\frac{3J}{8\nu}\right)^{1/2} \frac{r}{x} \qquad \text{is the similarity variable.} \tag{1.23d}$$

In the analysis of laminar flames by Ko, Chung, and Lee [25], the assumed velocity profile leaving the nozzle is parabolic (Poiseuille flow). The solution to the above differential equations then becomes:

$$u = \frac{3}{8\pi\nu x}\frac{J}{\rho}\frac{1}{\left(1+\eta^2/8\right)^2} \tag{1.24a}$$

where,

$$J = \rho\pi u_o^2 d^2/12 \tag{1.24b}$$

is the momentum invariant based on mean exit velocity and,

$$\eta = \sqrt{1/32}\left(\frac{u_o d}{\nu}\right)\frac{r}{x} \tag{1.24c}$$

These solutions are alike in that the velocity u is related to the similarity variable inversely to the second power. Both similarity variables depend on r/x, which makes them similarity variables. However, there are some differences in constants which are accounted for by the different velocity profiles.

1.8 Derivation of Turbulent Jet Relations [39]

The governing differential equations for a turbulent jet are the same as those for the laminar case, assuming that the velocities are the time averaged quantities and replacing the kinematic viscosity with the turbulent viscosity, ν_T.

$$\frac{\partial \bar{u}}{\partial x}+\frac{\partial \bar{v}}{\partial r}+\frac{\bar{v}}{r}=0 \qquad \text{mass (continuity)} \qquad (1.25)$$

$$\bar{u}\frac{\partial \bar{u}}{\partial x}+v\frac{\partial \bar{u}}{\partial r}=\frac{\nu_T}{r}\frac{\partial}{\partial r}\left(r\frac{\partial \bar{u}}{\partial r}\right) \qquad \text{momentum in the x-direction} \qquad (1.26)$$

A stream function approach is taken by these authors to solve these equations.

$$\bar{u}=-\frac{1}{r}\frac{\partial \psi}{\partial r} \qquad \text{and} \qquad \bar{v}=\frac{1}{r}\frac{\partial \psi}{\partial x} \qquad (1.27a,b)$$

Note that by using the stream function approach, that the continuity equation is automatically satisfied. A similarity solution in the form below is chosen to solve the momentum equation in terms of the stream function variable.

$$\psi=\nu_T x F(\xi) \qquad (1.28)$$

where F is a dimensionless function of ξ=r/x.

Putting the form above for ψ into the equations for u and v, yields:

$$\bar{u}=-\frac{\nu_T}{x}\frac{F'}{\xi} \qquad \text{and} \qquad \bar{v}=\frac{\nu_T}{x}\left(\frac{F}{\xi}-F'\right) \qquad (1.29a,b)$$

The boundary conditions are:

At ξ=0, $\qquad \frac{F}{\xi}-F'=0 \qquad$ and $\qquad \frac{F''}{\xi}-\frac{F'}{\xi^2}=0$

Expand F in a Taylor series expansion around ξ=0,

$$F(\xi) = a + b\,\xi + c\,\xi^2 + d\,\xi^3 + e\,\xi^4 + \ldots \tag{1.30}$$

The first boundary condition results in a = 0, and the second boundary condition results in b = d = 0. Putting the relations for u and v into the momentum differential equation yields:

$$\frac{d}{d\xi}\left(\frac{FF'}{\xi}\right) = \frac{d}{d\xi}\left(F'' - \frac{F'}{\xi}\right) \tag{1.31}$$

Integrating,

$$\frac{FF'}{\xi} = F'' - \frac{F'}{\xi} + C_1 \tag{1.32}$$

The second boundary condition from above determines that C_1 must be zero. Schlichting first solved this equation by setting $\xi = \ln \beta$. The result after another integration is:

$$\xi F' = 2F + \tfrac{1}{2} F^2 + C_2 \tag{1.33}$$

The authors conclude that C_2 must be zero because of the expansion of the function around ξ=0. The solution to the equation above is:

$$F(\xi) = \frac{(C_3\xi)^2}{1 + \tfrac{1}{4}(C_3\xi)^2} \tag{1.34}$$

Substituting this back into the relations for u and v yields:

$$\bar{u} = \frac{\nu_T}{x}\frac{2C_3^{\,2}}{\left[1 + \tfrac{1}{4}(C_3 r/x)^2\right]^2} \quad \text{and} \quad \bar{v} = \frac{C_3\nu_T}{x}\frac{(C_3 r/x) - \tfrac{1}{4}(C_3 r/x)^3}{\left[1 + \tfrac{1}{4}(C_3 r/x)^2\right]^2} \tag{1.35a,b}$$

To find C_3, the u and v equations are substituted into the momentum invariant relation, which can be determined at the nozzle in terms of initial flow velocity, density, and the turbulent viscosity.

$$C_3 = \sqrt{\frac{3}{16\pi}}\sqrt{\frac{J}{\rho}}\frac{1}{\nu_T} \tag{1.36a}$$

where,

$$J = \int_0^{2\pi}\int_0^{\infty} \rho \overline{u}^2 r dr d\theta = 2\pi\rho b^2 u_{\max}^2 \tag{1.36b}$$

and b is the width of the jet.

2. Experimental Apparatus, Procedure, and Raw Data

2.1. Experimental Apparatus

The burner is shown in Figure 2.1 below. It consists of a tube that contains the fuel for combustion surrounded by an annulus of co-flowing air. Two different stainless steel tubes with inner diameters of 2.5 mm and 4 mm are used.

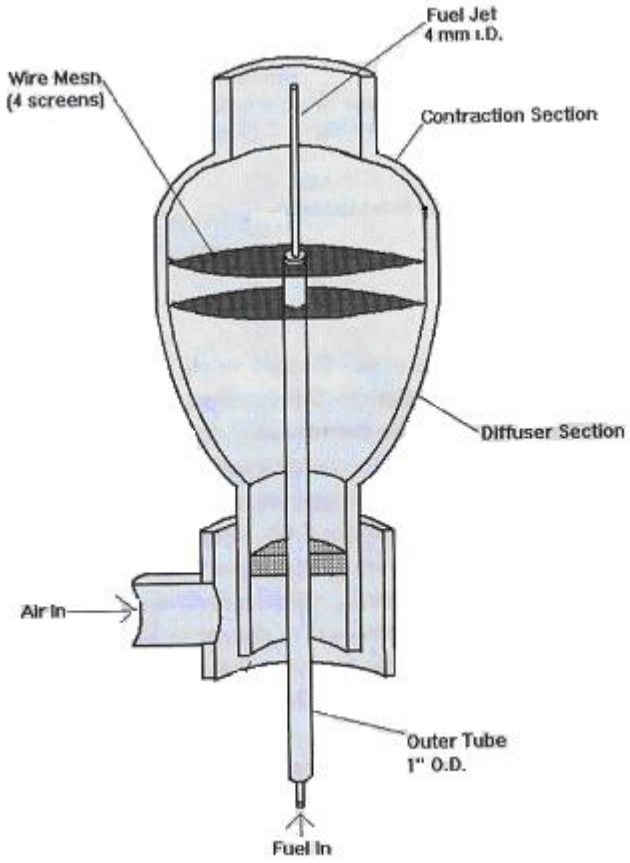

Figure 2.1 – Experimental Setup

The co-flow air is supplied by a Magnetek model 9467 centrifugal blower, with a variable speed drive to vary air flow and velocity. Flexible hose connects the blower to the burner assembly where the air is guided through a sharp turnaround and then forced upward through a 1 inch thick layer of honeycomb material. This material acts as a flow straightener. The air then enters a diffuser section where the cross sectional area increases. Four wire mesh screens dampen any flow irregularities and disrupt flow vortices. The diameter of the co-flow annulus is 5.75 inches at the burner tip.

Fuel flow was measured using an Advance Series 150 flowmeter. This rotameter was calibrated for use with air and methane. A small knob controls the flow, which is measured by determining the position of a stainless steel ball in glass chamber with graduated markings. Fuels used in the experiments include methane, propane, and ethylene. All fuels and the nitrogen are supplied in cylinders as compressed gases. A flow regulator reduces the pressure from 1,000 psig in the cylinder for use in the experiments.

Co-flow velocity was measured using a TSI Velocicalc model 8345 hot wire anemometer. The meter is capable of resolving velocity to the nearest 0.01 m/s with an accuracy of ±3% of full-scale. When measuring co-flow, many measurements were taken to account for small variations in the flow over the co-flow cross-sectional area.

2.2. Experimental Procedure

Data was collected on flame height as a function of fuel velocity out of the burner tube and co-flow velocity. The co-flow velocity is set using a dial controlling a variable speed drive on the blower. To obtain very low co-flow velocities, paper was taped over part or all of the air inlet. Air velocity was measured using a hot-wire anemometer. The co-flow

velocity varies somewhat around the cross-sectional area. About ten different measurements were made at various locations and a representative value used based on the judgment of the experimenter. Measurements were taken at various radial and circumferential locations. Some drift was noted in the velocity measurements. Over time, the readings tended to increase by about 0.1 m/s. Therefore, the burner was allowed to come to equilibrium by setting the co-flow velocity and waiting several minutes. Velocity measurements were taken again at the end of the experimental run to confirm the system was at steady state.

After establishing a base co-flow velocity, the gas flow is initiated and a flame lit using a standard propane lighter. The initial flame is typically attached and the gas flow is increased gradually until liftoff is achieved. Care is taken to increment the gas flow knob slowly so that a precise lift-off velocity is determined. Lift-off heights for different fuel velocities are recorded on a data entry form created for this investigation.

The lifted height is read using a graduated ruler that has been attached to the burner. Care was taken to insure that readings were taken such that the observer and the flame were at the same height. Lift-off heights were measured to within 1/8 inch, the smallest graduation on the ruler. At most lifted conditions, the flame height tended to vary periodically. An average or representative height was determined using the observer's best judgment. The variation in flame height was typically between 1/8 and ¼ inch.

After the lift-off height and velocity was recorded, the fuel flow was increased to some nominal value above lift-off. The height above the burner was recorded, for confirmation against data that has been collected by other experimenters in the purely lifted regime.

The fuel velocity was then reduced back to the lift-off velocity and the lift-off height compared to the original. Then, the fuel velocity is gradually reduced until the flame spontaneously reattaches to the burner. Using the graduations on the rotameter and based on the size of the hysteresis regime, data points corresponding to varying fuel nozzle velocities throughout the hysteresis regime were collected. For zero co-flow, the difference between lift-off fuel velocity and reattachment fuel velocity was often small, resulting in fewer data points. As the co-flow was increased in subsequent experimental runs, the velocity difference increased and more data points could be collected. Care was taken to precisely set the velocity at each value on the meter. The stainless steel ball was used for measurements and proper values were determined when the center of the ball was at the mark.

As before, lift-off heights were measured by first aligning the observer's line of sight at the level of the base of the flame. Then, the measurement is determined using the attached ruler to the nearest 1/8 inch. The data is recorded on the sheet along with any comments about the flow.

Experimental runs were made at various co-flows to cover a variety of conditions. The data was tabulated in Microsoft Excel and measured rotameter flows converted to fuel velocity using the following procedure:

1. The measured value on the rotameter was converted into a flow rate in standard liters per minute of methane using calibration data provided by the manufacturer.
2. The volumetric flow rate is converted into velocity using the inner diameter of the nozzle and determining an area.

   $$\text{Fuel Velocity} = \text{Volumetric Flow Rate} / (\pi \, ID^2 / 4) \qquad (2.1)$$

3. The fuel velocities are graphed against lift-off height for various co-flow velocities.

Although not as precise as a thorough analysis using high speed imaging and a complex computational analysis of flame location (as some other researchers have done), the methods used in these experiments to determine flame location are valuable in determining trends and approximate locations. The computations in the analysis to follow depend on the data collected, but are not progressive in that a few measurements are used in succession to compute results. Rather, a few relatively simple relations are applied to large numbers of data points, each with their own associated measurement error. However, this error over the course of many data points should effectively cancel out and don't cascade to render the results useless. Thus, the general trends and results are believable and not due to mathematical aberrations.

2.3 Raw Data Charts and Figures

Data from the experimental runs made for undiluted methane, ethylene, and propane fuels are shown below in tabular form and graphically.

Table 2.1 – Raw Data Set for Lifted Flame Heights (in inches) for Methane Fuel, Large Nozzle, No Dilution

Flowmeter	Fuel Vel	Co-Flow Velocity, m/s----------											
reading	m/s	0	0.05	0.12	0.18	0.22	0.3	0.38	0.5	0.53	0.6	0.7	0.72
40	44.37	1.25		1.75									
35	38.40	0.75		1.5	1.5			2.25					
30	32.42			1				2				3.25	
29	31.27				1.125								
28	30.08	0.6							2				
27	28.89			0.75	1								
26	27.74	0.5						1.75					
25	26.55	0.5	0.625	0.625	0.625			1.75	1.875				
24	25.40	0.5	0.5		0.5		1.75		1.875			3.25	
23	24.24			0.5		0.75		1.875	1.875				
22	23.09	0			0.375		1.75			2.625		3.375	3.75
21	21.93		0.5	0.375	0.25			1.75	1.875				
20	20.78			0.375	0.25	0.625	1.625	1.5		2.5	3.25	3.5	3.375
19	19.66		0.25	0.375	0.25		0.875	1.25	1.75				
18	18.54		0	0.375	0.25	0.5	0.75	1.125		2.5	3	3.375	3.25
17	17.42			0	0	0.3	0.875						
16	16.30					0	0.875	0.875	1.25	2.5	3	3.25	3.5
15	15.20						1	1	1.375	2.375	3.125	3.625	
14	14.16						0	1.25	1.5	2.375	3	3.625	3.5
13	13.11							1.375		2.5			3.625
12	12.09							0	1.5		3	3.5	3.625
11	11.03								1.75	2.625			
10	9.98								1.75	2.75	3	3.75	3.875
9	8.96								0	3		4	
8	7.94									0	3.5	4.25	4.25
7	6.89										4	4.625	5
6	5.90										0		0
5	4.82											0	

Table 2.2 – Raw Data for Lifted Flame Heights (in inches) for Methane Fuel, Small Nozzle, No Dilution

Flowmeter	Fuel Vel.	Co-flow Velocity, m/s						
Reading	m/s	0	0.13	0.2	0.26	0.36	0.47	0.55
21	16.50	1.375	1.9	2.25	2.5			
20	15.49							
19	14.48					2.75		
18	13.53	1.25		1.875				
17	12.63		1.875		2.25			
16	11.72	1.25	1.75	1.95	2.25	2.5		
15	10.88	1.2	1.75	1.9375	2.125	2.375		
14	10.08	0		1.875		2.5		
13	9.28		1.875	1.9375	2	2.5		
12	8.49			2	2.125	2.5		
11	7.75		2	2.0625	2.375	2.75	3.25	
10	7.00		0	2.125	2.5	2.875	3.5	
9	6.26			0	2.75	3.1	4	
8	5.52				3	3.5	4.75	4.25
7	4.83				0	0	0	5
6	4.08							0

Table 2.3 – Raw Data for Lifted Flame Heights (in inches) for Ethylene Fuel, Large Nozzle, No Dilution

Flowmeter	Ethy vel	Co-Flow Velocity, m/s----------								
reading	m/s	0	0.25	0.40	0.46	0.58	0.70	1.0	1.6	1.8
25	20.43	0.25								
24	19.55									
23	18.66	0.125								
22	17.77		0.25	0.375	0.375					
21	16.88	0.125				0.5	0.625			
20	15.99	0	0.25	0.25			0.56	0.875		
19	15.13		0.22		0.27	0.375				
18	14.27		0.2	0.25	0.27	0.36	0.42			
17	13.41		0.14	0.2	0.25			0.75		
16	12.55		0			0.35				
15	11.70			0	0.2	0.25	0.375	0.625		
14	10.90				0	0.25	0.35		1.5	
13	10.09					0	0.32	0.5		1.875
12	9.31						0.32	0.5	1.25	
11	8.49						0			
10	7.68							0	1.25	1.5
9	6.90								1.625	
8	6.11								0	2.25
7	5.30									3
6	5.29									0

Table 2.4 – Raw Data for Lifted Flame Heights (in inches) for Ethylene Fuel, Small Nozzle, No Dilution

Flow	Fuel Vel.	Co-Flow Velocity, m/s---------		
slpm	m/s	0	0.46	0.60
10	40.83	0.1875		
9.56	39.03	0.1875		
9.12	37.24	0.2		
8.91	36.38		0.375	
8.7	35.52	0	0.375	
8.49	34.67			
8.28	33.81			0.6
8.08	32.99		0.3125	0.5
7.88	32.17			0.47
7.68	31.36		0.3125	0.4
7.5	30.62			0.375
7.32	29.89			0.375
7.14	29.15		0.25	0.375
6.96	28.42			0.375
6.78	27.68		0.25	0.375
6.6	26.95			
6.42	26.21		0.25	0.375
6.24	25.48			
6.06	24.74		0.25	0.35
5.88	24.01			0.35
5.7	23.27		0.1875	
5.51	22.50			0.3
5.32	21.72		0	
5.12	20.91			0.3
4.92	20.09			0.3
4.72	19.27			
4.52	18.46			0

Table 2.5 – Raw Data for Lifted Flame Heights (in inches) for Propane Fuel, Small Nozzle, No Dilution

Flowmeter	Prop vel	Co-Flow Velocity, m/s----------		
Reading	m/s	0	0.23	0.31
18	11.25			
17	10.57			
16	9.89			
15	9.22			
14	8.59			
13	7.95			
12	7.34			
11	6.69	0.375		
10	6.06	0.28		
9	5.44	0.25		
8	4.82	0	0.625	
7	4.18		0.55	
6	3.58		0.625	
5	2.92		0	0.875
4	2.43			0

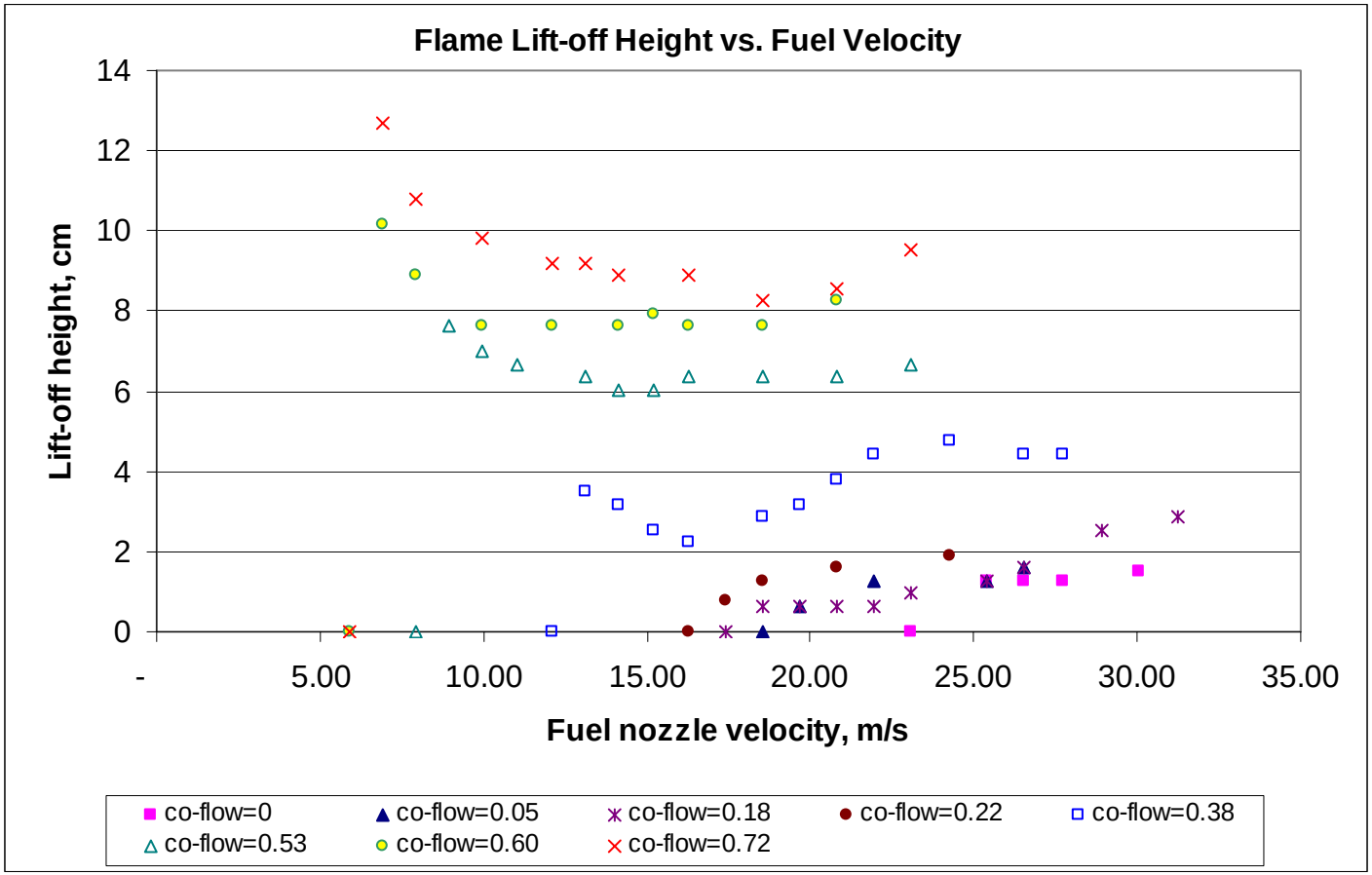

Figure 2.2 – Lift-off Flame Height vs. Fuel Velocities for Methane, Large Nozzle, No Dilution

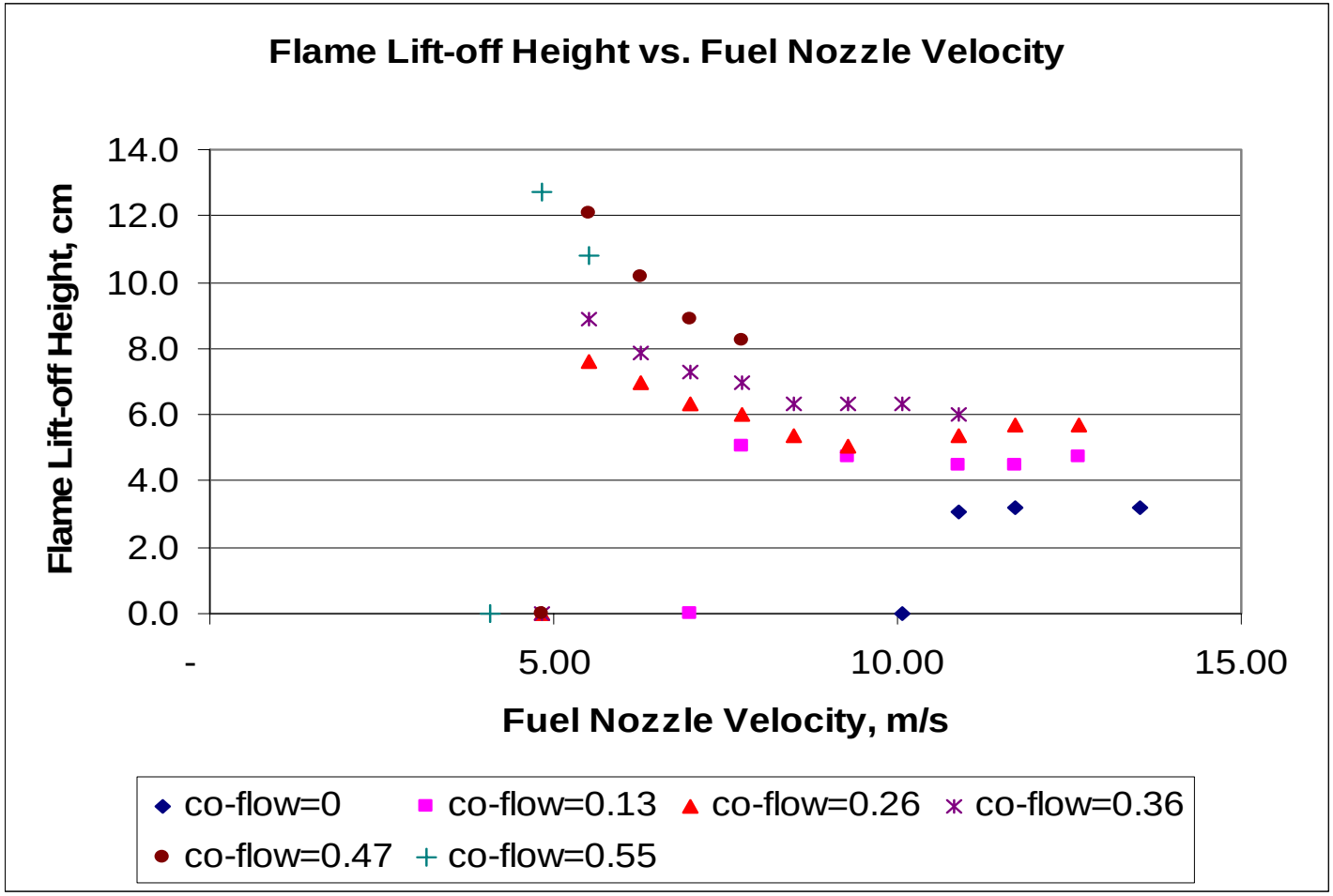

Figure 2.3 – Lift-off Flame Height vs. Fuel Velocities for Methane, Small Nozzle, No Dilution

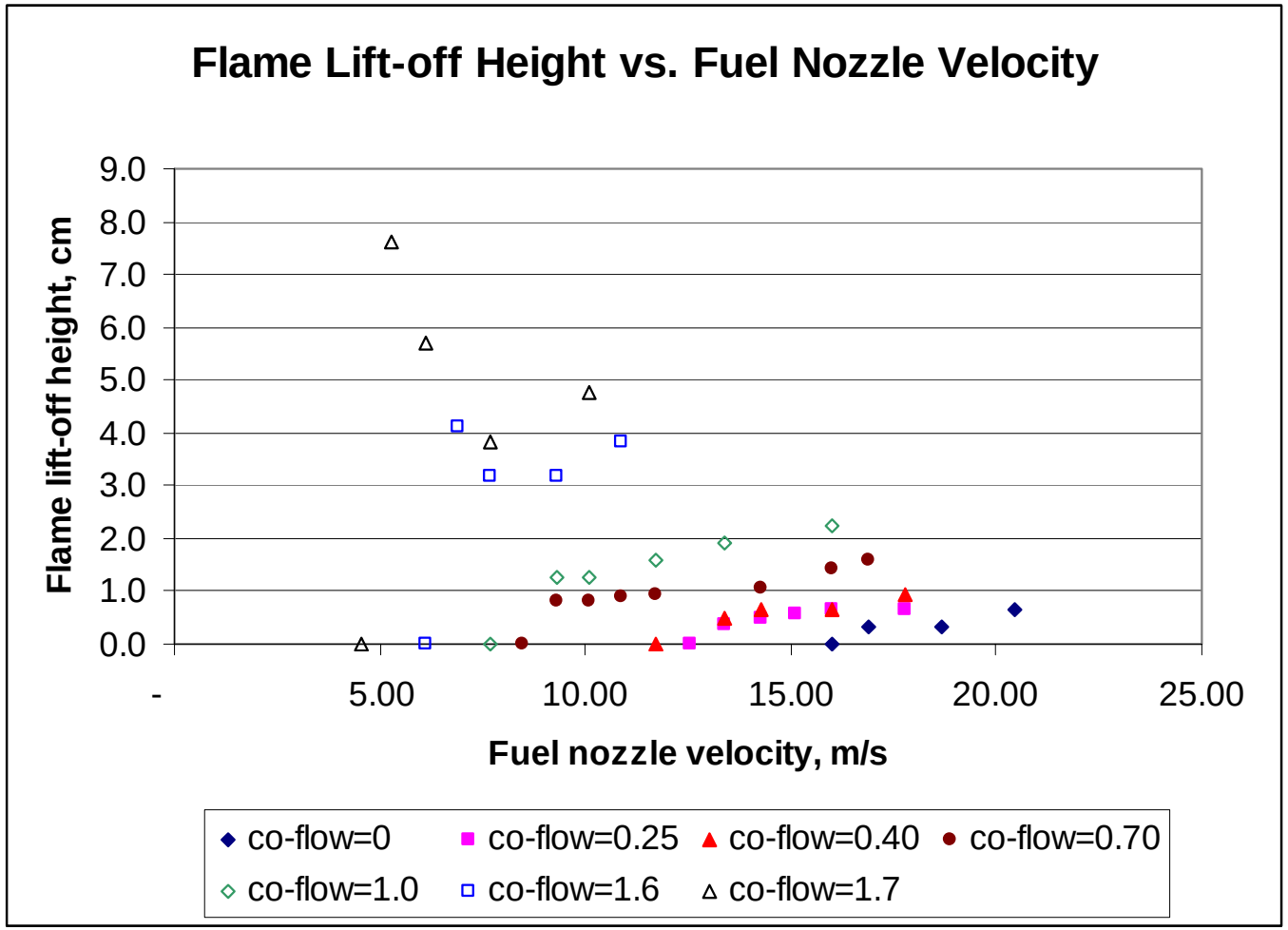

Figure 2.4 – Lift-off Flame Height vs. Fuel Velocities for Ethylene, Large Nozzle, No Dilution

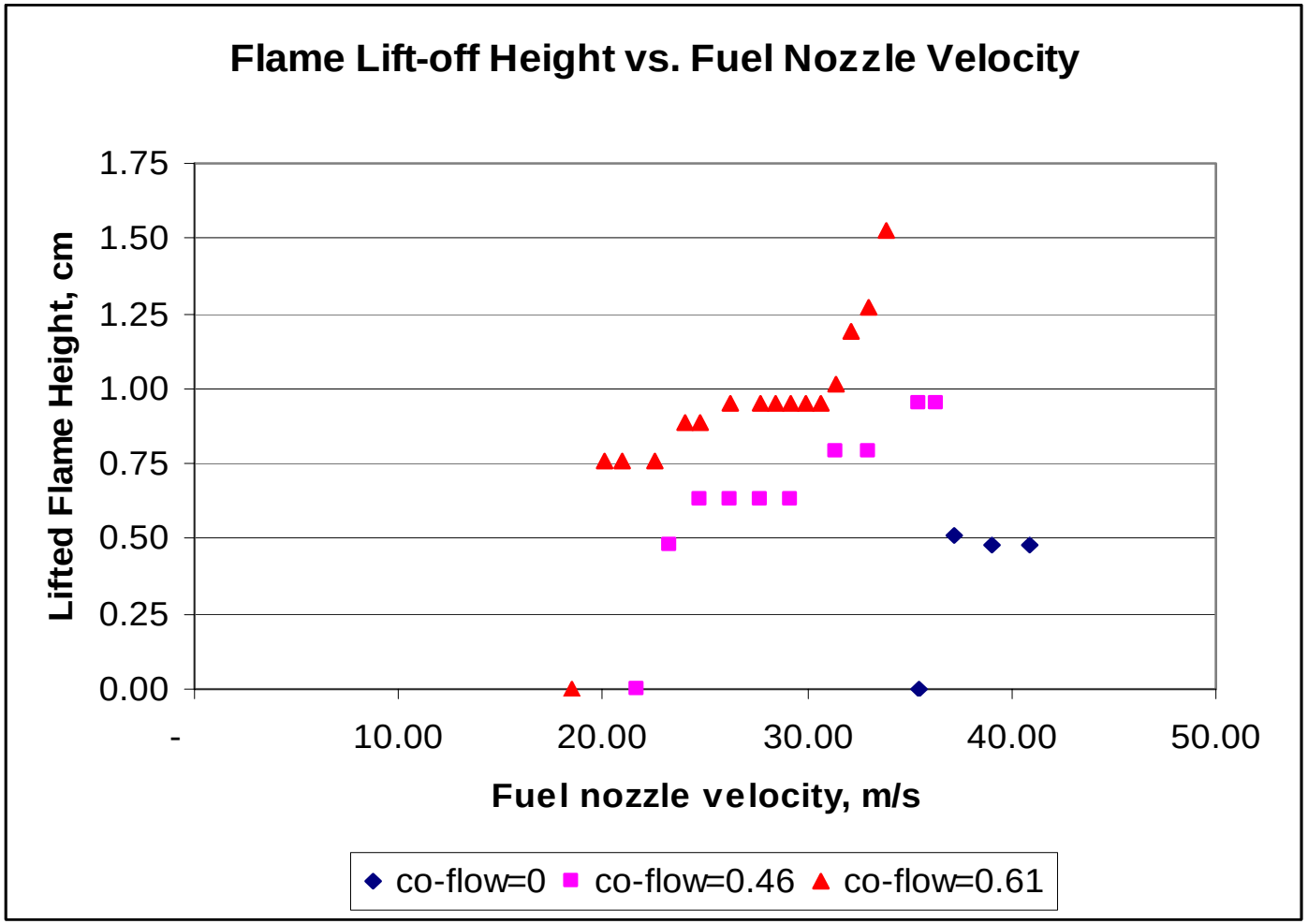

Figure 2.5 – Lift-off Flame Height vs. Fuel Velocities for Ethylene, Small Nozzle, No Dilution

2.4 Photographs and visual observations

The figures below illustrate some of the photographs taken during experimental runs with comments about basic flame structure and behavior.

2.4.1 Methane Large Nozzle

For methane with the large (4 mm nozzle) and zero co-flow, the following photographs illustrate the different regimes:

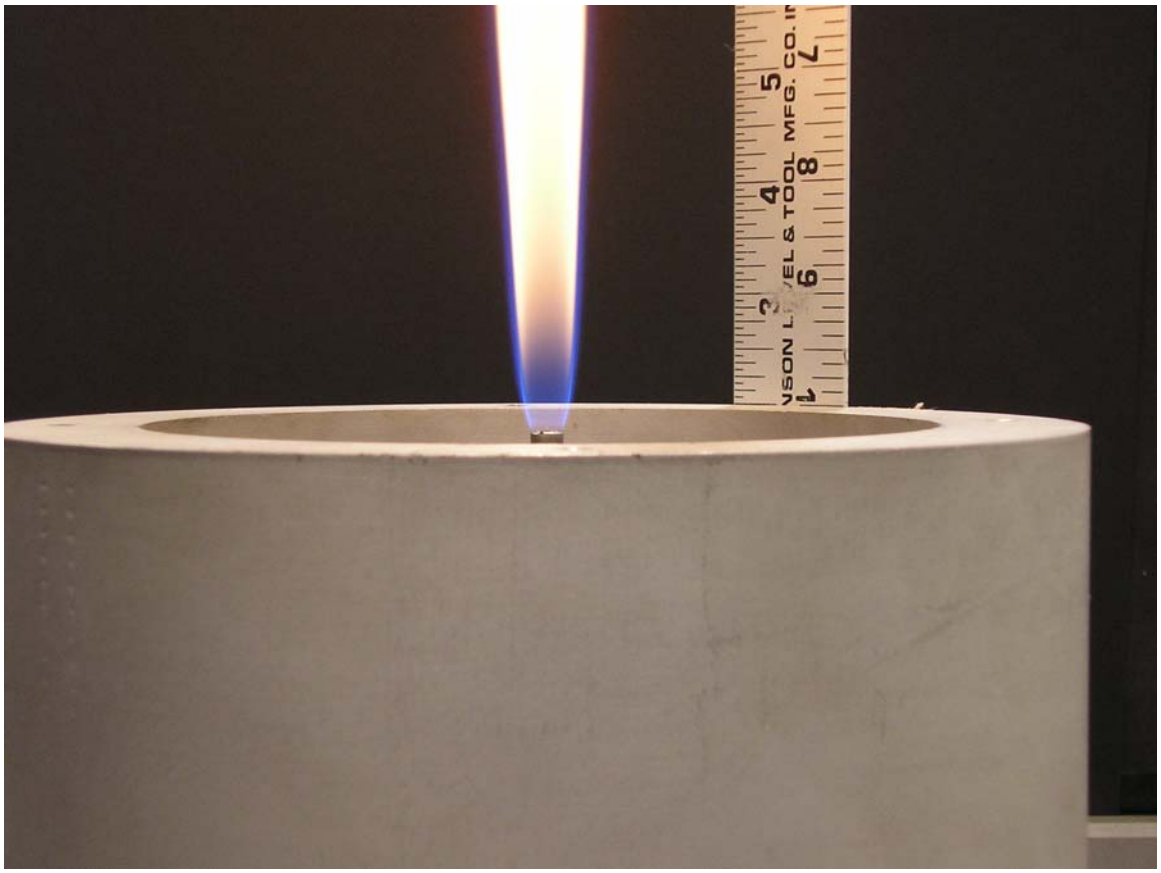

Figure 2.6 – Methane Large Nozzle, Zero Co-flow, Attached Region

The above photograph is for an attached flame for methane and zero co-flow. The fuel velocity at the nozzle exit is 11 m/s. Note the blue flame at the flame base, which transitions to a bright orange diffusion flame above. At this fuel velocity, the flame is steady without much flicker. Just prior to lift-off, the flame will begin to flicker and turbulence in the diffusion portion of the flame increases.

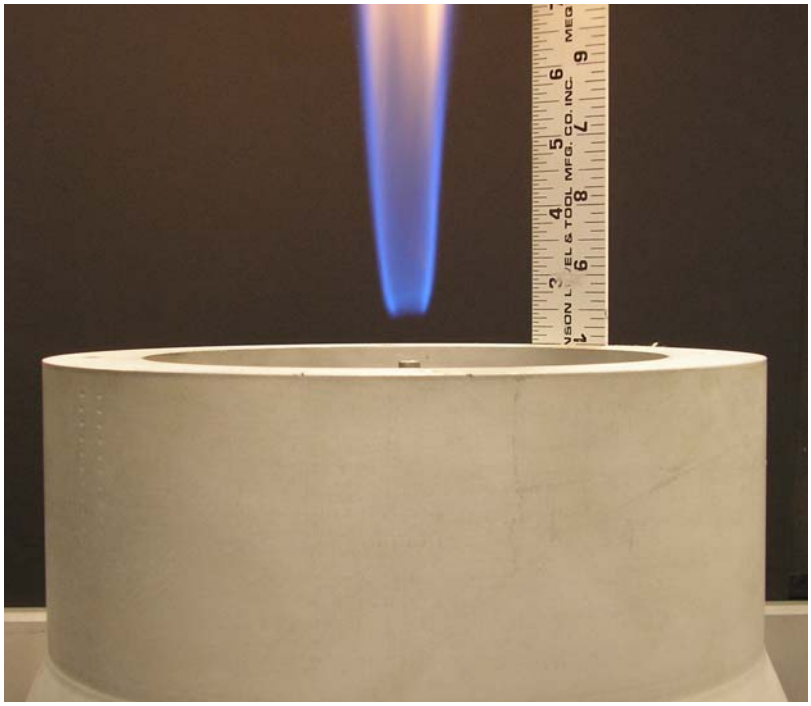

Figure 2.7 – Methane Fuel, Large Nozzle, Zero Co-flow, Lifted Flame

Lifted flames produce a different structure. The blue region is much larger, extending further downstream. This indicates that there has been some degree of premixing prior to combustion, which results in a hotter flame and less soot formation. As the flame lifts farther from the burner, the amount of orange in the flame decreases. Orange flame is indicative of soot luminescence and a cooler flame.

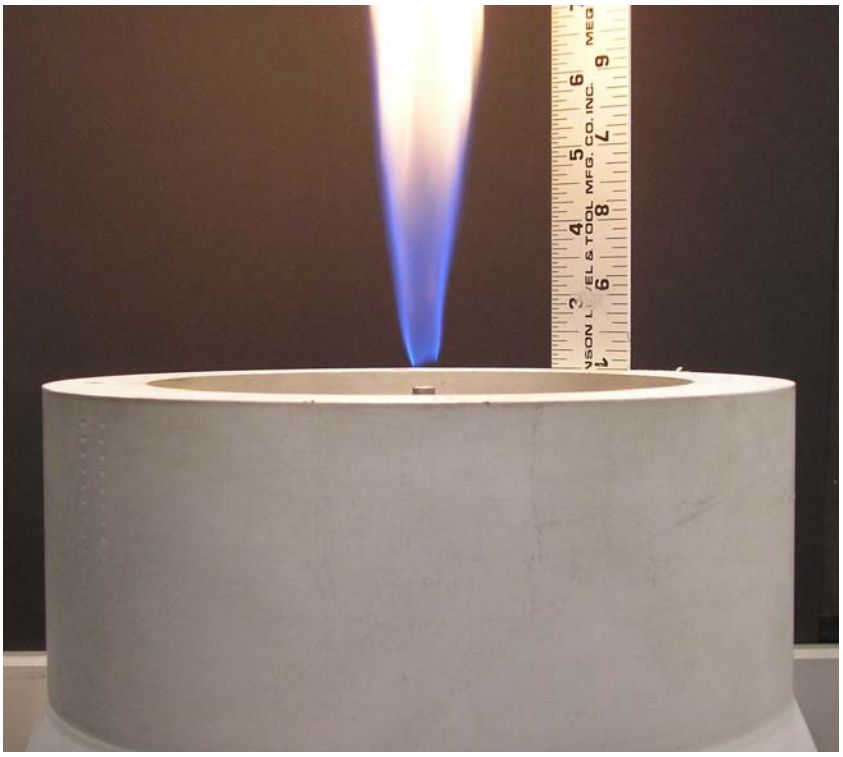

Figure 2.8 – Methane Fuel, Large Nozzle, Zero Co-flow, Lifted Flame in Hysteresis Regime

For the no co-flow case the flame lift-off height decreases as the fuel velocity decreases. The flame appears more and more like the initially attached flame, with a small lift-off height. Soot luminescent becomes more apparent closer to the leading edge, as seen in Figure 2.8 above. For the large nozzle and no co-flow, flames are lifted only a fraction of an inch above the nozzle. Mixing of fuel and air is limited, and the flame takes on properties of an edge flame – rather than the lifted flames that are the primary focus of this work. At some lower fuel velocity, the flame spontaneously reattaches.

When a small amount of co-flow is added, the lift-off and reattachment velocities are affected. Visually, the flame does not appear to be significantly affected by the co-flow. Figure 2.9 shows the attached flame subjected to a 0.30 m/s co-flow.

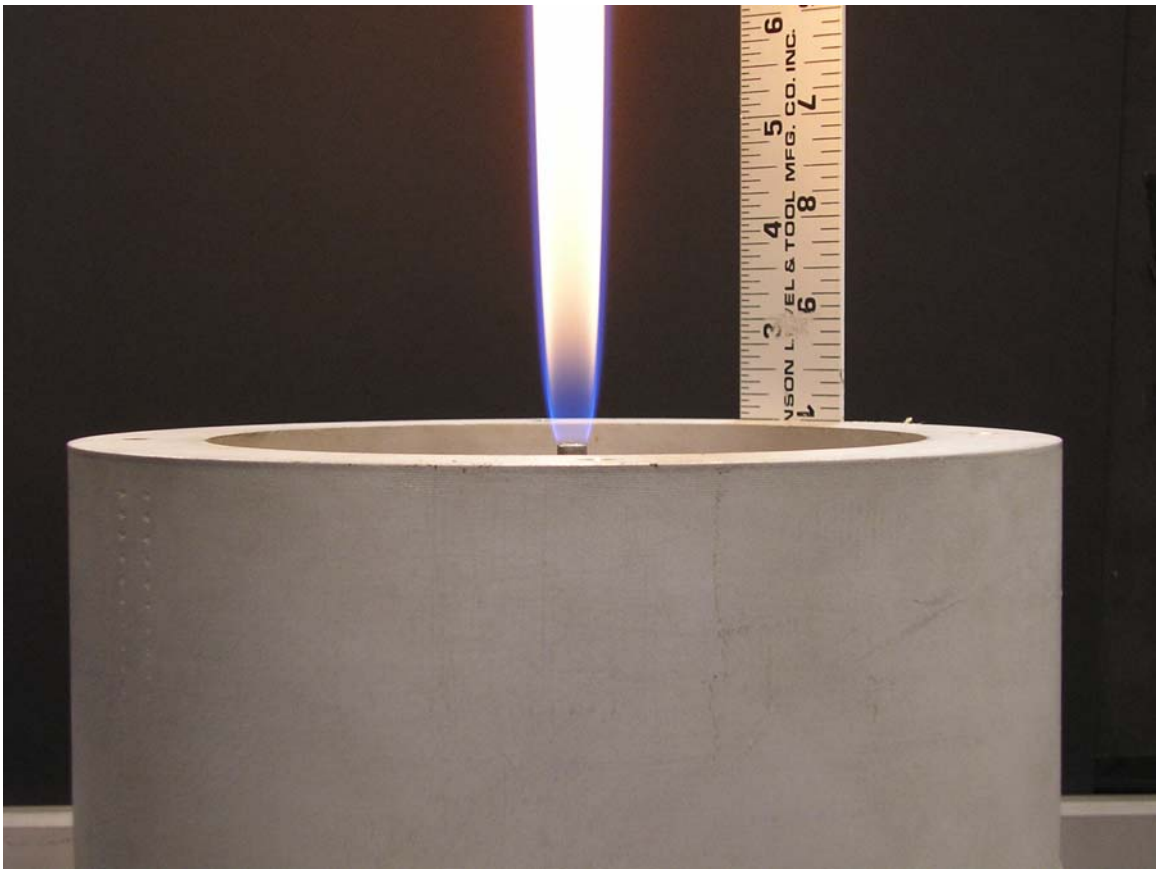

Figure 2.9 – Methane Fuel, Large Nozzle, Co-flow=0.30 m/s, Attached Flame

The appearance of the flame is almost unchanged from the zero co-flow case in Figure 2.6. The flame base is characterized by a blue flame and the orange soot luminescent region begins just above the burner. As for the zero co-flow case, increasing the fuel velocity gradually results in a longer flame. Near the lift-off velocity, the flame structure begins to flicker and lift-off occurs.

Figure 2.10 shows a lifted flame at the same co-flow conditions as Figure 2.9. Note the absence of orange luminescence. The flame base becomes much broader and the length of the flame shortens. Here, the lift-off height is about two inches and premixing of fuel and air is significantly more than for the zero co-flow case. The differences between this case (moderate co-flow) and the zero co-flow case are considerable.

Reducing the fuel velocity to near the reattachment velocity, results in the flame pictured in Figure 2.11. This flame appears more like a combination of the attached and lifted flames from the previous two figures. The flame is mostly blue, indicative of significant premixing – however orange begins to appears as the fuel velocity is reduced. The flame base is not as broad as for the previous case and the flame takes on an overall shape more like the attached flame. The lifted height is reduced in this picture to about one inch.

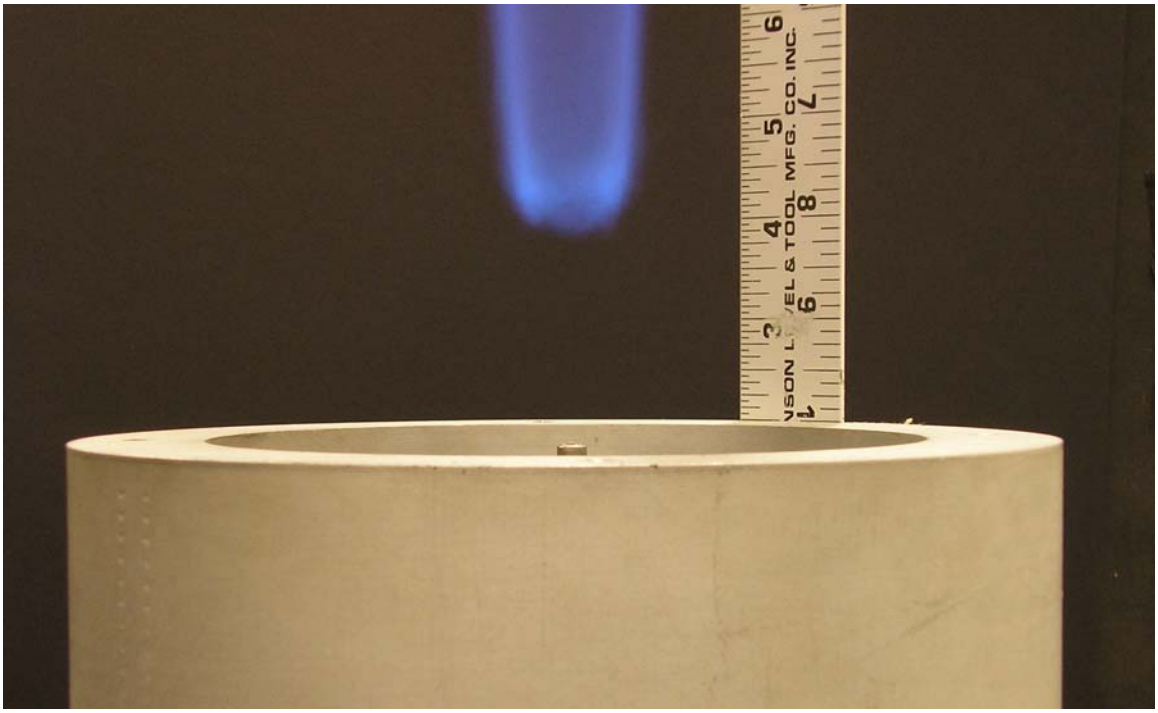

Figure 2.10 – Methane Fuel, Large Nozzle, Co-flow=0.30m/s, Lifted Flame

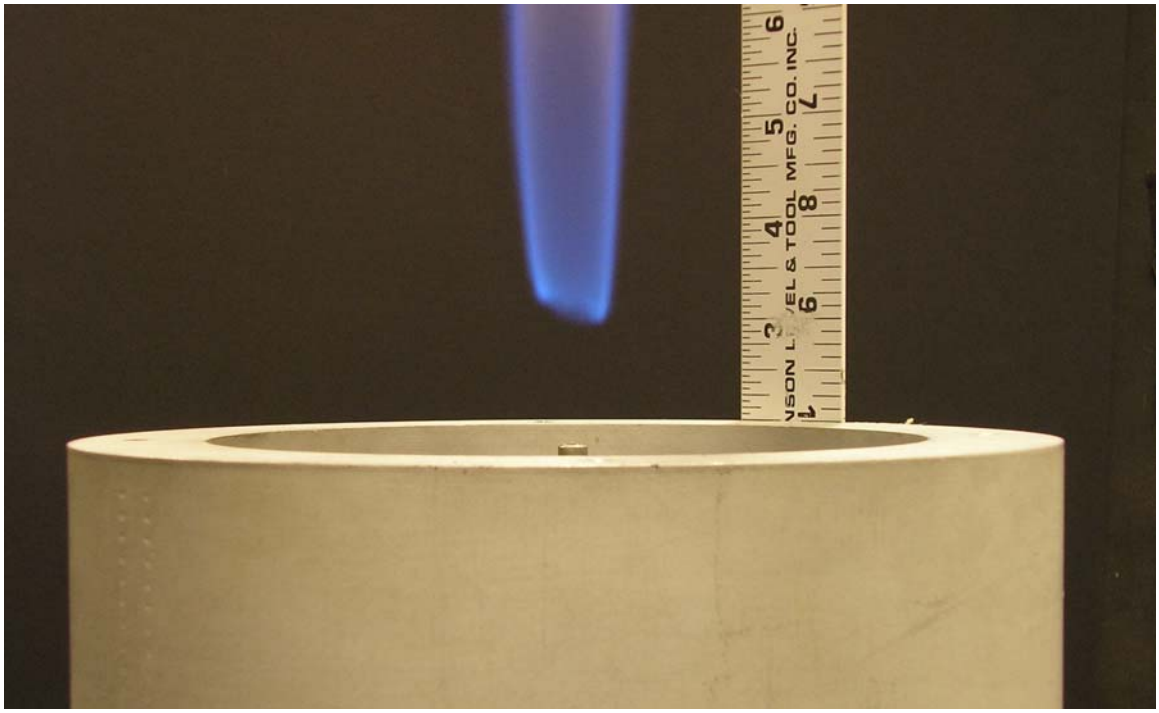

Figure 2.11 – Methane Fuel, Large Nozzle, Co-flow=0.30m/s, Hysteresis

When a relatively high co-flow (about 0.72 m/s) is applied to the flame, the unexpected phenomenon of the flame lifting as the fuel velocity is decreased becomes pronounced. Figure 2.12 shows the attached flame with a co-flow of 0.72 m/s. It again does not appear significantly different than the flames for the zero and moderate co-flow cases.

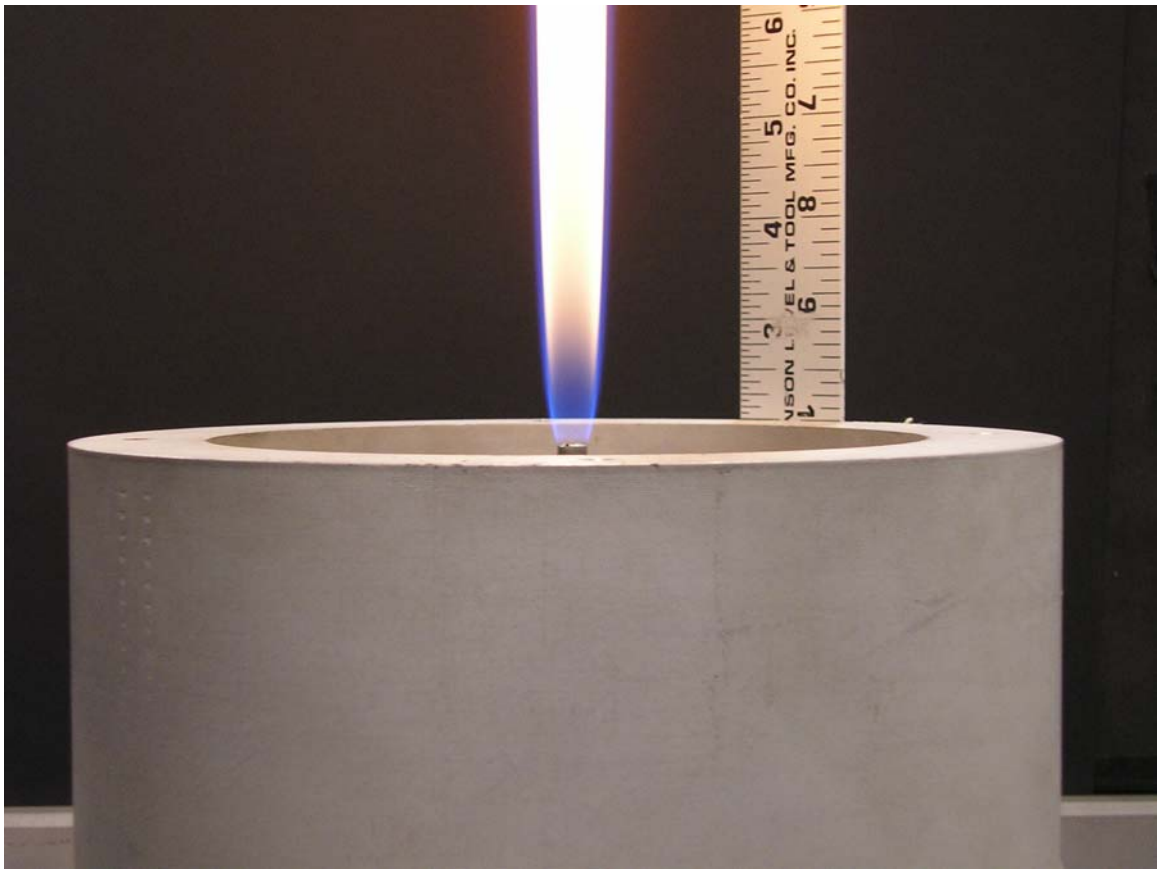

Figure 2.12 – Methane Fuel, Large Nozzle, Co-flow=0.72m/s, Attached Flame

As the flame lifts, the classic flame brush structure becomes apparent, as seen in Figure 2.13. The lift-off height for this case is in excess of 4.5 inches (11.5 cm) and the chemical reactions do not occur at one distinct height above the burner, but rather in a zone. Premixing is very significant and there is almost no orange flame. The flame brush is definitely turbulent and without any formal structure. This is different from the moderate co-flow case, in which the basic structure of a flame could be seen.

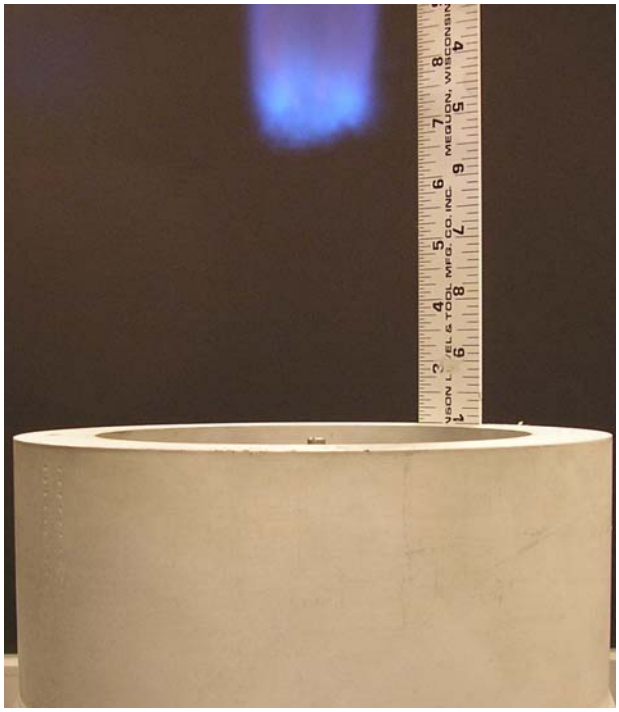

Figure 2.13 – Methane Fuel, Large Nozzle, Co-flow=0.72 m/s, Lifted Flame

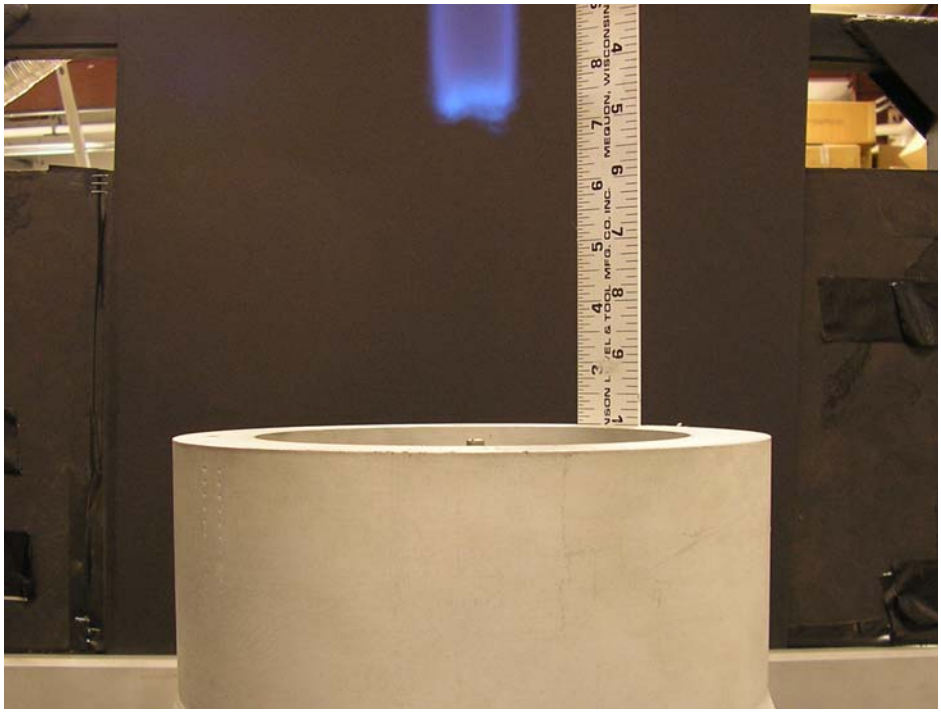

Figure 2.14 – Methane Fuel, Large Nozzle, Co-flow=0.72m/s, Hysteresis

Figure 2.14 shows the hysteresis case with high co-flow. The same flame brush shape can be seen as in the previous figure, but the structure above the brush appears to be transitioning to look more like the moderate co-flow case. The flame base is narrower and the brush thickness is much smaller – indicative of the diminished fuel supply at lower nozzle velocities. The lifted flame height here is about five inches, just a bit more than for the previous case.

Methane flame with the large (4 mm) nozzle show four different flame regimes. For low nozzle velocities, the flame is attached and visually does not vary as co-flow is increased. For lifted flames, the flame structure depends in part on the co-flow velocity and

in part on how close to the fuel velocity is to the reattachment velocity. For low co-flows, the flame is lifted only a fraction of an inch and behaves as an edge flame.

For moderate co-flows, the lift-off height is greater and the flame takes on a different structure. The basic shape of the attached flame is apparent, but the flame is almost completely blue in color and the flame is broader. As fuel velocity is reduced, the flame transitions to appear more like the attached flame, until it actually does reattach to the burner.

At high co-flows, the lifted flame appears more as a brush, with a reaction zone rather than a distinct flame base. The base is very broad and the lift-off height can exceed 4 inches. As the fuel velocity is reduced, the flame base becomes more narrow, the thickness of the flame brush smaller, and the region above the brush tends to transition to look more like the same region of a moderate co-flow lifted flame.

2.4.2 Small Nozzle and Methane Fuel

The results for the small nozzle with methane fuel are similar to those with the large nozzle, except with a notable exception. For the large nozzle, the flame can stabilize at low co-flows with lifted flame height of 1/4 – 1 inches (1 - 2.5 cm). All of the lifted flames for the smaller nozzle are in excess of one inch (2.5 cm). Figures 2.15 to 2.19 show results for low co-flow and high co-flow cases.

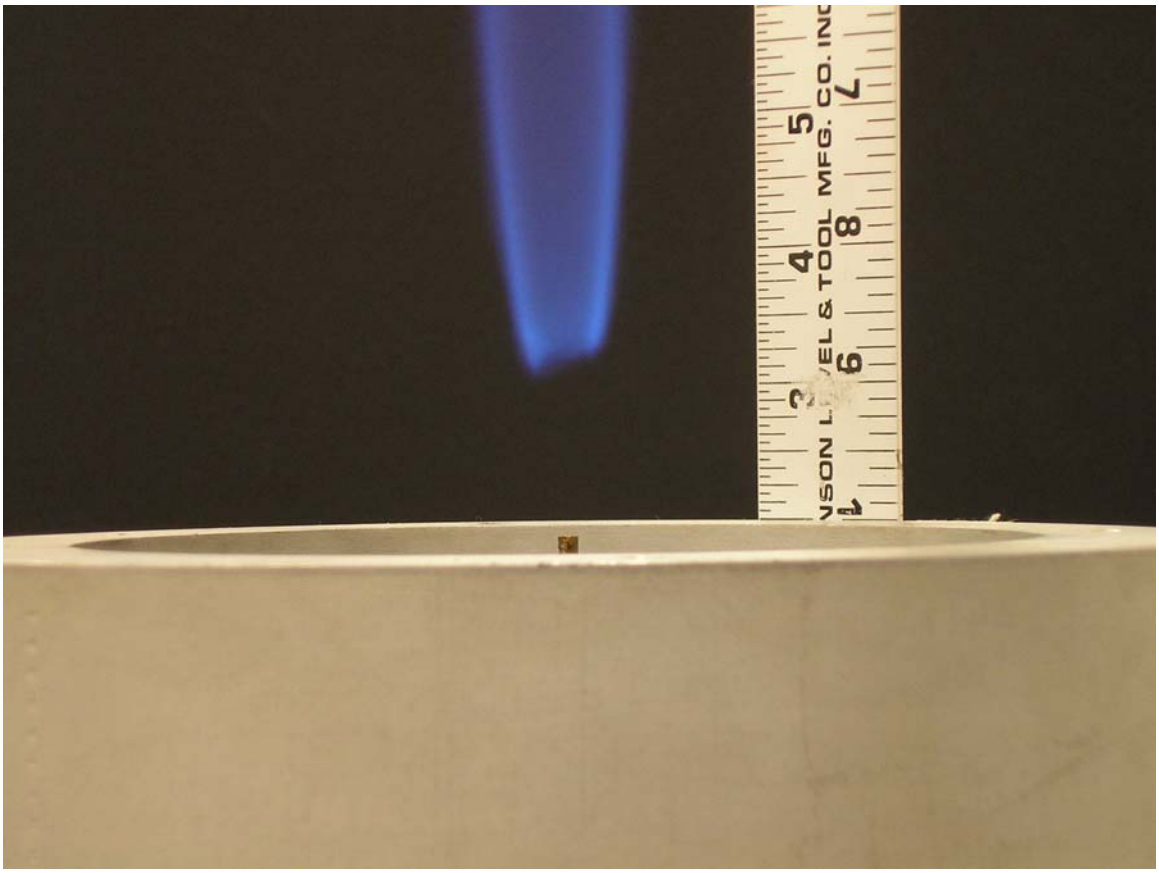

Figure 2.15 – Methane Fuel, Small Nozzle, No Co-flow, Lifted Flame

In Figure 2.15, a lifted flame with the small nozzle is shown. The lift-off height is about one inch. The flame is similar in structure to one produced by the large nozzle with moderate co-flow. The flame is almost completely blue with no indication of a flame brush. The flame base is broader than for the attached flame. Premixing is significant.

Figure 2.16 shows a flame in the hysteresis regime near reattachment. It is virtually identical to the flame in the previous figure. Flame heights, structure, and shape are unchanged.

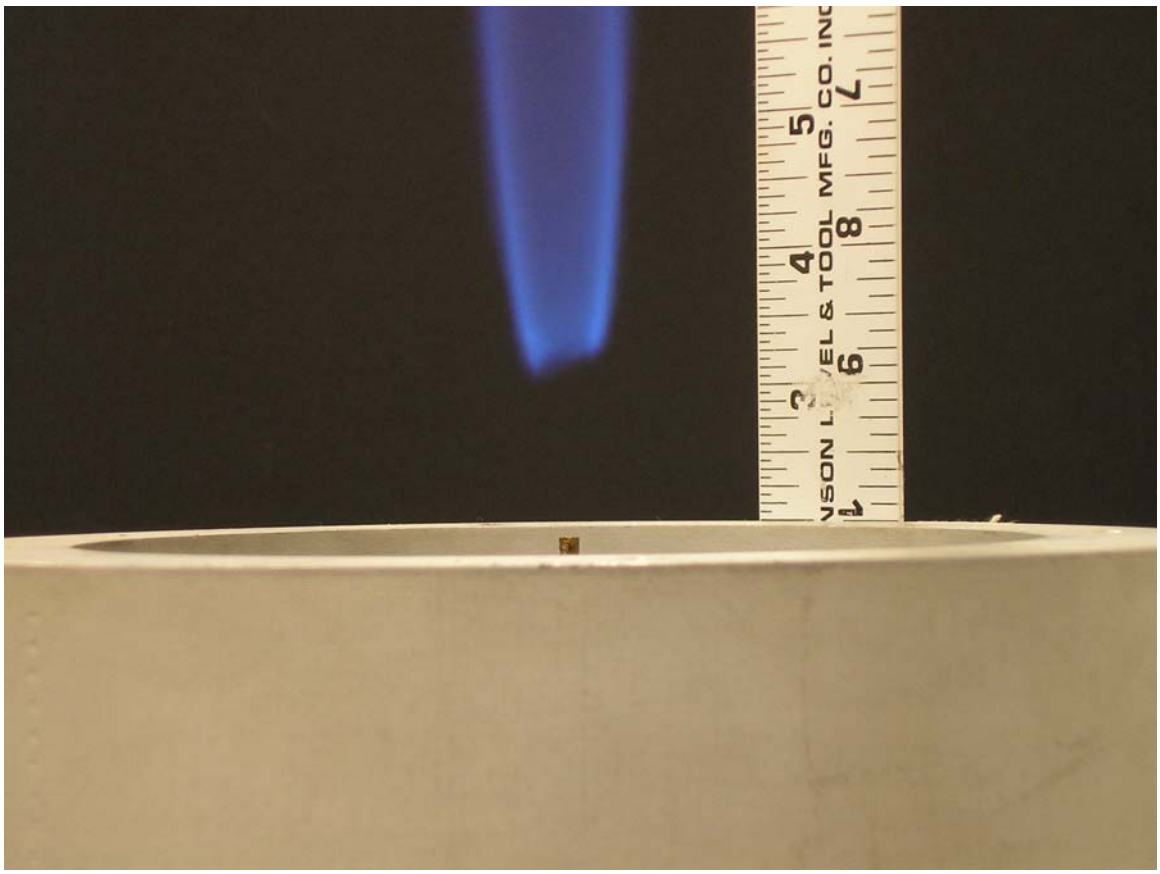

Figure 2.16 – Methane Fuel, Small Nozzle, No Co-flow, Hysteresis

Figure 2.17 shows an attached flame when there is a moderate 0.33 m/s co-flow. The attached flame is similar in structure to those for the large nozzle, except smaller. The flame base is blue and the trailing flame is orange.

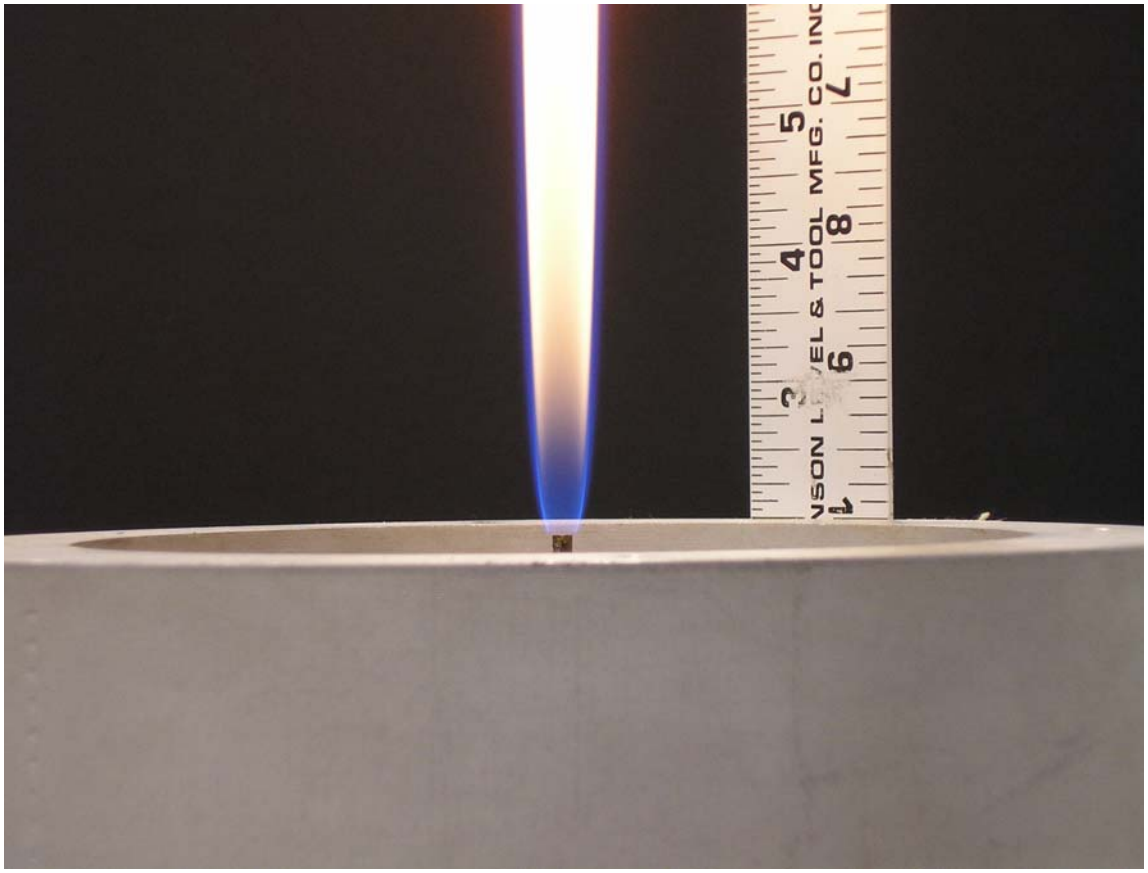

Figure 2.17 – Methane Fuel, Small Nozzle, Co-flow=0.33m/s, Attached Flame

Figure 2.18 shows a lifted flame for the 0.33 m/s co-flow case. Apparent are the beginnings of a flame brush structure, as for the high co-flow case with the large nozzle. The trailing flame above the brush does have small amounts of red and orange, just as for the large nozzle cases. The lift-off height is in excess of two inches.

Decreasing the fuel velocity to near the reattachment velocity results in the flame shown in Figure 2.19 below. The structure of the flame is mostly unchanged, but the flame base is smaller and lift-off height larger (about 3.5 inches).

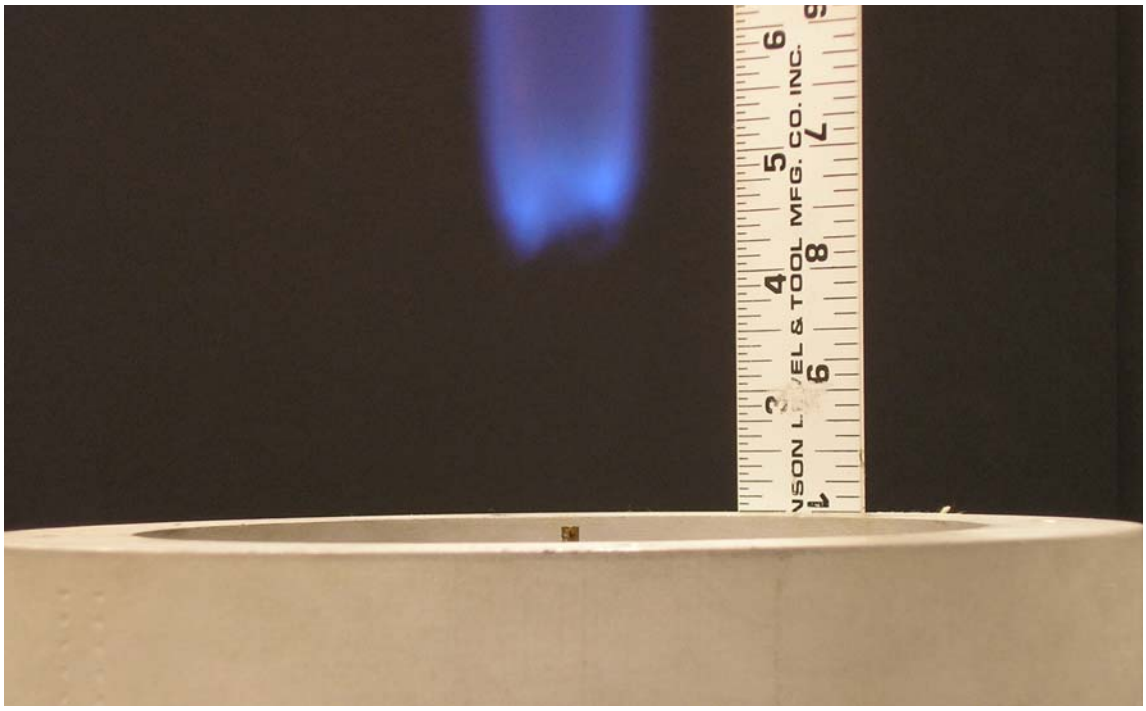

Figure 2.18 – Methane Fuel, Small Nozzle, Co-flow=0.33m/s, Lifted Flame

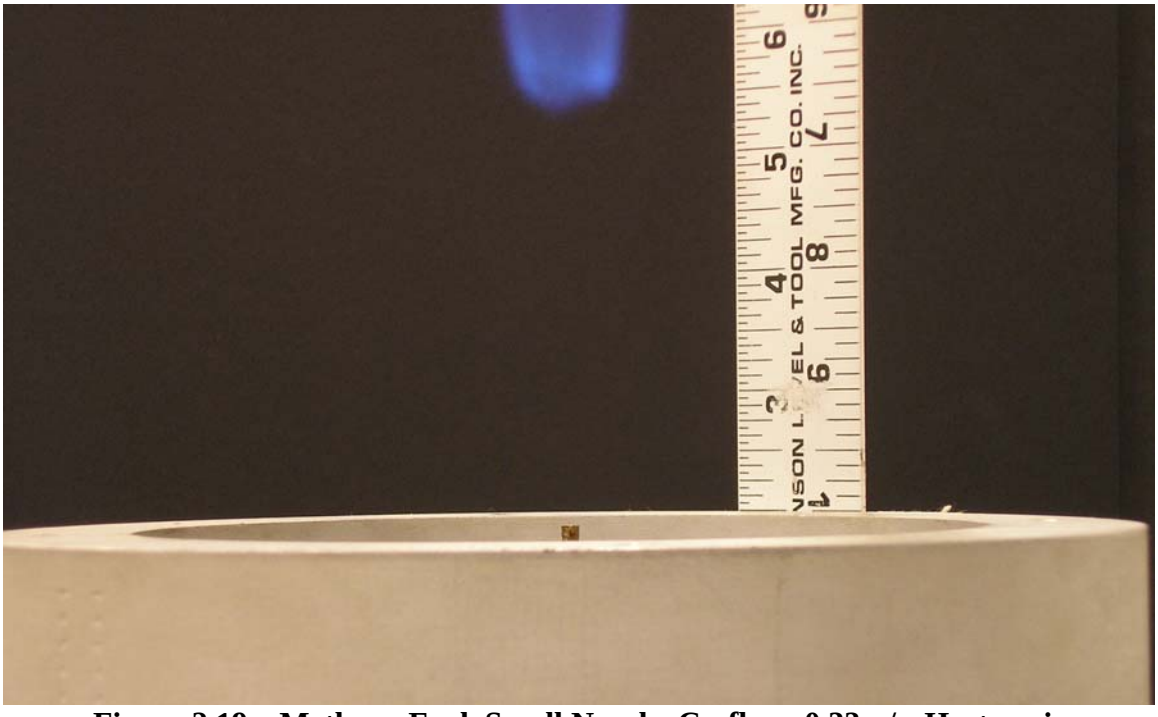

Figure 2.19 – Methane Fuel, Small Nozzle, Co-flow=0.33m/s, Hysteresis

2.4.3 Ethylene Fuel, Small Nozzle

Ethylene fuel burns brighter and produces more soot. The behavior of ethylene is similar to that of methane, except the range of fuel and co-flow velocities differ. Figure 2.20 shows an attached ethylene flame with no co-flow.

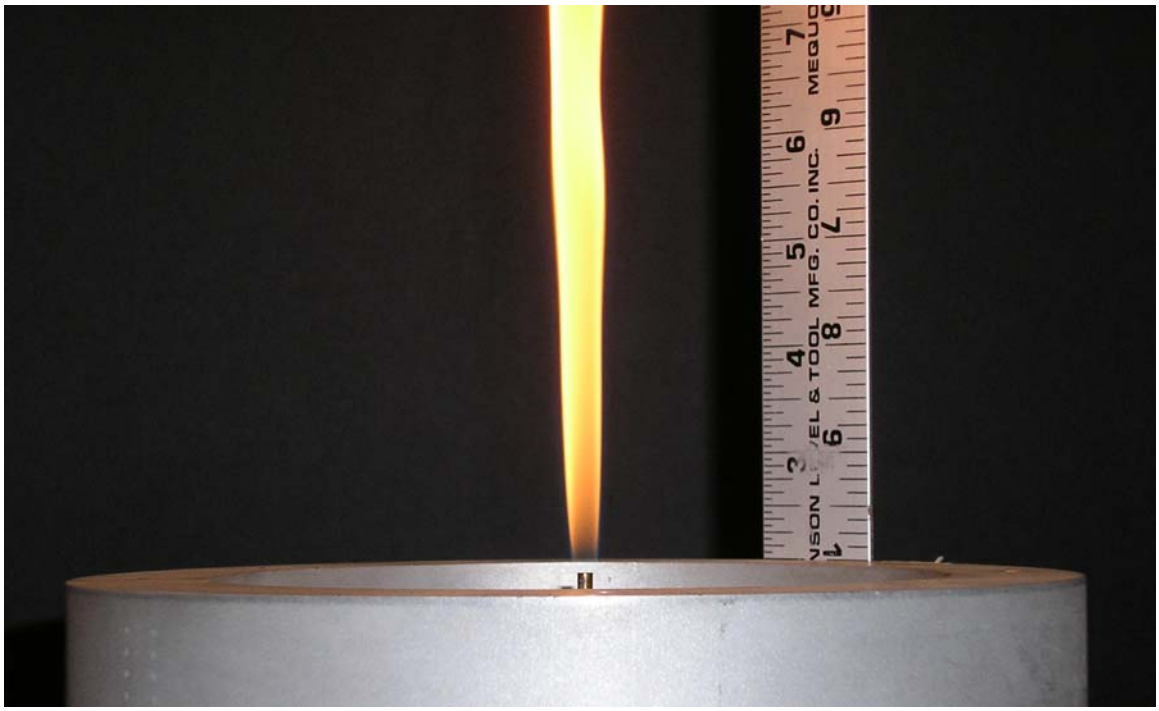

Figure 2.20 – Ethylene Fuel, Small Nozzle, No Co-flow, Attached Flame

The flame is much more orange than a methane flame. This is due to soot luminescence. At higher fuel flow, the flame appears more like a methane flame – with a blue flame base. This is shown for an attached flame near lift-off in Figure 2.21 below. For flames of ethylene the bright flame obscures some of the visible features in the photograph.

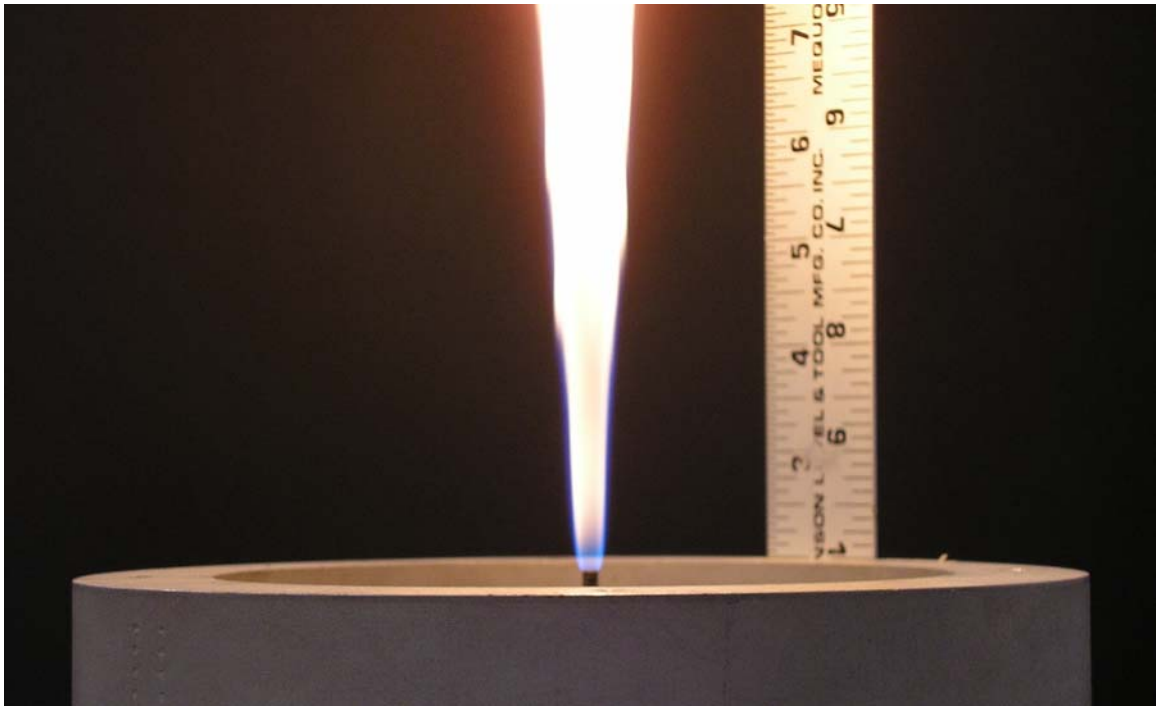

Figure 2.21 – Ethylene Fuel, Small Nozzle, No Co-flow, Attached Flame Near Lift-off

A lifted flame appears much as the methane lifted flames, as seen in Figure 2.22. Again, the brightness of the orange part of the flame obscures some of the blue parts of the flame. The lift-off height for low co-flows is typically less than an inch. As the fuel velocity is decreased, through the hysteresis regime, the flame moves closer to the burner, until finally reattaching. Figure 2.23 show the flame in the hysteresis regime, just prior to reattachment. Flame structure and behavior are similar between the lifted case and the hysteresis case.

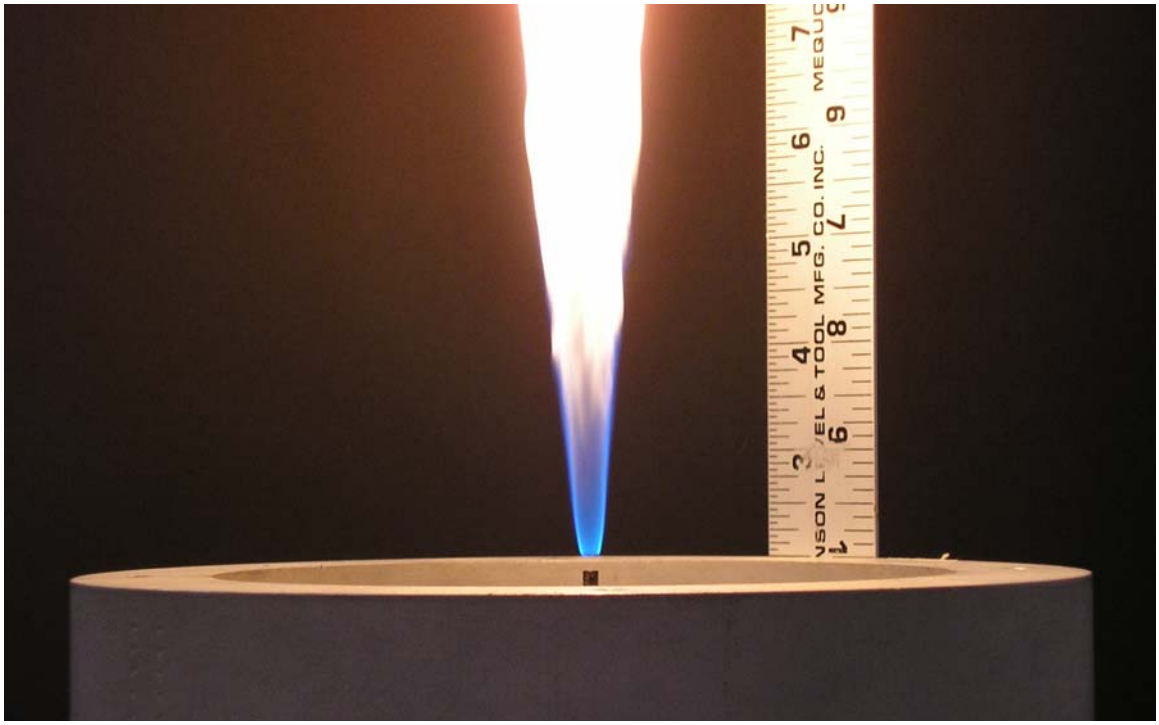

Figure 2.22 – Ethylene Fuel, Small Nozzle, No Co-flow, Lifted Flame

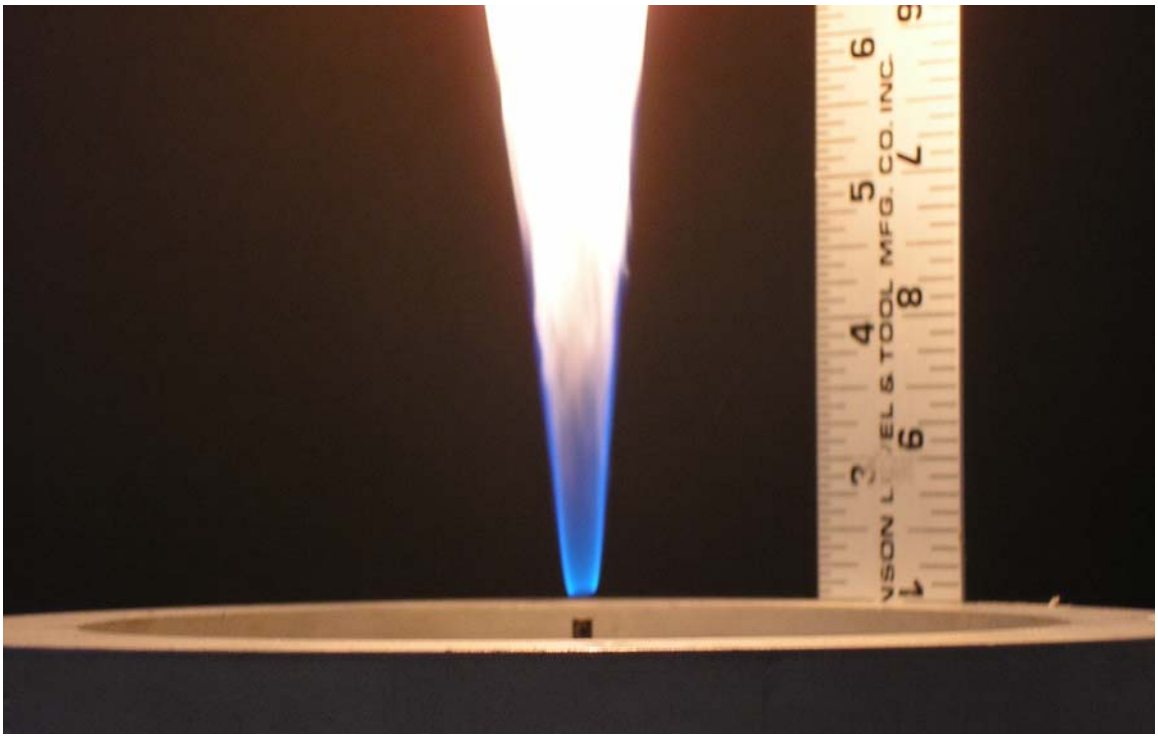

Figure 2.23 – Ethylene Fuel, Small Nozzle, No Co-flow, Hysteresis

With the addition of moderate co-flow (0.24 m/s), the structure and behavior of the flame is similar. Figures 2.24 – 2.26 show an attached flame, a lifted flame, and a flame in the hysteresis regime.

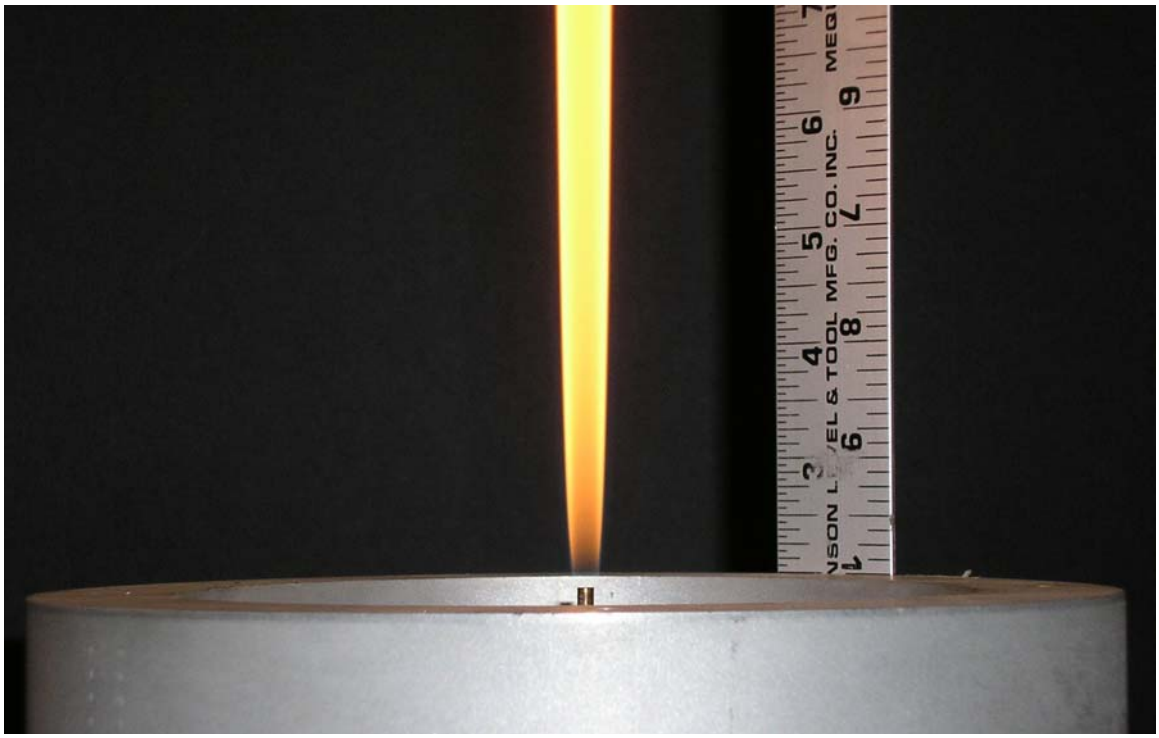

Figure 2.24 – Ethylene Flame, Small Nozzle, Co-flow=0.24m/s, Attached Flame

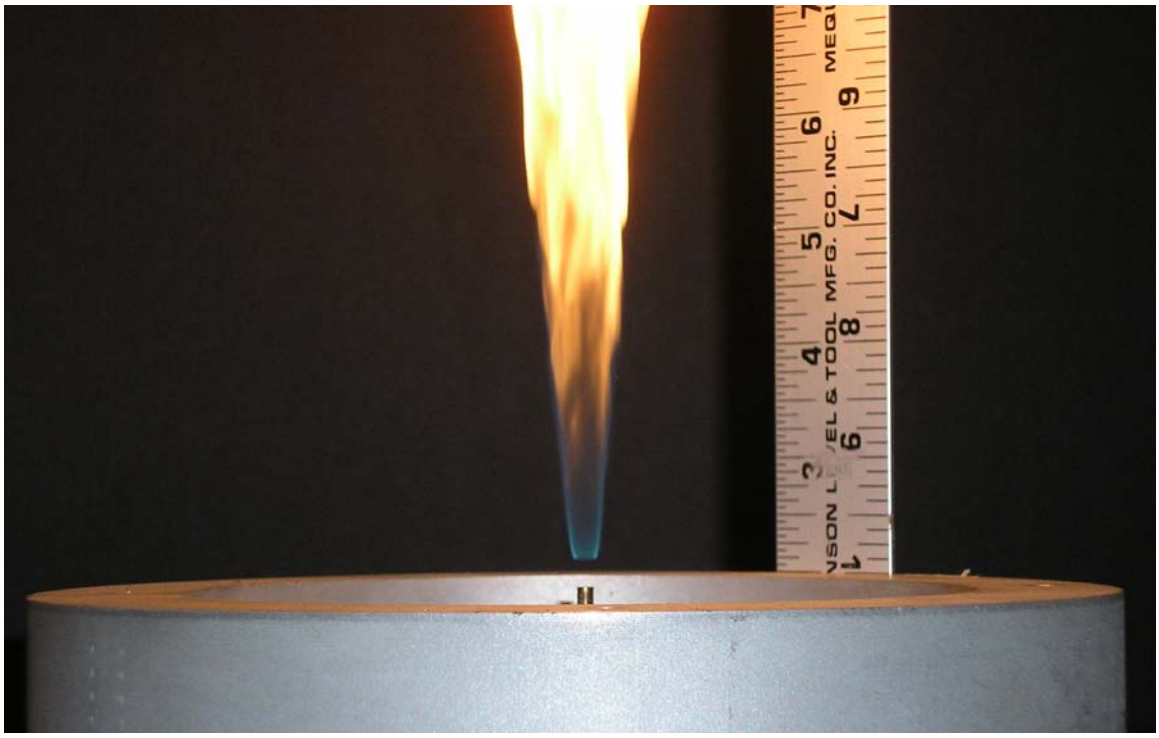

Figure 2.25 – Ethylene Flame, Small Nozzle, Co-flow=0.24m/s, Lifted Flame

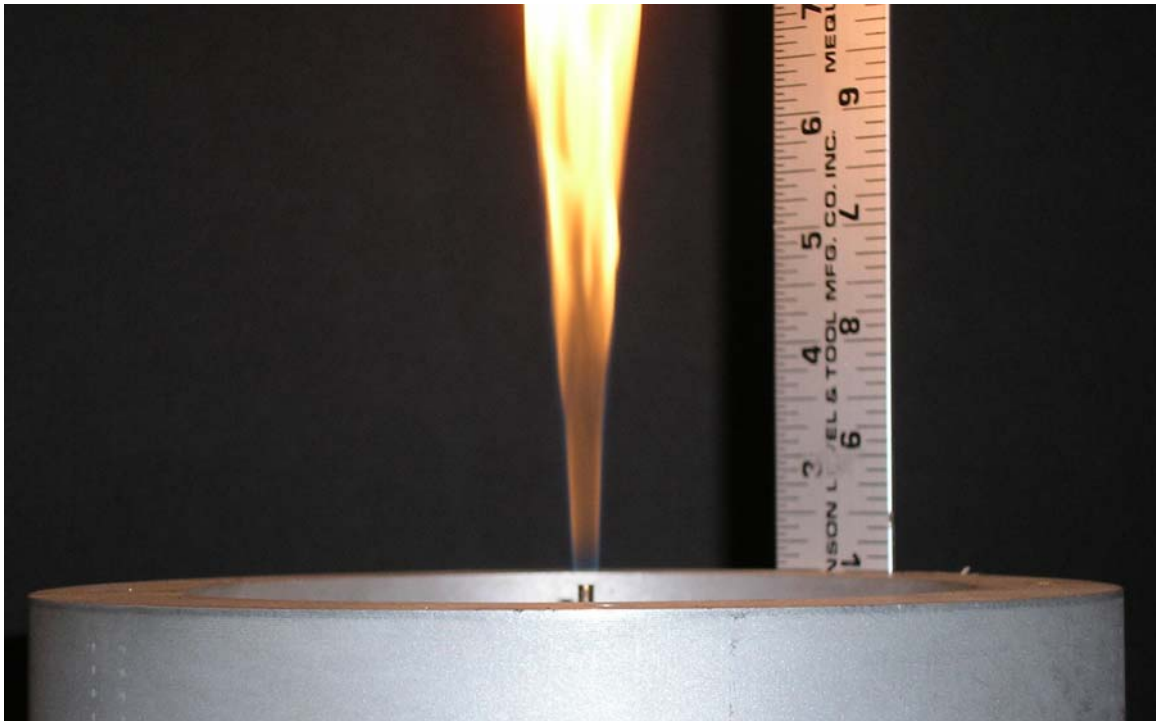

Figure 2.26 – Ethylene Fuel, Small Nozzle, Co-flow=0.24m/s, Hysteresis

At high co-flow (1.6 m/s) the behavior changes. As for methane, the flame will initially move towards the nozzle as the fuel velocity is decreased. Near the reattachment velocity, the flame height will begin to increase, becoming a maximum at the reattachment velocity. Figure 2.27 shows an attached flame at high co-flow.

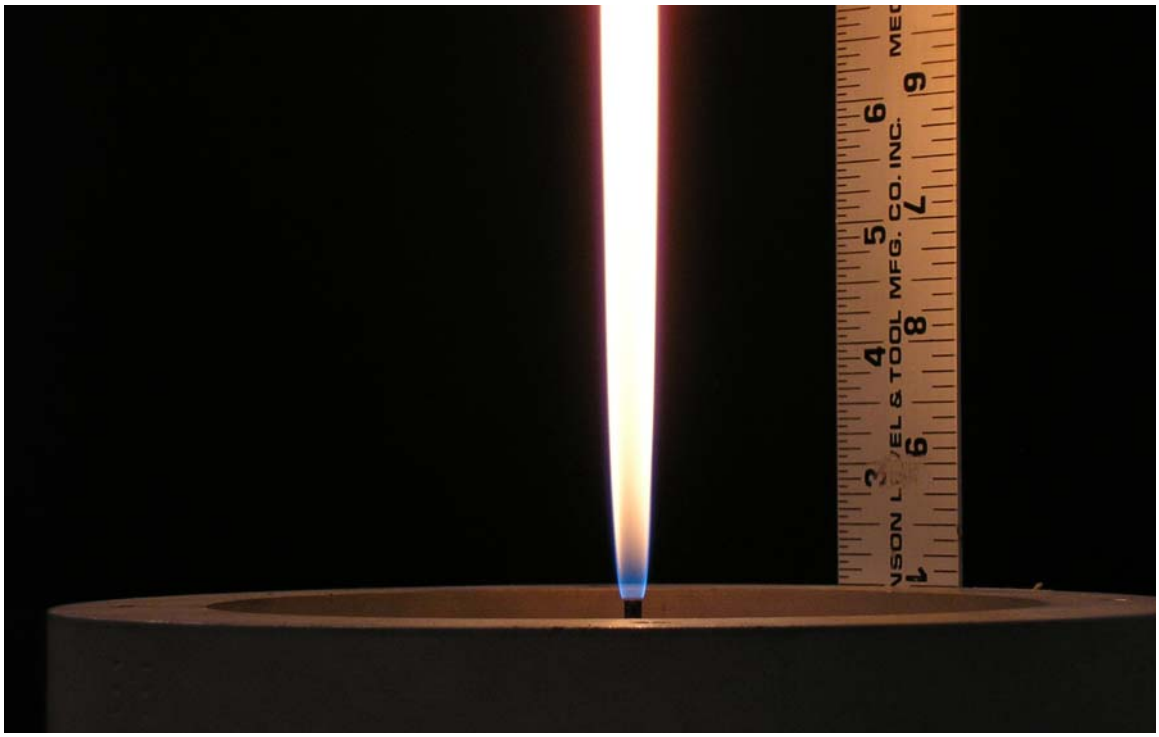

Figure 2.27 – Ethylene Fuel, Small Nozzle, Co-flow=1.63m/s, Attached

Figures 2.28 – 2.29 show a lifted flame and a flame in the hysteresis regime near reattachment. The lifted flame height is about two inches, while the lifted height of the flame just prior to reattachment is two inches. The bases of the flames are distinctly blue and transitioning to a flame brush.

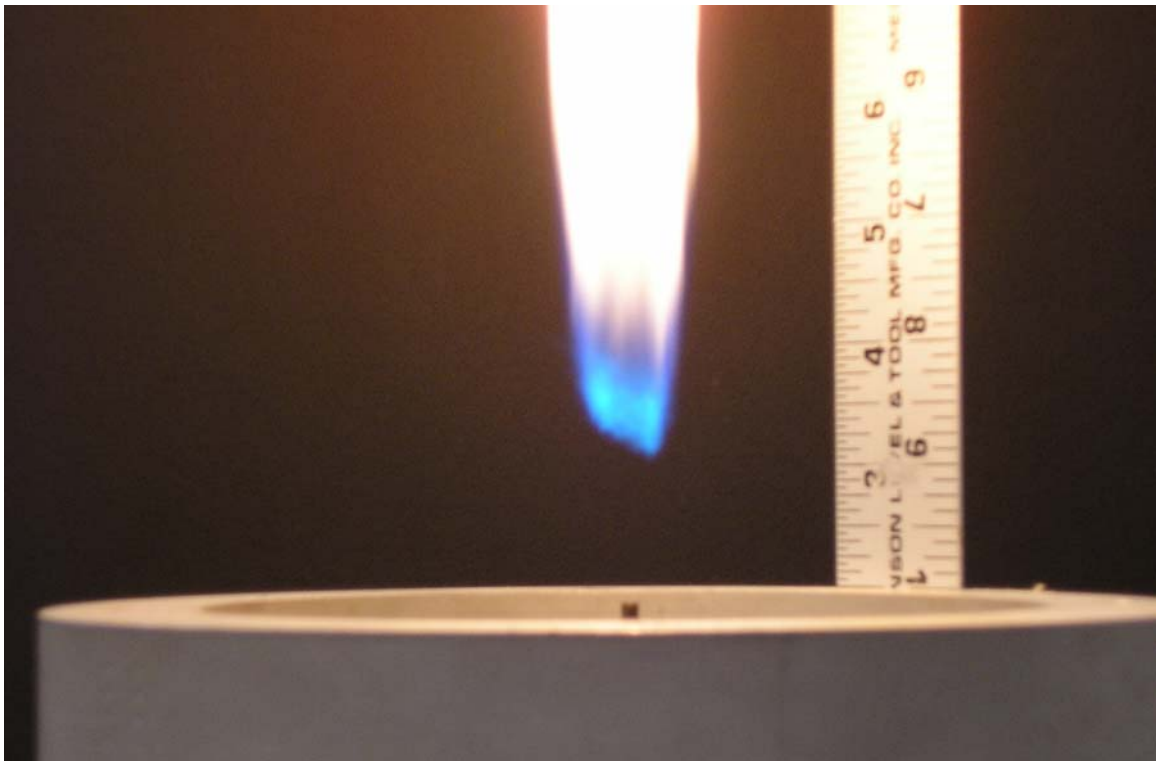

Figure 2.28 – Ethylene Fuel, Small Nozzle, Co-Flow=1.63m/s, Lifted Flame

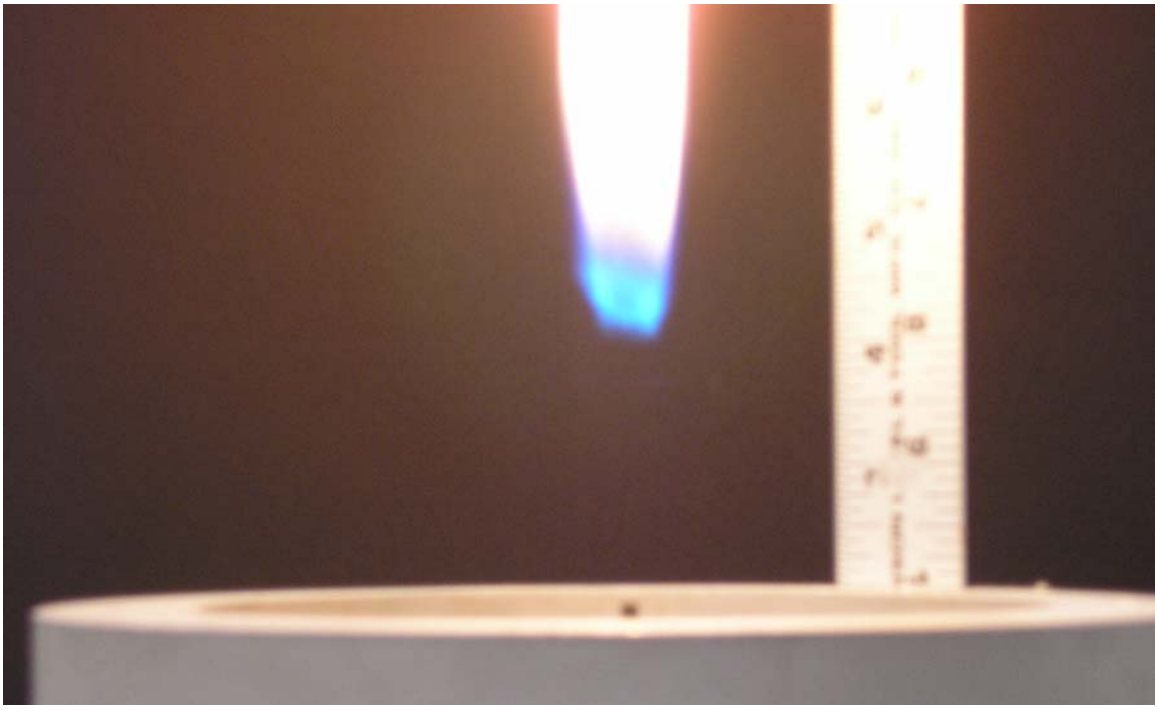

Figure 2.29 – Ethylene Fuel, Small Nozzle, Co-Flow=1.63m/s, Hysteresis

3. Analysis of Lift-off Heights, Lift-off Velocity, and Reattachment Velocity

3.1 Lift-off Heights

3.1.1 General Observations

Analyzing the raw data in Tables 2.1-2.4 and Figures 2.2-2.6, several interesting phenomena can be seen in the data. In many cases, as expected, as fuel velocity is decreased the flame lift-off height decreases – until some minimum nozzle velocity is achieved and the flame spontaneously reattaches. This behavior has been noted by many researchers, beginning with Scholefield and Garside in 1949 [1]. Prior to reattachment, the flame can be made to reattach by passing a hand near the flow so as to disrupt the flow patterns. Likewise, an attached flame with nozzle velocity in the hysteresis regime can be made to lift by simply blowing gently on the flame.

For nozzle velocities in the hysteresis regime, igniting the flame well above the lift-off height will cause a lifted flame to occur. Igniting the flame near the burner nozzle will cause an attached flame to occur. Therefore the location of the ignition has a significant effect on flame location. For most of the flames in this study, lift-off was achieved by starting with an attached flame with fuel velocity well below lift-off and reattachment nozzle velocities. The fuel velocity is increased gradually until lift-off occurs and then reduced until reattachment occurs.

When a small annular co-flow is applied, the same basic behavior occurs, but the magnitude of the velocities at which lift-off and reattachment occur change. Even when a barely detectable co-flow of 0.05 m/s is used, there is a definite change in behavior.

For some combinations of nozzle sizes and co-flow, the flame behavior changes as the fuel velocity is decreased towards to the reattachment velocity. After initially decreasing, the flame lift-off height unexpectedly increases as the fuel velocity is decreased. This phenomenon can be explained by the flame seeking out positions with favorable stoichiometric conditions. This is discussed in Chapter 4.

3.1.2 *Methane Fuel, Large Nozzle*

The results for methane fuel and the large nozzle are given in Table 2.1 and Figure 2.2. Co-flows between zero and 0.72 m/s were analyzed and lift-off heights throughout the hysteresis regime plotted. For relatively low co-flows, the flame height decreases gradually as the fuel velocity is decreased. This is in agreement with others who have noted behavior in the hysteresis regime [14, 15, 17]. At some much lower fuel velocity, the flame spontaneously reattaches to the burner and will not lift back off, until the fuel velocity is increased to the previous lift-off velocity.

At higher co-flow velocities, the flame lift-off height initially decreases, reaches a minimum, and then the flame lift-off height increases – even though the fuel nozzle velocity continues to decrease. This is contrary to what happens outside of the hysteresis regime and will be a point revisited later in this work. The maximum flame height, which is achieved just prior to reattachment, increases as the co-flow increases. Also, the size of the dip in flame heights with co-flow decreases as the co-flow increases, suggesting that that co-flow has a larger effect over flame height and the decrease in fuel nozzle velocity a lesser effect.

At some lower nozzle velocity, the flame spontaneously burns down to the nozzle and the flame reattaches to the burner. This transition occurs similarly to an ignition event that occurs well above the nozzle. It is not instantaneous, but occurs over the course of a few seconds. As for low co-flow velocities, the flame can be lifted from an attached condition by blowing gently and made to reattach by moving a hand near the flame. The reattachment velocity steadily decreases as the co-flow velocity is increased, becoming less than half of the value at zero co-flow.

What is immediately evident is that lift-off height is not linearly related to nozzle velocity. Kalghatgi [2] predicted a linear relationship between nozzle velocity and lift-off height for flames outside of the hysteresis regime (i.e., for nozzle velocities above the lift-off velocity). Instead, a new relation is needed, taking into consideration the location of the stoichiometric point and the jet velocity at the flame base to predict lift-off height.

3.1.3 Methane Fuel, Small Nozzle

The plot of flame height to nozzle velocity for the small nozzle is similar to that of the large nozzle. However, several differences become apparent. First, the flame lift-off heights for the small nozzle are actually much larger for lower nozzle velocity. This is a point that will be revisited in Chapter 4. The range of stable co-flows is much smaller for the small nozzle. Co-flows above 0.55 m/s were not attainable, compared to a maximum of about 0.72 m/s for the large nozzle. The tendency for the flame to simply decrease in height until reattachment is also only seen for the zero co-flow case. Even for a co-flow of 0.13 m/s the lift-off height was found to increase slightly as the fuel velocity is decreased. Therefore

this phenomenon is proposed to be related to nozzle size, as well as the magnitude of the co-flow velocity.

The nozzle velocity required for lift-off is much smaller for the smaller nozzle, usually about half of the value as for the larger nozzle. However, the reattachment velocities are relatively constant and on the same order as for the larger nozzle. This reinforces the notion that lift-off and reattachment are governed by different physics, as proposed by Gollahalli [15].

3.1.4 Ethylene Fuel, Large Nozzle

Many of the same trends seen with methane flames are also seen with ethylene fuel. The main differences between methane and ethylene is the higher burning velocity (0.70 m/s versus 0.40 m/s for methane) and the Schmidt number (about 0.7 for methane and about 0.8 for ethylene). It is believed that the burning velocity plays a significant role in flame behavior, as will be discussed below.

At low and moderate co-flows, the lift-off heights are small – typically less than an inch – and the flame lift-off height decreases as the fuel velocity is decreased. At some much lower fuel velocity, the flame will spontaneously reattach. This is similar to the behavior of methane with a low co-flow.

Only at extreme co-flow (greater than about 1.5 m/s), does this behavior change. When a co-flow of 1.6 or 1.7 m/s is applied, the flame lift-off height will initially decrease, then it dramatically increases until reattachment.

3.1.5 Ethylene Fuel, Small Nozzle

The results for ethylene fuel and the small nozzle are presented in Figure 2.5. Lift-off heights are small, typically less than ¾ inches. For all of the cases analyzed, the lift-off heights decrease as the fuel flow is decreased, as it does for the large nozzle case. Co-flow definitely affects lift-off heights. The no co-flow lifted flame height at lift-off is 0.2 inches (0.5 cm), while it is three times that value when a 0.6 m/s co-flow is applied. The lift-off velocity is not greatly affected by co-flow, although it is reduced as co-flow is increased.

The reattachment velocity is greatly affected by co-flow. For the no co-flow case, the reattachment velocity is about 35 m/s. When a 0.46 m/s co-flow is applied, the reattachment velocity is reduced to about 22 m/s. With a 0.6 m/s co-flow the reattachment velocity is 18 m/s.

3.1.6 Propane Fuel

Limited data using propane and the small nozzle was collected. Lift-off heights are small, similar to ethylene. The size of the hysteresis regime is small, typically only a few gradations on the flow meter. At a co-flow of 0.31 m/s, the lift-off and reattachment velocities were almost identical. The lifted flame heights also did not change significantly in the hysteresis regime. Co-flows above 0.31 m/s were not attainable. Since only a few data points were collected, this work will not consider propane fuel to any great extent.

3.1.7 Effect of Co-flow on Lift-off Heights

The noticeable effect on a flame of even the smallest of co-flows has been attributed by some researchers [6] to the relative magnitude of the co-flow when compared to the speed of the jet at the flame base. Such a co-flow (i.e., 0.05 - 0.20 m/s) is almost insignificant when compared to the nozzle velocity – of order 10-30 m/s. It is however very significant when compared to typical local flame speeds of 1 – 1.5 m/s.

For laminar flames, Lee et al. [35] proposed a relation for the flame lift-off height for flames in co-flow. The relation for the non co-flow case [equation 1.24a] is modified by the subtraction of the co-flow from the tribrachial burning velocity (about twice the laminar burning velocity). Such a procedure may be useful for turbulent flames, but the exact formulation has not been determined. An alternative method to handle co-flow was proposed by Montgomery et al. [8]. The procedure involves the computation of an effective nozzle velocity, given as equation (1.5). The effective velocity consists of the nozzle velocity at the nozzle exit, plus the co-flow velocity multiplied by a weighting factor. The weighting factor is a function of the square root of the density ratio of the two fluids and an empirical constant. This method is utilized in this work as part of procedure using jet velocities at the flame base, discussed in Section 4.2.

3.2 Lift-off Velocity

3.2.1 General Observations

The data in Tables 2.1 - 2.4 can be analyzed to determine trends in lift-off and reattachment points, as co-flow varies. Lift-off occurs when the fuel velocity is increased and an initially attached flame spontaneously lifts from the nozzle. As seen by other researchers [6, 15], the fuel velocity required for lift-off varies with the fuel, the amount of dilution of the fuel, the nozzle size, and any co-flow. Figures 3.1-3.5 show the trend of fuel velocity at lift-off as co-flow is varied.

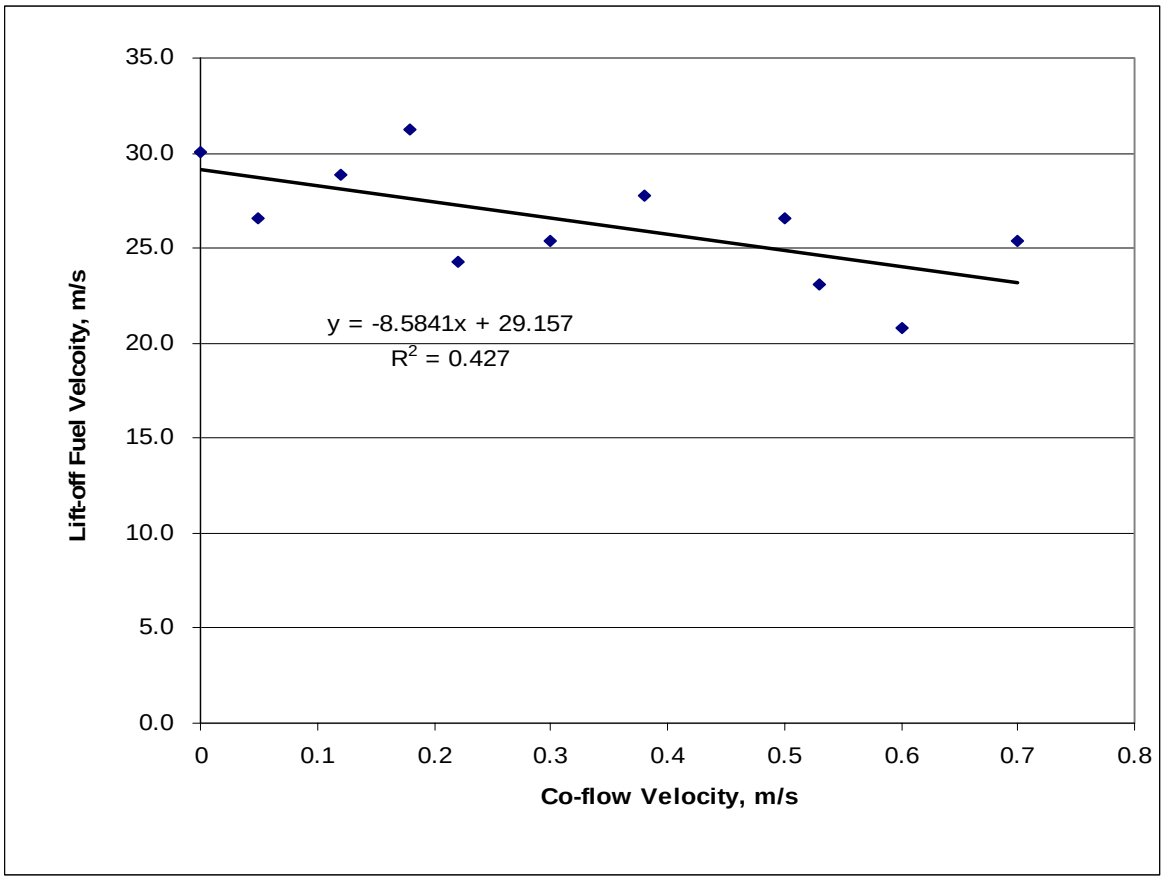

Figure 3.1 – Lift-off Fuel Velocities vs. Co-flow, Large Nozzle, Methane Fuel

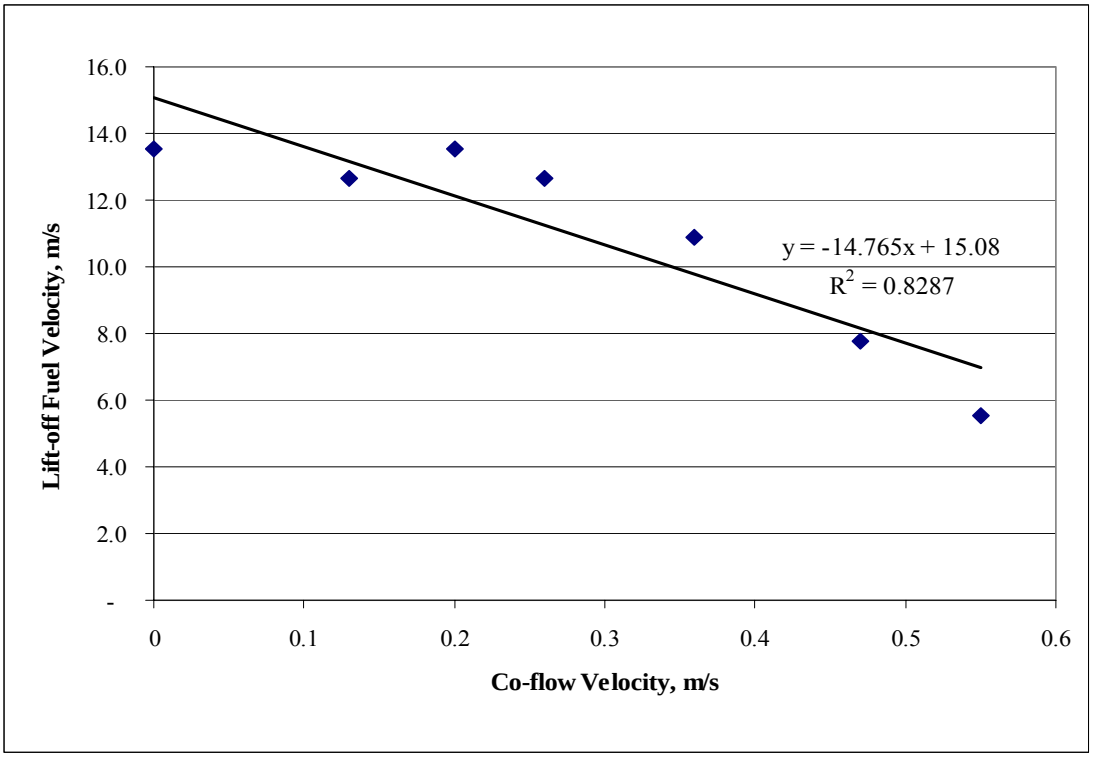

Figure 3.2 – Lift-off Velocity vs. Co-flow, Small Nozzle, Methane Fuel

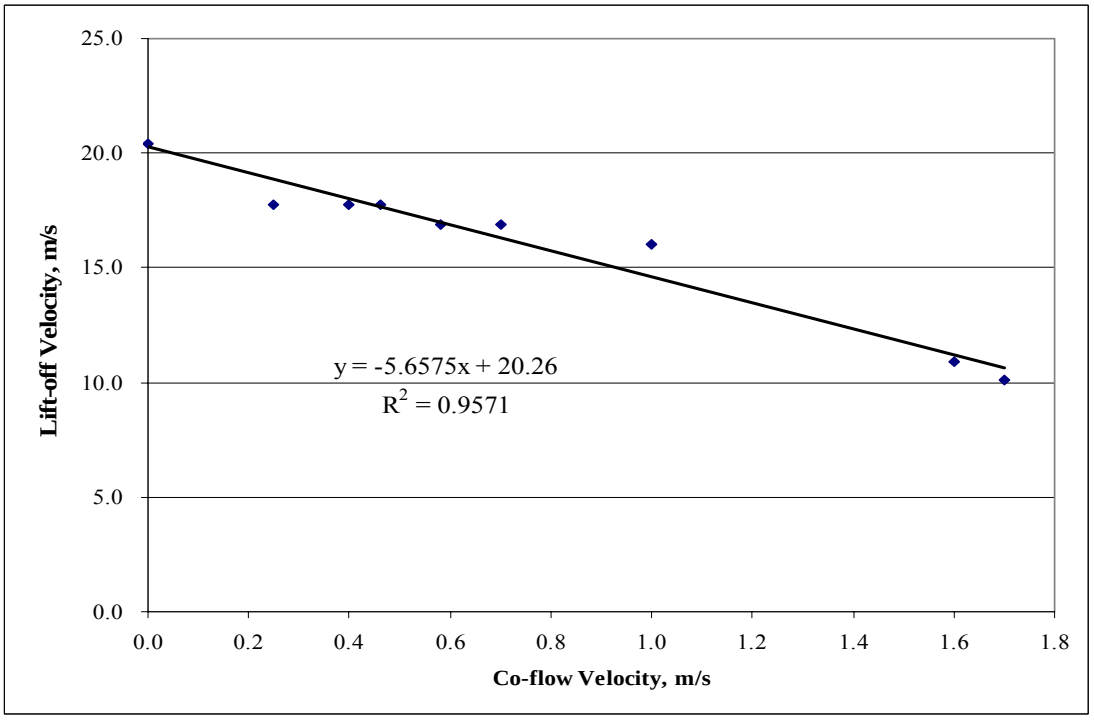

Figure 3.3 – Lift-off Velocity vs. Co-flow, Large Nozzle, Ethylene Fuel

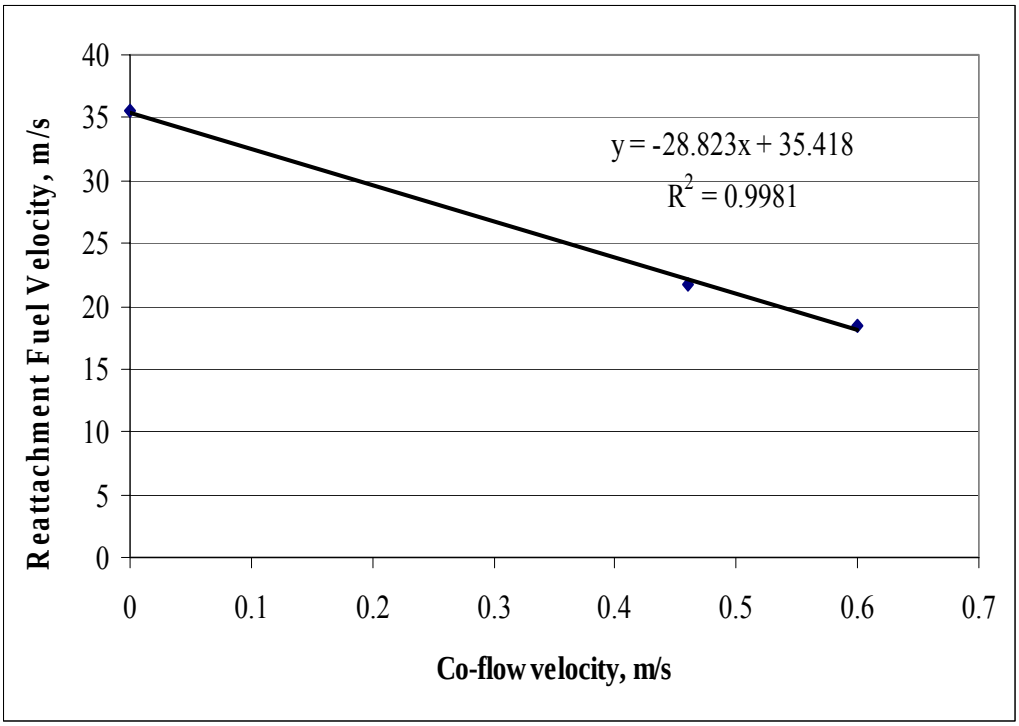

Figure 3.4 – Lift-off Velocity vs. Co-flow, Small Nozzle, Ethylene Fuel

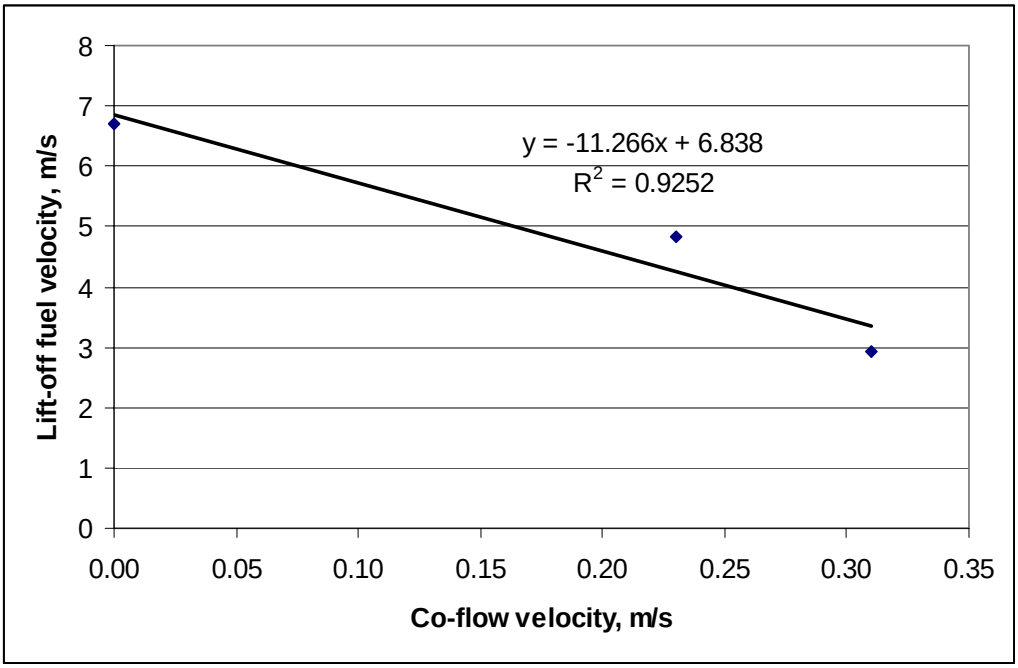

Figure 3.5 – Lift-off Velocity, Small Nozzle, Propane Fuel

The general trend for the plots is for lift-off fuel velocity to decrease as the co-flow is increased. There is definite linear trend to the results, though individual points vary significantly from the trend lines. It also appears that the slope of the line formed by connecting the points is a function of the nozzle diameter. The slope of the line increases proportionally as the nozzle diameter decreases (i.e., the slope is inversely proportional to nozzle diameter). However, without additional nozzle sizes to experiment with, the exact correlation cannot be made with any certainty.

Lift-off is attributed to a complex interaction of heat transfer and flow conditions at the burner tip. At some point, conditions no longer favor a flame being attached and the flame lifts. This analysis will not consider the mechanics of lift-off, except to mention that there is a hysteresis effect in lift-off. When the fuel velocity of an initially lifted flame is reduced to the original lift-off fuel velocity, the flame stays lifted. The flame will remain lifted until the fuel velocity is reduced to a much lower fuel velocity, the reattachment fuel velocity. For a range of fuel velocities, there are two stable points – one lifted and one attached, which constitutes the hysteresis regime.

3.2 Plots of Reattachment Velocity

The reattachment fuel nozzle velocity is also a function of fuel used, nozzle size, and co-flow. It is not, however, a function of dilution in the fuel [15]. Gollahalli instead suggested that reattachment was a function of the large scale structures of the flow. This makes sense, since dilution would not appreciably change these structures. Other parameters, such as heat release, would change significantly with dilution. The parameters

affecting reattachment are also expected to be totally different from lift-off, since reattachment is a behavior occurring to lifted flames, while lift-off occurs to attached flames – a totally different environment.

Figures 3.6 – 3.10 show how the reattachment fuel velocity varies with co-flow. Here, the linear trend is very evident for both fuels and nozzle sizes.

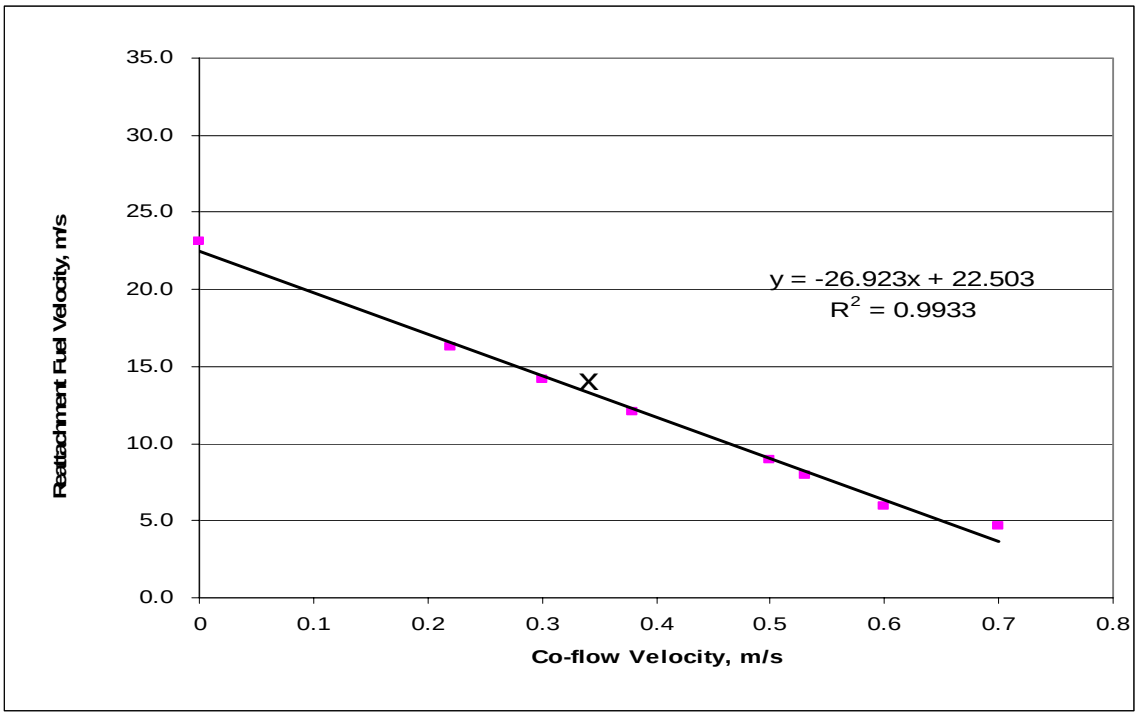

Figure 3.6 – Reattachment Fuel Velocity vs. Co-flow, Large Nozzle, Methane

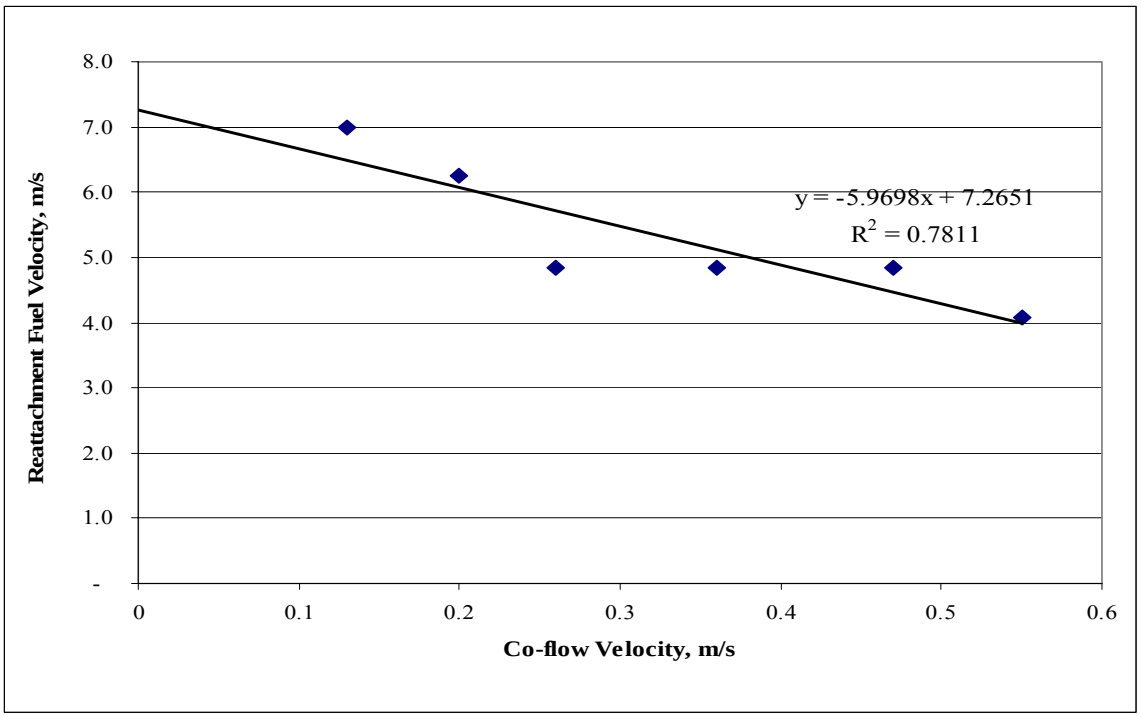

Figure 3.7 – Reattachment Fuel Velocity vs. Co-flow, Small Nozzle, Methane

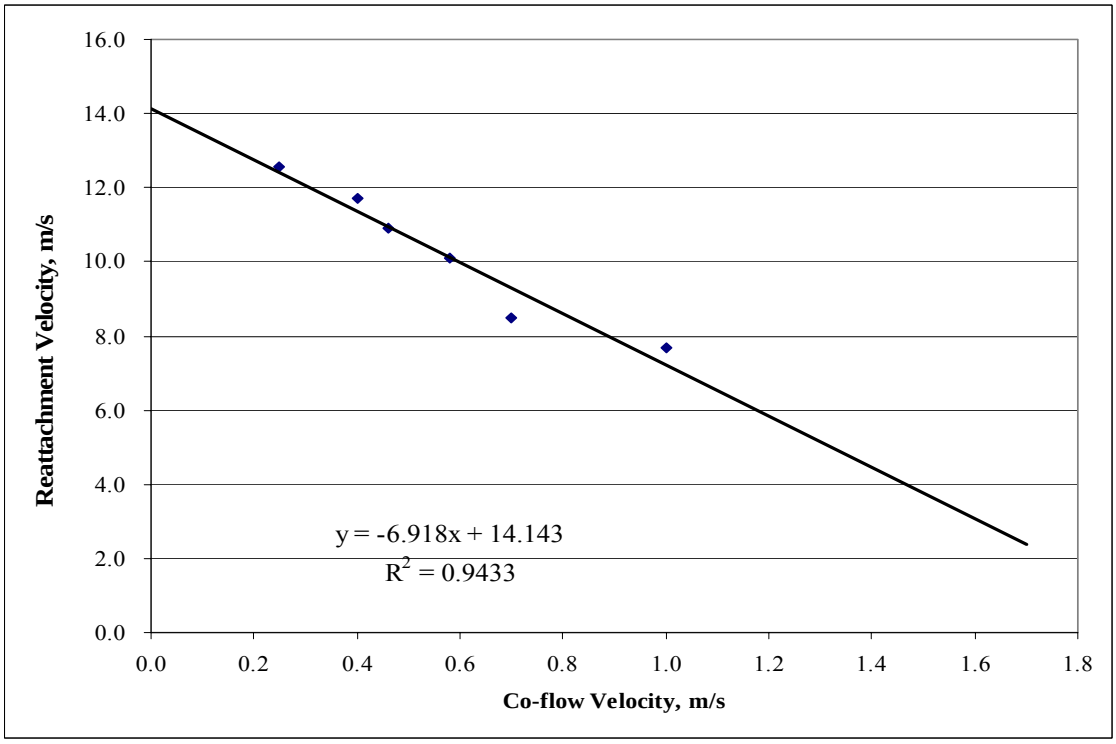

Figure 3.8 – Reattachment Fuel Velocity vs. Co-flow, Large Nozzle, Ethylene

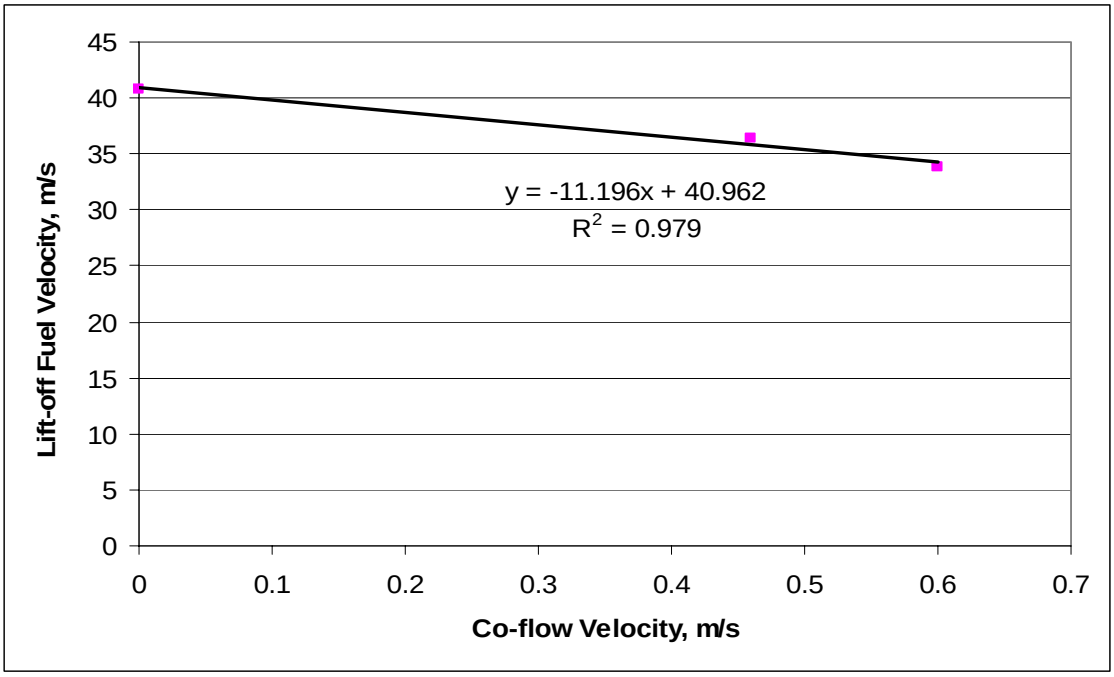

Figure 3.9 – Reattachment Fuel Velocity vs. Co-flow, Small Nozzle, Ethylene

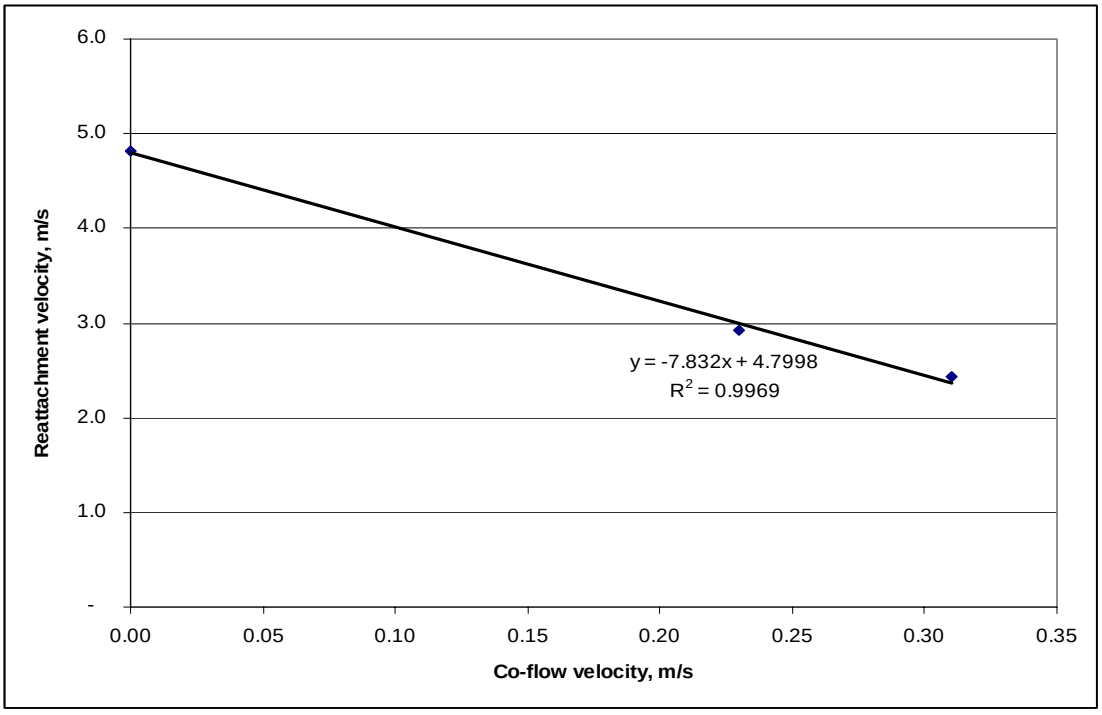

Figure 3.10 – Reattachment Fuel Velocity vs. Co-flow, Small Nozzle, Propane

The reattachment velocities decrease as the co-flow velocity increases. The change is dramatic at large values of co-flow. Examining the plots, it is apparent that co-flow significantly affects lift-off velocity and reattachment velocity. For the large nozzle and methane fuel, the lift-off fuel velocity at zero co-flow was measured to be 30 m/s, while reattachment occurred at 23 m/s from Figure 3.1. Even if a very small co-flow of 0.05 m/s is applied, significant changes in flame behavior occur. The lift-off fuel velocity is reduced to 26 m/s and the reattachment velocity is reduced to 18 m/s. For larger co-flows (e.g., the 0.53 m/s case), the reattachment velocity decreases to about 8 m/s, a reduction of about 75%. It is clear that the co-flow significantly affects reattachment and plays a significant role in lift-off behavior.

For example, ethylene fuel in the small nozzle has a reattachment velocity of 35 m/s at zero co-flow. When 0.6 m/s of co-flow is applied, the reattachment velocity is decreased to less than 20 m/s.

For reattachment, the relation of reattachment velocity line slope to nozzle diameter is less obvious. For laminar flames, the diameter squared is an important part of the relation for lift-off height. Working with this assumption, the turbulent flames here can be assessed. If for methane, small nozzle the zero co-flow point is removed, the best fit line has a slope of about -6, instead of –9.5. The points on the line for the large nozzle, methane fuel fit reasonably well. For methane, the reattachment line slope seems to vary directly as the nozzle diameter squared.

Similarly for ethylene and the large nozzle, if the two extremely high co-flow values are removed, the slope of the best fit line is about –7, while the slope for the small nozzle

case is about –29. Since the smaller nozzle is about half the size of the large nozzle, the functional relationship appears to be diameter squared, but the relation is reversed. The larger magnitude slope for the ethylene fuel is for the smaller nozzle, while the larger magnitude slope is for the larger nozzle for methane fuel. It is not certain if these relationships are the result of coincidence or some underlying theory.

While the functional relationship for reattachment appears to be related to the nozzle diameter squared, for lift-off it is the inverse of the nozzle diameter. This conclusion reinforces the notion that lift-off and reattachment are governed by different phenomenon, as stated by Gollahalli [15].

The results for the reattachment fuel velocities can be made to collapse to a single curve if the reattachment velocities (y-axis) are non-dimensionalized by the reattachment velocity for the particular fuel and nozzle size at zero co-flow, and if the co-flow velocity (x-axis) is non-dimensionalized by the laminar burning velocity of the fuel. The results are presented in Figure 3.11 below.

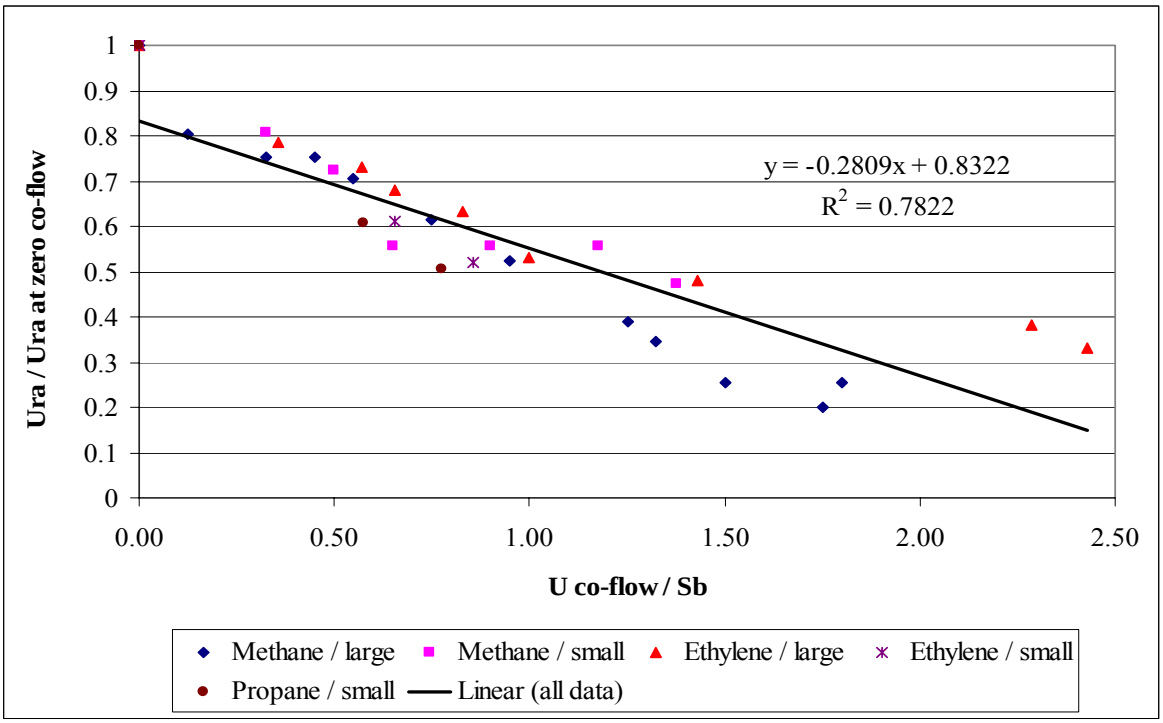

Figure 3.11 – Non-dimensional Reattachment Velocity vs. Non-dimensional Co-flow

The figure above shows how the laminar burning velocity may play into the reattachment phenomenon. Non-dimensionalization using the zero co-flow value allows for the removal of the nozzle size and some of the fuel parameters from the analysis. The agreement is quite good, up to a co-flow values order of the laminar burning velocity. From there, the curves diverge somewhat, though the agreement is still fair.

What is apparent from all of these observations is that there is still much work to be done on flames in the hysteresis regime. Definite trends in the data suggest that parameters can be predicted using measurable quantities, such as fuel nozzle velocity, fuel parameters, and burner size. The effects of co-flow are also not fully understood, but appear to shift the range of stable nozzle velocities downward and the range of stable lift-off heights up.

4. Computation of Jet Velocity at the Flame Base

4.1 Tieszen's Relations

In the introduction section of this work, two relations provided by Tieszen were presented to describe local velocity and fuel mass fraction in a turbulent jet (equations 1.3 and 1.4). The first relation, which relates the local excess jet velocity to the initial jet velocity from the nozzle exit, is a function of the position (in r and z coordinates), the density ratio of the fuel and co-flow, and the nozzle size. It is repeated here for convenience:

$$\frac{\overline{U}}{U_o} = 11.8\left(\frac{\rho_o}{\rho_\infty}\right)^{1/2}\left(\frac{r_o}{z}\right)e^{-93.7\left(r/z\right)^2} \tag{1.3}$$

The local excess jet velocity is defined as the component of the actual velocity at a point, due only to the jet. The actual velocity can be found by adding the local excess jet velocity to the co-flow velocity. Therefore, the local excess jet velocity is the velocity of the fuel, with respect to the co-flow (or as seen by an observer traveling at the speed of the co-flow).

The second of the Tieszen relations presented describe the fuel mass fraction in the jet. It is also a function of the position, the density ratio of the fuel and air, and the nozzle size.

$$Y = 10\left(\frac{\rho_o}{\rho_\infty}\right)^{1/2}\left(\frac{r_o}{z}\right)e^{-57\left(r/z\right)^2} \tag{1.4}$$

Equation (1.4) is not specifically derived for jets in co-flow and will be assumed to be approximate for this analysis. This assumption was also made in Brown et al. [6]. For laminar jets, Lee et al. [35] also determined that the relation for fuel mass in a laminar co-flowing jet remained unchanged, as seen in equation (1.13). The main assumption given by

Tiezsen is that these relations only work 20 or more nozzle diameters downstream. Our results deal mostly with flames located 10 to 30 diameters above the nozzle, therefore our results will be considered approximate. Some authors have utilized a virtual origin technique to work with smaller lift-off heights. This analysis will not consider these effects important, since this analysis does not apply to flames at very low lift-off heights.

4.2 Analysis of the Data at the Flame Base

Tieszen's relations can be applied to the experimental data collected and a local excess jet velocity at the flame base computed. The flame base is assumed to be located at the stoichiometric point at the measured lift-off height, which is then in turn used to compute the local excess jet velocity. Fuel properties, such as density were determined from tabulated values [40].

4.2.1 Methane Large Nozzle

The data for methane fuel and the large nozzle is presented in Figure 4.1 below. Immediately apparent from the figure is that the data forms three lines. The rightmost line is for low co-flows where most of these flames are in a region close to the burner where diffusion effects are expected to dominate. As will be seen later in this chapter, these flames do not necessarily behave as well lifted flames. The leftmost line represents well-lifted turbulent diffusion flames in high co-flow. In spite of a range of co-flows measured, the data seems to fall near one of these three lines. The significance of this is unknown.

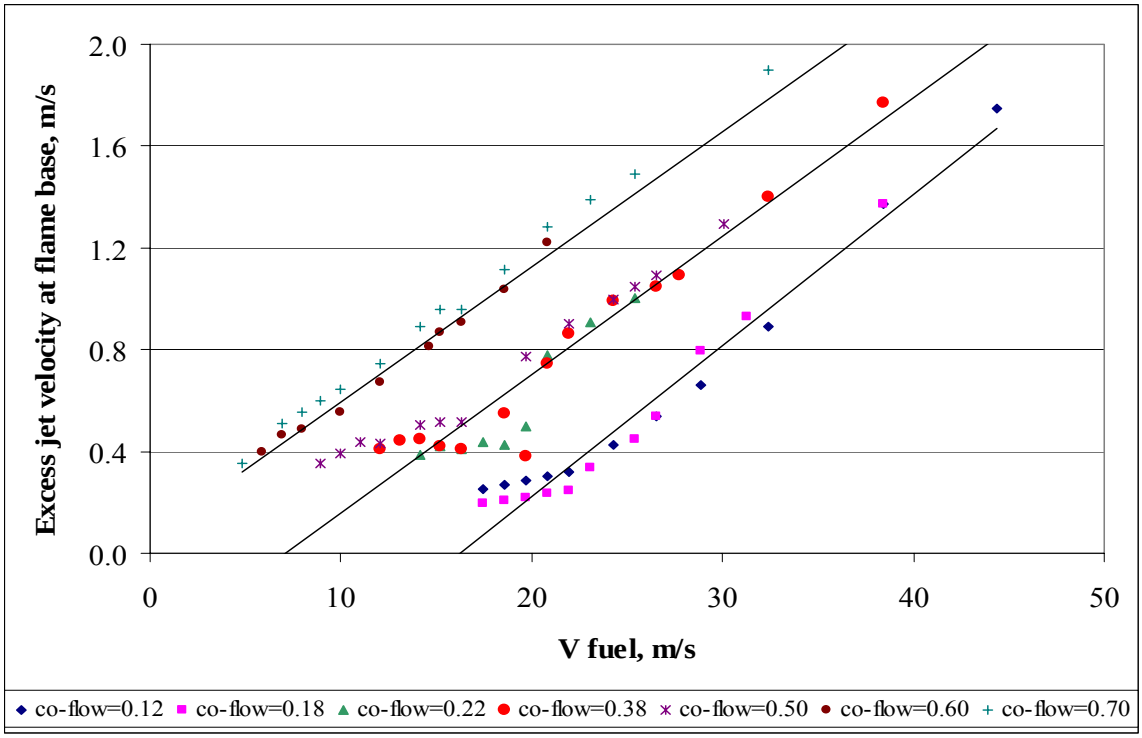

Figure 4.1 – Excess Jet Velocity vs. Fuel Nozzle Velocity

The linear behavior between local excess jet velocity and the nozzle velocity is good for excess jet velocities down to about 0.4 m/s. This is in spite of the non-linearity of the lift-off heights. Thus, we can say that the local excess jet velocity and the nozzle velocity are linearly related into the hysteresis regime, for flames outside of the jet development region (about 8 nozzle diameters). This is similar to Khalghatgi's statement that the lift-off height is linearly related to the nozzle velocity and is an important finding of this work.

The relation between lift-off height and the local excess jet velocity is partially a consequence of the Tieszen relations. The right hand side of equation (1.3) can be plotted at the stoichiometric radius to determine the fraction of the nozzle velocity that is experienced

at the local, lifted position. Figure 4.2 shows the results for methane fuel and the large nozzle.

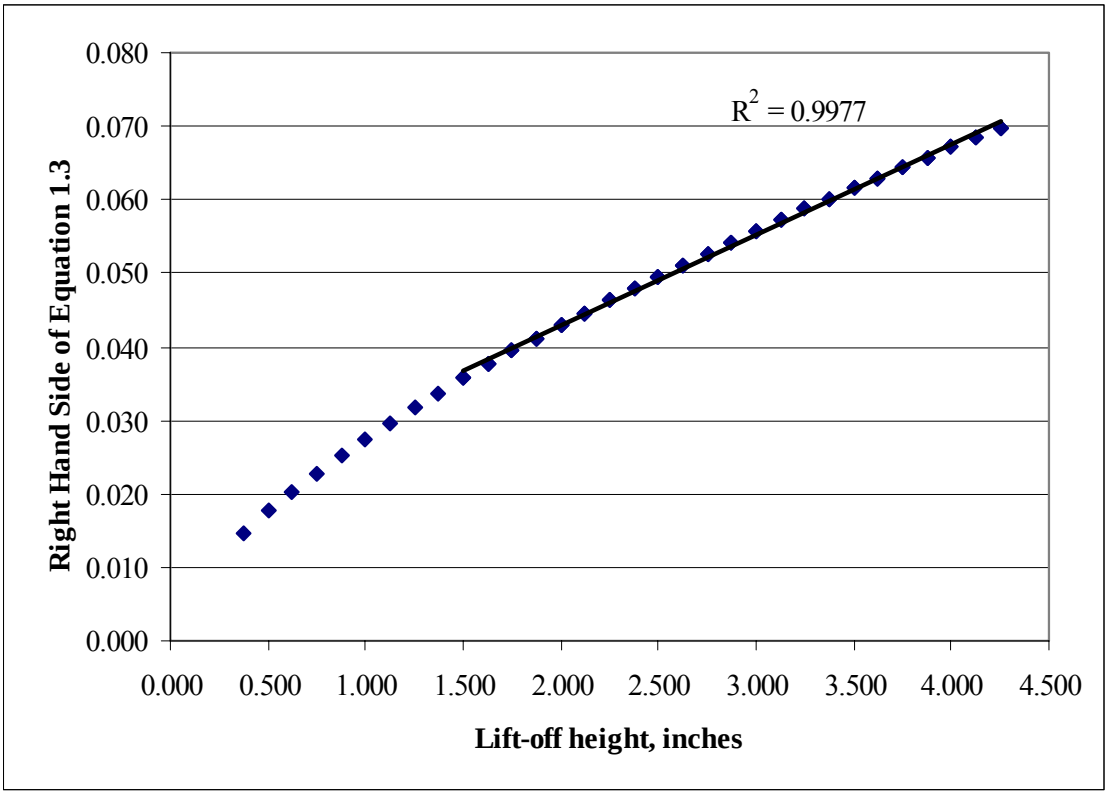

Figure 4.2 – Plot of Right Hand Side of Equation (1.3) at Different Lift-off Heights

The plot shows a relatively non-linear region at low lift-off height. Above 1.5 inches, the curve becomes much more linear, as indicated by the excellent R^2 value computed during the linear regression. This plot demonstrates the linearity of the lift-off height and the local excess jet velocity, for a particular nozzle velocity. The plot of the right hand side of equation 1.3, including the determination of the stoichiometric radius, not is dependent on the nozzle velocity, nor the co-flow. Fuel properties are accounted for in the density ratio and

the use of the stoichiometric fuel mass fraction to determine the value of r at a particular height. It is also dependent on the radius of the nozzle, through the term r_o.

Khalghatgi proposed that the lift-off height is linearly related to the nozzle velocity (equation 1.1). Since the lift-off height is linearly related to both the nozzle and the local excess jet velocities, the linearity of the local excess jet velocity and the nozzle velocity can also be surmised, as seen in Figure 4.1.

What is novel here is that while Khalghatgi's linear relation describes flames that are outside of the hysteresis regime, the linearity of the excess jet velocity to the nozzle velocity holds well into the hysteresis regime. For methane flames with a co-flow of 0.6 m/s or more, the linearity holds to the reattachment point. A change in the linearity is observed when the local excess jet velocity approaches 0.4 m/s. This will be discussed in Section 4.3 below.

Therefore, it is postulated that the local excess jet velocity is an important parameter in determining flame stability. The local excess jet velocity is a strong function of the nozzle velocity, but also incorporates density and fuel concentration through the relation for fuel mass fraction (equation 1.4). Its linearity will into hysteresis regime, even when flame lift-off heights are highly non-linear is indicative of its fundamental nature to the flame. It is also easy to see how flame behavior would be directly affected by velocity at the flame base.

What is not as clear is what role the co-flow plays in the lift-off height. Co-flows allow the experimenter to have the same fuel velocity, but have different flame locations, as well as to use lower fuel velocities than could be achieved without co-flow. Flames with the same local excess jet velocity, but at different co-flows, propagate at different speed with respect to the stationary nozzle.

Montgomery et al. [8] suggest modifying the nozzle velocity by adding a factor related to the co-flow. Then, flame properties for a turbulent flame in co-flow can be determined using the zero co-flow results. Included in the factor is the density ratio of air to fuel and a constant.

$$V_{eff} = V_{jet} + C\sqrt{\frac{\rho_{coflow}}{\rho_{jet}}}V_{coflow} \qquad (4.1)$$

The authors of the study suggest using 5.2 for the constant C for methane fuel and a 10 mm nozzle diameter. Our results using the local excess jet velocity, instead of the nozzle velocity, show that a constant of about 30 gives good results. Since the local excess jet velocity and the nozzle velocity are linearly related in the region of interest (as per Figure 4.1), we would expect equation (4.1) to hold if the local excess jet velocity is used, but perhaps with a different constant.

Below a local excess velocity of about 0.4 m/s, the line connecting the points changes and becomes shallower in slope. Lift-off heights in this region are very small, typically less than ½ inch (1.25 cm), and this region is a part of the developing region of the jet where Tieszen's jet relations do not hold. Therefore the proposed behaviors are expected to change.

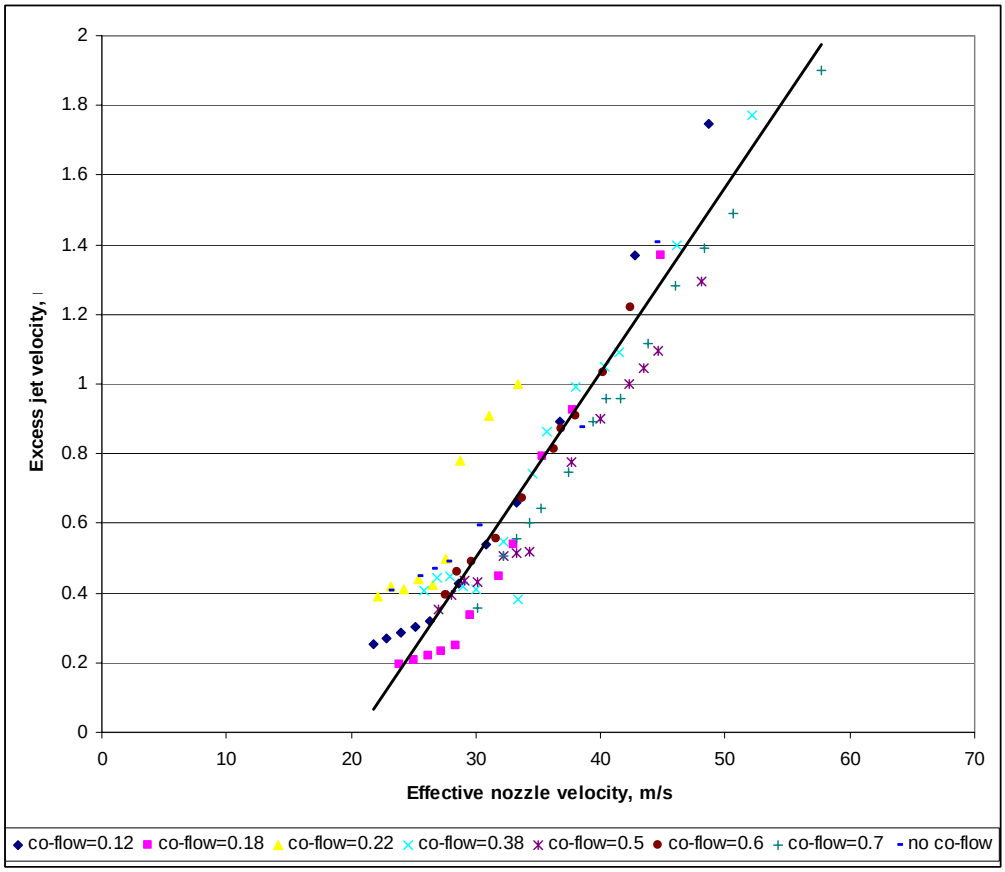

Figure 4.3 – Excess Jet Velocity vs. Effective Nozzle Velocity for Methane, Large Nozzle

4.2.2 Methane Fuel Small Nozzle

A similar analysis can be conducted for methane fuel and the smaller 2 mm nozzle. The results are presented in Figures 4.4 and 4.5.

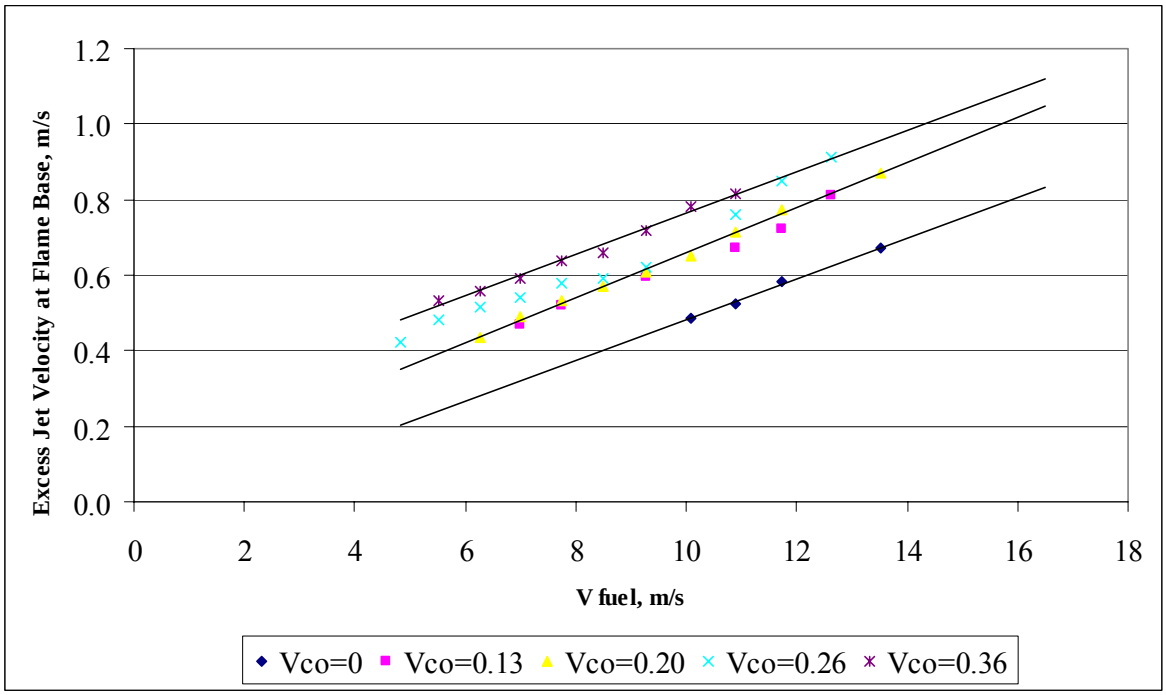

Figure 4.4 – Excess Jet Velocity vs. Fuel Nozzle Velocity, Methane Fuel, Small Nozzle

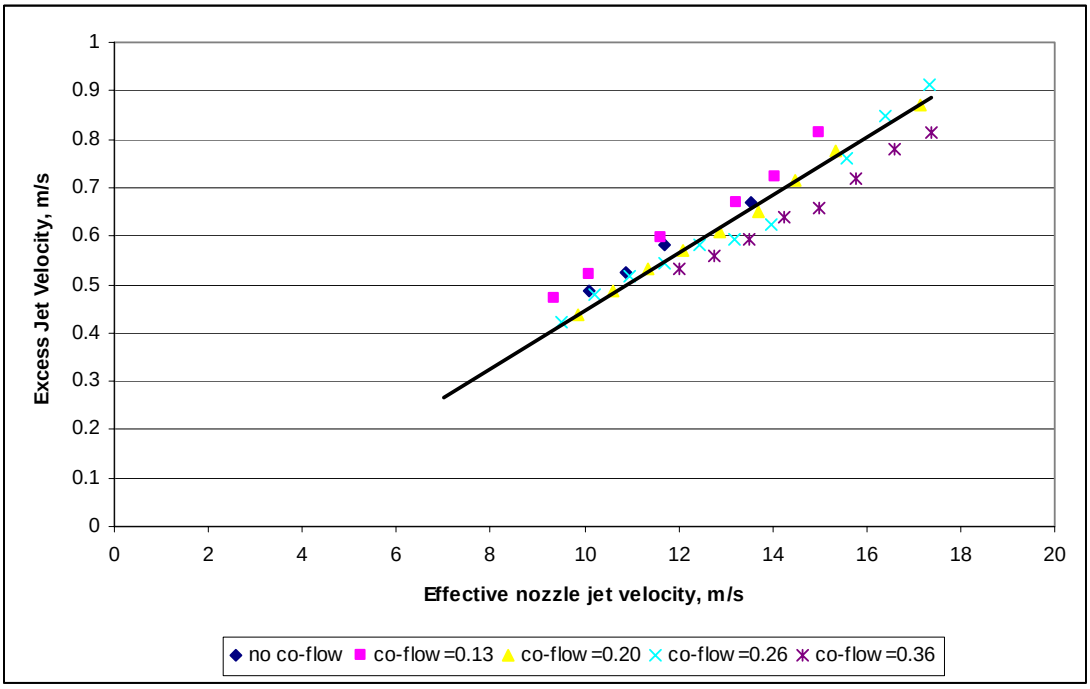

Figure 4.5 – Excess Jet Velocity vs. Effective Jet Velocity, Methane Fuel, Small Nozzle

For the case of the smaller nozzle, the effective jet velocity can also be estimated. Using equation (4.1) and analyzing different cases, the constant with the best fit is about 15. This scales roughly with the nozzle size. Also note that the data on the low end of the curve does not diverge due to entering the jet development region – a consequence of using the smaller nozzle where all lifted flame stabilize outside of the jet development region.

4.2.3 Ethylene Fuel, Large Nozzle

Continuing the analysis for ethylene fuel with the large nozzle, we come across some difficulty in using the Tieszen relations. Although some liberty has been taken with the 20 nozzle diameter minimum suggested by Tieszen, the lift-off heights for flames of ethylene,

except at extreme co-flow, are very small – typically less than an inch (2.5 cm), or 6 nozzle diameters. As expected, the methodology applied to methane does not work well in this region. However, for the large co-flow cases where the lift-off heights are well in excess of 10 nozzle diameters, the methodology does give consistent results. Figure 4.6 shows the results for ethylene fuel, large nozzle.

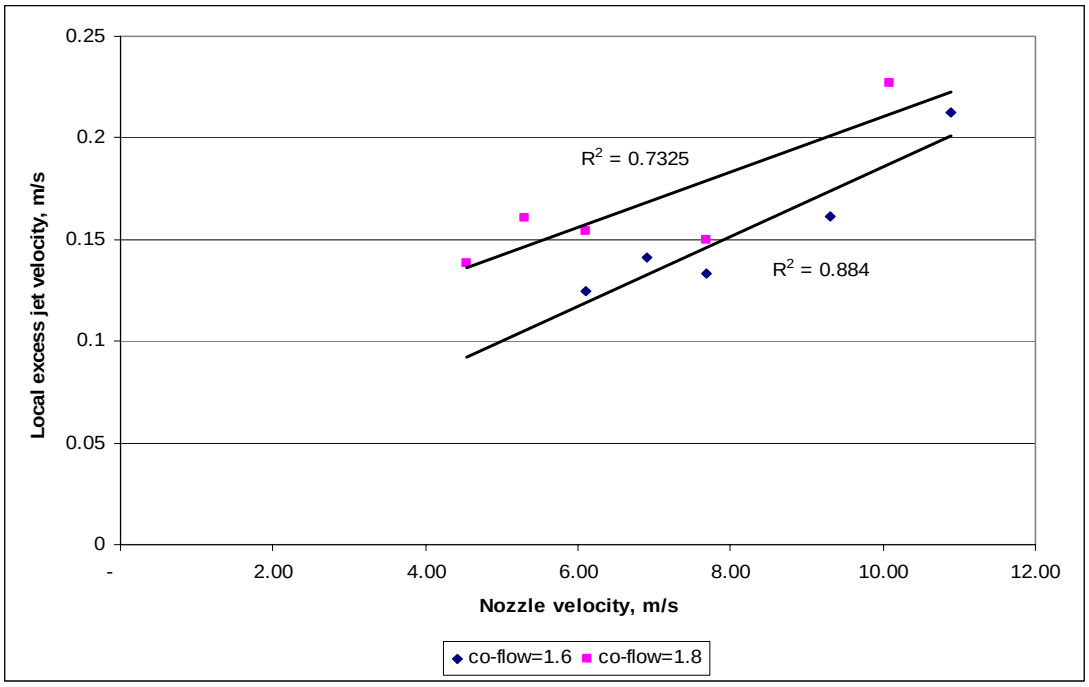

Figure 4.6 – Local Excess Jet Velocity vs. Fuel Nozzle Velocity, Ethylene Fuel, Large Nozzle

In applying the technique of effective local excess jet velocity a constant of 15 was chosen, though it is fairly insensitive to changes between 10 and 20. These results demonstrate that the work of Montgomery et al. [8] describes the effect of co-flow well, if the appropriate constant is chosen.

Results for ethylene, small nozzle and propane fuels did not expected to yield any significant results because the measured lift-off heights for flames at all co-flows are less than one inch and are therefore too small for the Tieszen relations to be valid.

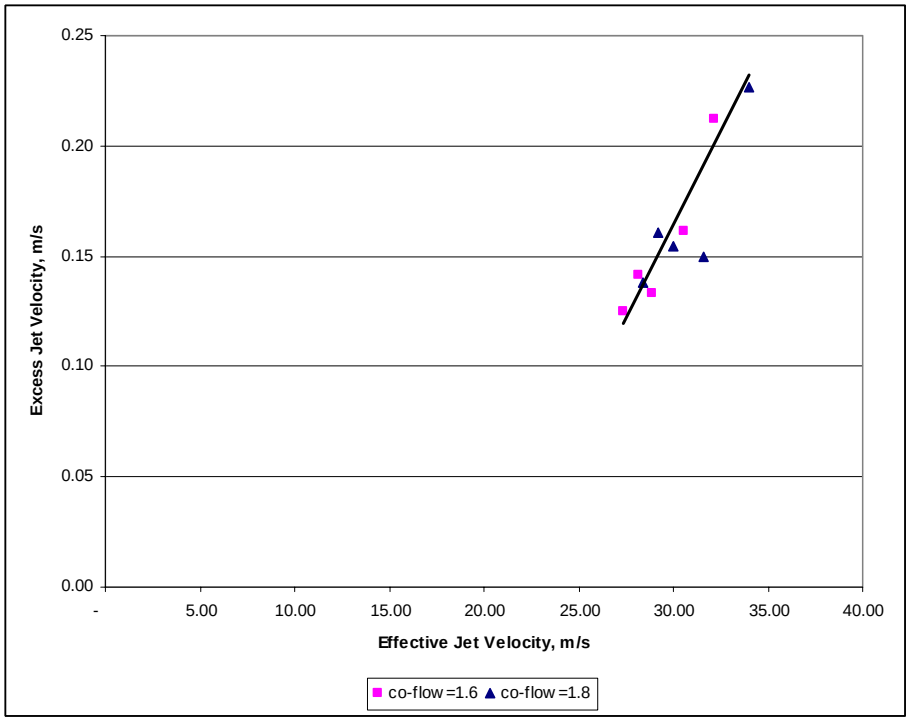

Figure 4.7 – Excess Jet Velocity vs. Effective Jet Velocity, Ethylene Fuel, Large Nozzle

Tieszen's jet relations can be used to compute a local excess jet velocity. The local excess jet velocity appears to describe the location of the flame well, even into the hysteresis regime where Khalghatgi's relation does not appear to hold. This linear relation can be further refined to include the effects of co-flow if an effective local excess jet velocity is computed. Montgomery et al. [8] proposed an effective nozzle velocity, which works well for flames outside the hysteresis regime in describing lift-off heights using equation (1.1)

from Khalghatgi. Our work extends that result and proposes an effective local excess jet velocity, which holds well into the hysteresis regime. Computation of the weighting constant, C, for the co-flow term is still unclear. This is an area for further study.

4.3 Computation of Local Jet Velocity at Reattachment

4.3.1 Methane Fuel

Looking at the figures above, the reattachment points can be singled out and analyzed separately from the remaining points. Figure 4.8 shows the total and excess jet velocities at reattachment for methane fuel and both nozzle sizes. What can be seen is that the filled points (squares and diamonds) for both nozzle sizes form a well-defined line. If the co-flow velocity is subtracted from the computed velocities (giving the local excess jet velocity), the result is a relatively horizontal line around 0.4 m/s, the laminar burning velocity for methane. The slope of the rising line is computed to be 0.88, which is consistent with a relation that varies proportionally with co-flow velocity.

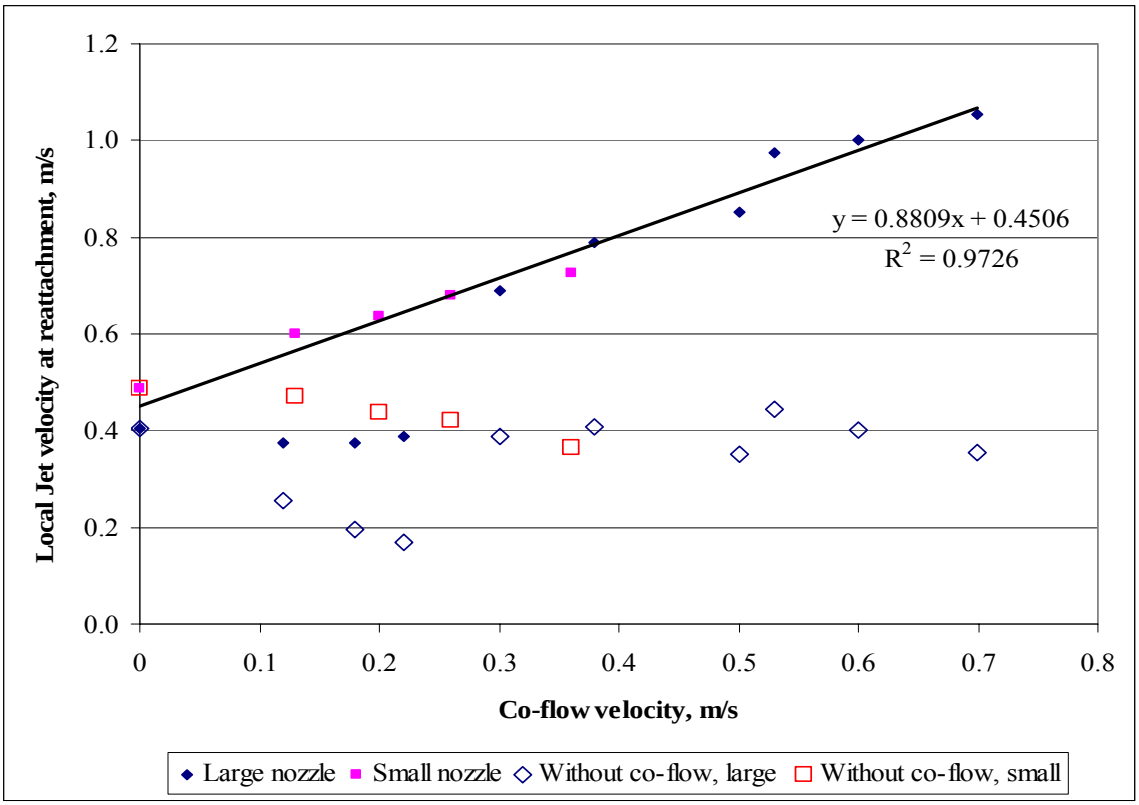

Figure 4.8 - Plot of Local Jet Velocity at Reattachment Point

This suggests that the phenomenon of reattachment occurs when the local excess jet velocity approaches the laminar burning velocity for methane. The flame, which according to some researchers burns at the laminar burning velocity relative to the modified flow at the flame base, cannot exist when its relative velocity falls below the laminar burning speed, except for cases where it is very close to the burner.

It is not difficult to see this idea. If the flame at reattachment continues to burn at the laminar burning velocity the flame will begin to move upstream, since the flame speed is now in excess of the oncoming jet velocity. The fuel velocity at the stoichiometric points continues to decrease with decreasing lift-off height and the flame burns all the way back

down to the burner. Factors that influence lift-off now take over and the hysteresis loop is complete.

For flames with fuel velocities above the reattachment velocity, the local excess jet velocity is still in excess of the laminar burning velocity. Reducing the nozzle velocity reduces parameters such as heat release, turbulence intensity, and the formation of large-scale structures. However, the flame is able to compensate for the reduction in nozzle velocity by reducing the local jet velocity at which it moves upstream against the oncoming jet. Perhaps heat release changes the size and shape of the region immediately around the flame. As the nozzle velocity is reduced, the flame's heat release is also reduced and its ability to deflect jet streamlines diminished.

This line of thinking does not explain why the laminar burning velocity appears to be the cut-off. A flame just at the reattachment point still has considerable heat release and has the ability to deflect streamlines. Either the idea of heat release affecting the flame position is not the primary influence, or the cut-off velocity just happens to be the laminar burning velocity for methane.

Another explanation is the transition to laminar flow in the jet. At some velocity, the jet will transition from a turbulent jet to a laminar jet. Stable, lifted laminar flames of methane have not been achieved (though recently they were using dilution with helium [41]). Given that the fluid properties at the flame base are likely similar, regardless of velocity since the stoichiometric mass fraction of fuel is very small when compared to air, the observed threshold velocity may be a transition from turbulent flow to laminar flow. The Reynolds number, which is related to the local velocity, fluid properties, and a characteristic length

scale would reduce to a functional relationship with the local velocity relative to the co-flow – the local excess jet velocity. Additional work using visualization techniques could be performed to confirm this hypothesis.

4.3.2 Ethylene Fuel

The same methodology can be applied to ethylene fuel and the large nozzle. The results are less definitive, since for co-flows of less than about 0.7 m/s the lift-off height is less than ¼ inch (0.6 cm), well into the region where diffusion plays the biggest role in flame behavior. For the 0.7 m/s co-flow and the 1 m/s co-flow the computed local jet excess velocity is about 0.07 m/s. For the 1.6 and 1.8 m/s co-flows the reattachment local excess jet velocities are 0.125 and 0.138 m/s, respectively. For ethylene fuel and the small nozzle, lift-off heights of ½ inch (1.25 cm) or more were possible for only a few fuel and co-flow combinations.

These values are well below the laminar burning velocity for ethylene, which is about 0.7 m/s. Thus, the idea from the section above that the laminar burning velocity is the cut-off velocity for reattachment is not supported. It appears that the cut-off velocity decreases as the heat release (laminar burning velocity) increases. Kalghatgi [4] suggests using the inverse of the laminar burning velocity squared as a way to account for heat release in flames. The relation for lift-off height includes this factor. If the cut-off velocity for methane, 0.4 m/s, is multiplied by the ratio of the laminar burning velocities, squared (i.e., $[0.4/0.7]^2 = 0.32$), the resulting cut-off local excess jet velocity is reduced to about 0.13 m/s. This is in the range of local excess jet velocities measured for ethylene at high co-flows.

Of course, this supposition cannot be fully supported with just two fuels. Additional testing with other fuels, as well as diluted methane and ethylene could help shed light on this idea. What is clear is that the factor $1/S_L^2$ is an important parameter not only for turbulent lifted flame height, but also for reattachment.

Analyzing the Khalghatgi's relation for lift-off height, note the dependence of the lift-off height to the heat release through the $1 / S_L^2$ term. Therefore, we propose the following relation for the local excess jet velocity at reattachment for methane:

$$V_{\text{reattachment, local excess}} = 0.064 / S_L^2 \qquad (4.2)$$

where 0.064 is an empirical constant computed from the data for methane fuel, where the constant has units of $(m/s)^3$. The thermal diffusivity could be incorporated into the result so that the functional relationship is with the characteristic chemical reaction time. There is not data to support whether the threshold velocity is based on laminar burning velocity, or thermal diffusivity, or both.

Equation (4.2) predicts the local jet excess velocity to be approximately 0.4 m/s for methane. This relation holds throughout the range of co-flows shown in the figure. This makes the computed local excess jet velocity at reattachment for ethylene 0.13 m/s, using 0.7 m/s as the laminar burning velocity for ethylene, and this is close to the measured values, which ranged from 0.120 – 0.138 m/s. This agreement for both methane and ethylene reattachment phenomena indicates that fuel type is indeed important, in contrast with the Gollahalli study [15].

The laminar burning velocity can be correlated with heat release. Therefore, ethylene has a higher heat release than does methane. Looking at the burning velocities, it is easy to

see why ethylene can burn in higher co-flows. The higher heat release and burning velocity suggests that it can better affect it environment through heat release – according to a theory proposed by Upatnieks et al. [22] and can propagate against larger incoming jet velocities. It does not immediately explain why ethylene can also exist at lower local excess jet velocities than methane.

This explanation will also have to consider co-flow. For methane, the threshold local excess jet velocity is about the laminar burning velocity. At very low co-flow velocities, the local excess jet velocities at reattachment were found to be even lower, though this was postulated to relate to the very small lift-off height and the lack of mixing. For these cases, the total velocity, including co-flow, seems a better measure.

For ethylene, data points where Tieszen's jet relations apply are for co-flows in excess of 1.5 m/s. With these co-flows, the local excess jet velocity may be much smaller than the laminar burning velocity, but the velocity at which the flame propagates against the stationary burner is still much larger than the laminar burning velocity. The total effect of co-flow must be considered when looking at reattachment phenomenon.

Using equation (4.2) and the Tieszen relations (equations 1.3 and 1.4), a computed lift-off height just prior to reattachment can be estimated. This is also equivalent to the maximum lift-off height of the flame before reattachment:

$$Z_{RA} = \frac{0.1083\left(\rho_o / \rho_\infty\right)^{1/2} r_o}{S_L^{3.106} U_o^{1.553} Y_{F,st}^{2.553}} \tag{4.3}$$

Thus, the lift-off height at reattachment is directly proportional to the nozzle size, inversely proportional to fuel parameters S_L and $Y_{F,st}$, and inversely proportional to the nozzle velocity.

The measured data for both fuels and nozzle sizes, and co-flows at their respective reattachment point is plotted with the results from equation (4.3) in Figure 4.8.

A good agreement is noted, as the curves follow the trends of the data well. Fuel effects are well captured by the S_L and $Y_{F,\,st}$ terms. Equation (4.3) provides a method to compute the reattachment height as a function of fuel and nozzle velocity. It does not predict what co-flow velocity is required to achieve a reattachment point for the input nozzle velocity.

Equation (4.2) and the Tieszen relations can also used to determine the nozzle velocity required for reattachment, as a function of nozzle size and fuel. Rearranging the terms and solving for U_o, the nozzle velocity yields:

$$U_{o,ra} = \frac{\left(\rho_o / \rho_\infty\right)^{0.32} \left(r_o / z\right)^{0.64}}{4.224 Y_{F,st}^{\;1.64} S_L^2} \tag{4.4}$$

The dependence of the nozzle velocity on laminar burning velocity squared is apparent, as it is for the local excess jet velocity. The dependence on the fuel through the stoichiometric mass fraction term and the density ratio term is seen as well. The nozzle velocity at reattachment is also a function of the lifted flame height at reattachment.

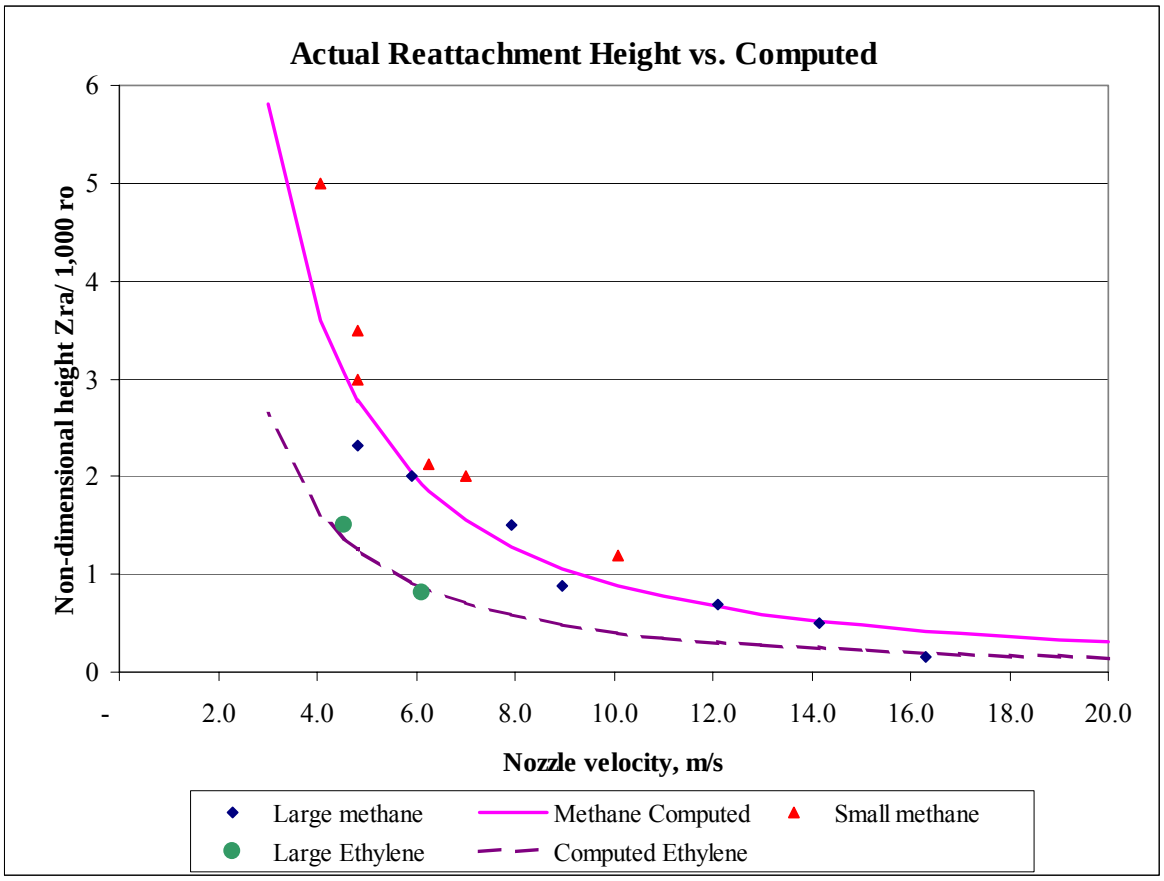

Figure 4.8 – Non-dimensional Lift-off Height as a Function of Fuel Nozzle Velocity

Equation (4.4) for the reattachment nozzle velocity is plotted against measured nozzle velocities at reattachment and shown in Figure 4.9. The line drawn diagonally in the figure indicates where there is a perfect match for the empirical data on the ordinate against the calculated on the abscissa. Most of the points fall near the line, indicating good agreement of our model with experiment.

Equations (4.2), (4.3) and (4.4) provide some insight into flame stability. Equation (4.2) predicts that the minimum local jet excess velocity is a function only of the laminar

burning velocity. Other fuel related parameters, such as stoichiometric fuel mass fraction, and nozzle construction (size) do not play a role in going over the peak from a lifted flame to one that reattaches**.** This does not directly support Gollahalli's assertion that lifted flame stability is a function of the flow structure rather than fuel. However, equation (4.2) determines the local excess jet velocity and not the actual nozzle velocity, which Gollahalli et al. measured and reported on.

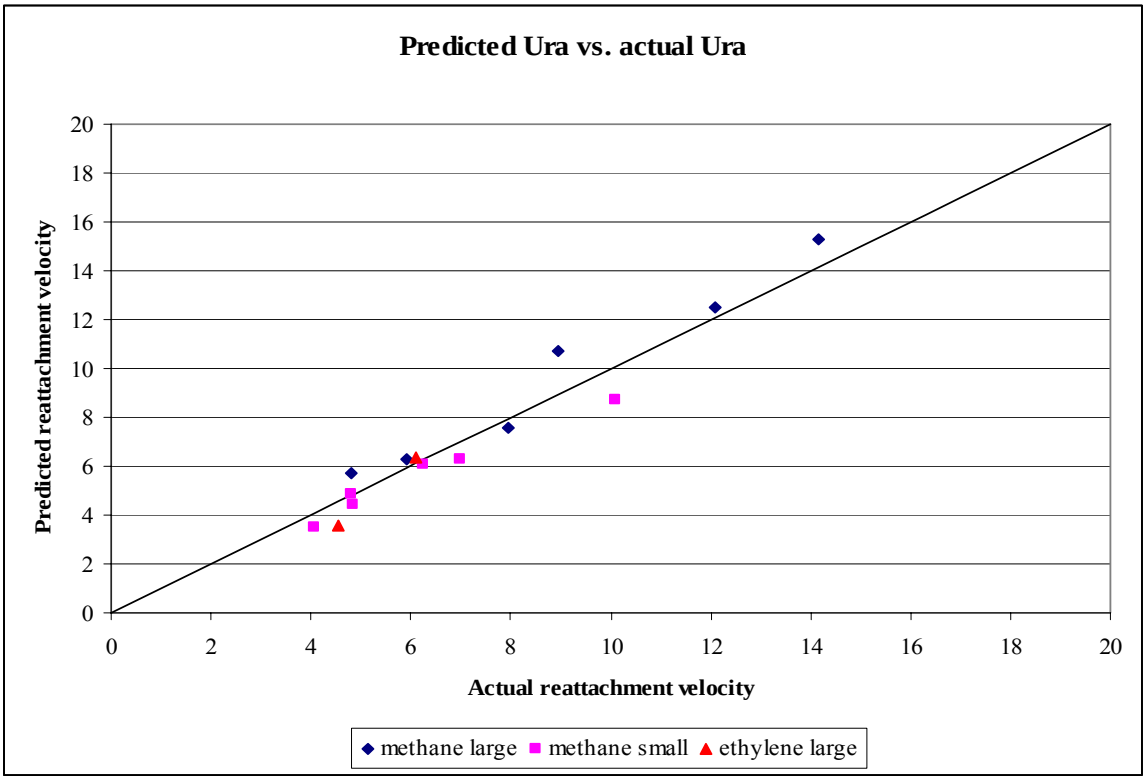

Figure 4.9 – Comparison of Actual Reattachment Velocity to Reattachment Velocity Estimated by Equation (4.4)

Equation (4.3) provides insight into what determines flame lift-off height. Included is the nozzle velocity, laminar burning velocity, the nozzle size, the fuel's stoichiometric mass fraction, and the ratio of fuel density to co-flow density. Therefore, flame height is much more complex, incorporating chemical kinetics, flow parameters, and construction of the nozzle. Using the relation proposed by Montgomery et al. [8], the nozzle flow velocity can be modified to include the effects of co-flow.

Equation (4.4) provides an empirical relation for fuel nozzle velocity at reattachment. The relation includes fuel parameters, such as stoichiometric fuel mass fraction, the density ratio of fuel to air, and the laminar burning velocity. There is also a functional dependence on nozzle size. However, there is a dependence on the lift-off height at reattachment, which must be measured.

Thus, we propose that the flame lift-off height can be determined using fuel properties, the co-flow, and the nozzle size for a particular fuel velocity. Though not all of the pieces of such a relation have been determined, the work discussed above gives glimpses of what the relation might involve.

The equations above can predict local excess jet velocity from nozzle velocity, co-flow velocity, and some constant – based on results shown in Figures 4.3, 4.5, and 4.7. From there, the local excess jet velocity can be used to determine the lift-off height using the properties of the fuel fired, the nozzle size, and the co-flow fluid properties. What is not known is how the constant in the effective velocity relation (equation 4.1) varies with fuel, nozzle size, or other parameters. However, if one set of experiments is performed with a nozzle, then it should be possible to predict what will happen at other co-flows and nozzle

fuel velocities. This represents a step forward in our understanding of flame behavior. Additional work needs to be done to help determine this constant varies for different fuels, nozzles, and fuel dilutions.

4.4 Lift-off Heights for Small Nozzle vs. Large Nozzle

An interesting consequence of applying the Tieszen relations (equations 1.3 and 1.4) to the flames is how flame lift-off varies with nozzle diameter. Experimentally, flames from the smaller nozzle were found to stabilize farther downstream than flames with the large nozzle and the same fuel velocity. This is a bit counterintuitive, since a large nozzle would supply more fuel and more momentum. Tieszen's jet relations can explain this unexpected result.

The explicit dependence of nozzle size on local excess jet velocity and fuel mass fraction is seen in the r_o term.

$$\frac{\overline{U}}{U_o} = 11.8\left(\frac{\rho_o}{\rho_\infty}\right)^{1/2}\left(\frac{r_o}{z}\right)e^{-93.7(r/z)^2} \tag{1.3}$$

$$Y = 10\left(\frac{\rho_o}{\rho_\infty}\right)^{1/2}\left(\frac{r_o}{z}\right)e^{-57(r/z)^2} \tag{1.4}$$

In both equations, r_o is directly related to the parameter computed – either ratio of the local excess jet velocity to nozzle velocity, or to the fuel mass fraction. Since flames of methane tend to stabilize in a region where the local excess jet velocity is between the laminar burning velocity (0.4 m/s for methane by coincidence) and about three times the laminar burning velocity [6, 7] the effect of the nozzle diameter (radius) can be seen. With all other

parameters remaining the same – notably fuel composition and nozzle velocity – reducing the nozzle size will reduce the right hand side of both equations. This can be offset by increasing the lift-off height, z, which in absence of the exponential term, would vary directly as the nozzle radius to produce the same fuel mass fraction and velocity ratio.

However, the exponential term is a very important term in the relations, particularly for the large nozzle. Table 4.1 shows the relevant parameters for methane and the large nozzle for a nozzle velocity of 22 m/s.

The stoichiometric radius is given by the following:

$$r_{st} = z\sqrt{\frac{\ln\left(\frac{10}{Y_{st}}\frac{r_o}{z}\sqrt{\rho_{fuel}/\rho_{\infty}}\right)}{57}} \qquad (4.5)$$

The column for exponential term and 1/z term breakdown the different parts of equation (1.3). The last column labeled Right Hand Side includes all of the terms and represents the ratio of the local excess jet velocity to the nozzle velocity. This data is plotted in Figure 4.2 above.

The column for Local Excess Jet Velocity is the Right Hand Side value multiplied by the nozzle velocity – 22 m/s in this case. The Total Jet Velocity is the sum of the Local Excess Jet Velocity and the co-flow – 0.38 m/s in this case. The column for Height in Diameters is used as a reference in determining the applicability of the Tieszen relations. As can be seen, for lift-off heights less than 1.5 inches (3.8 cm), z / D is less than 10 and the correlation is expected to be poor, so we confine our results for higher flame heights.

What Table 4.1 illustrates is the interaction of the exponential term and the 1/z term. For the large nozzle, the exponential term for small nozzles is quite small and the 1/z term

quite large for small lifted flame heights. At this fuel velocity and the assumed 0.38 m/s co-flow, the lifted flame height is 1.75 inches (4.5 cm). At this height, the exponential term is about 0.089 and the 1/z term 22.5. Variations in either term therefore can affect flame height dramatically.

Table 4.1 – Breakdown of Terms in Equation 1.3 for Methane, Large Nozzle

Lift-off Inches	Stoich. Radius, m	Local Excess Jet Velocity m/s	Total Jet Velocity m/s	Height Nozzle Diameters	Exponential Term	1/z term	Right Hand Side of Equation 1.3
0.500	0.00278	0.38702	0.76702	3.2	0.011	78.740	0.018
0.625	0.00332	0.44682	0.82682	4.0	0.016	62.992	0.020
0.750	0.00384	0.50247	0.88247	4.8	0.022	52.493	0.023
0.875	0.00433	0.55490	0.93490	5.6	0.029	44.994	0.025
1.000	0.00479	0.60472	0.98472	6.4	0.036	39.370	0.027
1.125	0.00523	0.65236	1.03236	7.1	0.043	34.996	0.030
1.250	0.00565	0.69815	1.07815	7.9	0.051	31.496	0.032
1.375	0.00605	0.74234	1.12234	8.7	0.060	28.633	0.034
1.500	0.00643	0.78511	1.16511	9.5	0.069	26.247	0.036
1.625	0.00679	0.82664	1.20664	10.3	0.079	24.228	0.038
1.750	0.00714	0.86703	1.24703	11.1	0.089	22.497	0.039
1.875	0.00746	0.90642	1.28642	11.9	0.100	20.997	0.041
2.000	0.00778	0.94488	1.32488	12.7	0.111	19.685	0.043
2.125	0.00807	0.98249	1.36249	13.5	0.123	18.527	0.045
2.250	0.00835	1.01932	1.39932	14.3	0.135	17.498	0.046
2.375	0.00862	1.05543	1.43543	15.1	0.148	16.577	0.048
2.500	0.00887	1.09087	1.47087	15.9	0.161	15.748	0.050
2.625	0.00911	1.12568	1.50568	16.7	0.174	14.998	0.051
2.750	0.00933	1.15991	1.53991	17.5	0.188	14.316	0.053
2.875	0.00954	1.19358	1.57358	18.3	0.202	13.694	0.054
3.000	0.00973	1.22674	1.60674	19.1	0.217	13.123	0.056
3.125	0.00991	1.25941	1.63941	19.8	0.232	12.598	0.057
3.250	0.01008	1.29162	1.67162	20.6	0.247	12.114	0.059
3.375	0.01023	1.32339	1.70339	21.4	0.263	11.665	0.060
3.500	0.01037	1.35474	1.73474	22.2	0.279	11.249	0.062
3.625	0.01050	1.38570	1.76570	23.0	0.296	10.861	0.063
3.750	0.01061	1.41628	1.79628	23.8	0.313	10.499	0.064
3.875	0.01070	1.44650	1.82650	24.6	0.330	10.160	0.066
4.000	0.01079	1.47637	1.85637	25.4	0.348	9.843	0.067

The data can be tabulated for methane fuel and the small nozzle. Using the same conditions as in Table 4.1 (fuel velocity of 22 m/s and co-flow of 0.38 m/s), Table 4.2 shows relevant results for equations 1.3 and 1.4.

Table 4.2 – Breakdown of Terms in Equation 1.3 for Methane, Small Nozzle

Lift-off Inches	Stoich. Radius, m	Local Excess Jet Velocity m/s	Total Jet Velocity m/s	Height Nozzle Diameters	Exponential Term	1/z term	Right Hand Side of Equation 1.3
0.500	0.00240	0.60472	0.98472	6.4	0.0356	78.740	0.0275
0.625	0.00283	0.69815	1.07815	7.9	0.0514	62.992	0.0317
0.750	0.00321	0.78511	1.16511	9.5	0.0694	52.493	0.0357
0.875	0.00357	0.86703	1.24703	11.1	0.0894	44.994	0.0394
1.000	0.00389	0.94488	1.32488	12.7	0.1113	39.370	0.0429
1.125	0.00418	1.01932	1.39932	14.3	0.1351	34.996	0.0463
1.250	0.00444	1.09087	1.47087	15.9	0.1607	31.496	0.0496
1.375	0.00467	1.15991	1.53991	17.5	0.1879	28.633	0.0527
1.500	0.00487	1.22674	1.60674	19.1	0.2168	26.247	0.0558
1.625	0.00504	1.29162	1.67162	20.6	0.2473	24.228	0.0587
1.750	0.00519	1.35474	1.73474	22.2	0.2793	22.497	0.0616
1.875	0.00530	1.41628	1.79628	23.8	0.3129	20.997	0.0644
2.000	0.00539	1.47637	1.85637	25.4	0.3479	19.685	0.0671
2.125	0.00545	1.53514	1.91514	27.0	0.3843	18.527	0.0698
2.250	0.00548	1.59269	1.97269	28.6	0.4222	17.498	0.0724
2.375	0.00548	1.64911	2.02911	30.2	0.4615	16.577	0.0750
2.500	0.00545	1.70448	2.08448	31.8	0.5020	15.748	0.0775
2.625	0.00537	1.75888	2.13888	33.3	0.5440	14.998	0.0799
2.750	0.00527	1.81236	2.19236	34.9	0.5872	14.316	0.0824
2.875	0.00511	1.86498	2.24498	36.5	0.6317	13.694	0.0848
3.000	0.00491	1.91679	2.29679	38.1	0.6775	13.123	0.0871
3.125	0.00465	1.96784	2.34784	39.7	0.7245	12.598	0.0894
3.250	0.00433	2.01816	2.39816	41.3	0.7728	12.114	0.0917
3.375	0.00392	2.06780	2.44780	42.9	0.8222	11.665	0.0940
3.500	0.00339	2.11679	2.49679	44.5	0.8729	11.249	0.0962
3.625	0.00266	2.16516	2.54516	46.0	0.9247	10.861	0.0984
3.750	0.00148	2.21294	2.59294	47.6	0.9777	10.499	0.1006

The variation of the exponential term is much smaller in magnitude for the small nozzle since the stoichiometric radius is lower. This is a result of the nozzle radius effects on

equation (1.4). For the same lift-off height, the 1/z term is the same between the two cases. The product of the exponential term, the 1/z term, the value of r_o, and various constants is higher for the smaller nozzle than for the larger nozzle. This makes the local excess velocity higher, for a given nozzle velocity. Since there is a range of local excess fuel velocities for which a stable flame is possible, the smaller nozzle must utilize lower fuel velocities to achieve the same local excess jet velocity.

For a given lift-off height, the stoichiometric radius for the small nozzle is smaller than for the large nozzle. This actually increases the exponential term for the smaller nozzle, since the exponent power becomes less negative (i.e., the power approaches zero and thus the result of the exponential approaches unity). At 2 inches (5 cm), the exponential for the large nozzle is about 0.11, while it is 0.35 for the small nozzle. The density ratio is constant between the two cases, as is the 1/z term for a given lift-off height. The r_o term reduces the effect proportionally to the change in radius. The right hand side for equation (1.3) is about 50% larger for the small nozzle than for the large nozzle.

This means that the velocity at the stoichiometric radius is higher for the smaller nozzle than for the larger nozzle. The gradients of velocity and concentration are also higher for the smaller nozzle, since the diffusion of momentum is related to the inverse of the radius (i.e., 1/r). A stable flame requires that the gradients not be too high (else the flame is strained out) and that the local jet velocity at the flame base be comparable to the some net burning velocity. The flame for the smaller nozzle lifts higher to overcome the higher gradients.

4.5 Implications on Flame Stability Theory

The present work does shed some light on current flame stability theory. Work in the hysteresis regime, near one of the extremes of flame stability allows the determination of flame behavior as heat release and flow velocities are minimized. Co-flow contributes the ability to analyze similar jet flow parameters (i.e., local excess jet velocity and heat release), but have flames with different overall total jet velocity.

There are two major theories that used to describe flame stability. Both have their supporters and detractors, and both describe some aspects of flame behavior well. As was presented in Chapter 1, one theory invokes the use of a turbulent burning velocity, and the other theory uses large-scale structures as a stabilizing mechanism.

In the analysis above, jet velocity and fuel concentration relations were used to determine flow parameters at the base of lifted flames. The results show that the excess jet velocity at the base is roughly linear with nozzle velocity. Stable flames respond to lower nozzle velocities by burning in a region where the jet velocity at the base is correspondingly lower. The linearity between nozzle velocity and local excess jet velocity is significant because the flame lift-off heights are highly non-linear for many of the points in Figures 4.1, 4.4, and 4.6. Varying linear paths in these figures for different co-flow velocities can be collapsed to a single line by using an effective velocity, as proposed by Montgomery et al. [8]. These results, shown in Figures 4.3, 4.5, and 4.7 show most points following a single line. The effective velocity, however, requires the use of a constant to scale the effect of co-flow. In each nozzle / fuel case a different constant was chosen, which could not be determine a priori. These concepts are more indicative of a stability mechanism that is

derived from a turbulent flame speed, or some representation based on the nozzle velocity, the co-flow velocity, and other parameters.

The reattachment phenomenon, in particular, can support both theories. The reattachment fuel velocities are plotted in Figures 3.6 to 3.10. Each is apparently linear, fitting the least squares regression fit quite well. The data can be collapsed into a single line by non-dimensionalizing the reattachment nozzle velocity at varying co-flows by the velocity at zero co-flow, and non-dimensionalizing the co-flow by the laminar burning velocity for each fuel. The linear fit is very good for co-flows up to about 1.2 times the laminar burning velocity. This is again indicative of the importance that some effective burning velocity has on flame stability.

Adding weight to this idea is the analysis of the local excess jet velocity at the flame base, at reattachment. Figure 4.8 shows the local jet velocity at reattachment for methane fuel. For lift-off heights greater than about an inch, the local excess jet velocity, represented as the open symbols, is nearly constant for the full range of stable co-flows and for both nozzle sizes. This concept was expanded into an equation for local excess jet velocity at the flame base (equation 4.2), which depends on laminar burning velocity only. The relation was confirmed for ethylene, which has a very different burning velocity.

Gollahalli [15] proposed that the reattachment nozzle velocity depends on the organized structures and not on dilution of the fuel, and varied little between fuels used. Our results show that fuel plays a major role in determining the local excess jet velocity at reattachment. The reattachment local excess jet velocity for ethylene is one-third the value

for methane fuel. Similarly, the nozzle velocities at reattachment we found are also quite different.

Gollahalli worked with propane and methane fuels, both of which have very similar undiluted laminar burning velocities. Since ethylene has a much higher laminar burning velocity than does methane (0.7 m/s vs. 0.4 m/s), it would have been a good choice as a third undiluted fuel in Gollahalli's experiments. For equation (4.2) to hold when the fuel is diluted, the change in laminar burning velocity due to dilution must also cause a change in flame position that maintains the local excess jet velocity constant. This could only hold if heat release, related through S_L^2/α is the primary contributor to flame stability. This would support the turbulent burning velocity idea of stability, rather than the large-scale structures approach.

Although all of our data supports the idea of an effective burning velocity being a primary mechanism of flame stability, it is important to note that flames from reattachment to blowout have different behaviors [23]. Flames that are lifted only a fraction of an inch above the burner do not behave as flames lifted an inch or more from the burner tip. The jet relations provided by Tieszen do not work well for the near nozzle flames. Part of this may be attributed to the singularity at the origin, since the relations depend on 1/z, or perhaps to the developing nature of the jet. Flames lifted many inches above the burner are burning in a region where fuel and air are almost completely premixed. These flames appear as burning zones rather than as a typical flame with a base and trailing diffusion flame.

Therefore this work does not offer any definite conclusions on which theory is correct, though our work tends towards the concept of turbulent burning velocities.

Additional work in the hysteresis regime is warranted, to collect additional data at more co-flows and with different fuels and dilutions. Analysis of the flames at reattachment using visualization techniques and velocity mapping would also provide insight into flame stability by studying the mechanism that causes a flame to no longer burn in a stable lifted condition.

5. Conclusions / Future Work

This work describes experiments and analysis of turbulent lifted jet flames in co-flow in the hysteresis regime. In the hysteresis regime, two stable flame locations exist – one lifted above the burner at some height and one attached. The regime represents the lower boundary of fuel velocity where a lifted flame can exist and hence can provide evidence to support or disprove current flame stability theories. Methane and ethylene fuels are burned to provide evidence of the effect of fuel properties on stability and two different nozzle sizes used. The addition of co-flow allows for multiple cases where fuel velocity is constant that results in different flame lift-off heights or behavior.

Although Scholefield and Garside [1] were the first to document the existence of the hysteresis regime, very few researchers have explored turbulent jet flames in the hysteresis regime – particularly with co-flow. Notably, Gollahalli [15] worked several fuels with several nozzle sizes using dilution to determine some basic trends. However, the experiments did not utilize co-flow and only lift-off and reattachment fuel velocities were presented. Some of the major contributions of this study are summarized below:

This study is the first to generate a dataset of flame lift-off heights as a function of fuel velocity for methane, ethylene, and propane fuels in the hysteresis regime using two different sized nozzles. The results show that flame lift-off height around the lift-off velocity is linear – as predicted by Khalghatgi [4]. As the fuel velocity is reduced to the reattachment velocity, the lift-off heights become highly non-linear with respect to the fuel velocity. At some co-flows, **the lift-off heights can actually increase as the fuel velocity is decreased**. The maximum lift-off height occurs just prior to reattachment and may be in

excess of four or five inches. **The lifting of the flame as fuel velocity is decreased is a phenomenon that has not been observed and documented by any previous researchers.**

Co-flow can also be seen as having a significant effect on flame behavior. For flames in co-flow, the flame lift-off heights are generally higher. The lift-off and reattachment fuel velocities are less than for flames in no co-flow. Even a seemingly insignificant co-flow of 0.05 m/s has a recognizable effect on flame behavior. Flames in co-flow may also exhibit the aforementioned lifting of the flame as the fuel velocity is reduced.

The lift-off velocities were plotted against co-flow and the results show a general linear trend, but that individual points varied significantly from the predicted line. **Reattachment velocities show a linear trend with respect to co-flow for all three fuels and both nozzle sizes.** Data for methane and ethylene can be reduced to a single line, by non-dimensionalizing by the laminar burning velocity.

Data on lift-off heights, fuel velocities, and co-flows can be analyzed using jet relations derived by Tieszen [5]. These relations allow for the determination of the stoichiometric radius and the local excess jet velocity at the flame base using the data collected in experiments. **The results show that local excess jet velocity varies linearly for stable flames well into the hysteresis regime. For flames in high co-flow, the linearity is for the entire range of stable lifted fuel velocities.** This is similar to Khalghatgi's relation [4] that flame lift-off height is linearly related to fuel nozzle velocity. Here, the linearity of the local excess jet velocity is in spite of the non-linear lift-off heights seen in the data.

Montgomery et al. [8] proposed the use of an effective fuel velocity, which is a function of the co-flow velocity, the ratio of densities of the fuel and air, and some predetermined constant, to explain the behavior of flames in co-flow. Extending their results to local excess jet velocity, our results confirm that this approach has merit. For the three different cases in which the Tieszen relations can be reasonably applied **the data can be collapsed to a single line describing the local excess jet velocity as a function of an effective jet velocity**. However, the value of the constant changes not only with fuel, but with nozzle size.

A similar method was used on the laminar flames studied by Chung, Lee, and co-workers. Their analysis shows that the effect of co-flow is to reduce the tribrachial flame speed by the value of the co-flow. Since the tribrachial flame speed is much lower than the nozzle speed, about twice the laminar burning velocity for laminar flames, the effect of a small co-flow can be seen.

The relations from Tieszen can also be used at the reattachment point. Local excess jet velocities were computed and plotted as a function of co-flow. **The results show that there appears to be a threshold value for the local excess jet velocities.** Flames with lower values can exist, albeit in a region close to the burner where diffusion effects are likely to dominate, rather than the partially premixed combustion typical of useful lifted flames. For methane this threshold value is about 0.40 m/s, the laminar burning velocity of methane. This threshold velocity may also be related to the transition of the jet from turbulent to laminar flow.

The value for ethylene is much lower, around 0.13 m/s, which is well below its laminar burning velocity. This result leads to **a relation for threshold local excess jet velocity, which just includes the inverse of the laminar burning velocity squared multiplied by a constant**. The laminar burning velocity squared is related to heat release, which is anticipated to have a major effect on flame stability, particularly in the low fuel velocity region.

Using Tieszen's jet relations and the proposed relation for threshold local excess jet velocity, t**he lift-off height at reattachment and the velocity at reattachment can be predicted**. The results are good and both co-flow and fuel properties are well accounted for.

While these experiments do not completely explain flame stability, even in the hysteresis regime, they do shed light on some previously unobserved aspects of what a comprehensive theory might contain. The local excess jet velocity, modified by co-flow, is certainly a parameter to be included. **These results support the turbulent burning velocity model** more than the model of flame stability that just incorporates large-scale structures.

Additional work is warranted to further confirm our results for additional cases. These cases should include a variety of additional fuels, such as ethane and hydrogen. In addition, dilution using nitrogen and carbon dioxide will allow additional laminar burning velocity cases to be studied. More nozzle sizes should be incorporated to determine the effect of nozzle size and to determine a lower bound of Reynolds number to which these theories apply. The area of transition flows, where the flow changes from laminar to turbulent is also worthy of investigation.

Since many of the flames exist in a region relatively close to the burner, additional jet models that accurately can predict jet velocity and concentrations in the developing region should be employed to analyze these flames. Studying flames in the hysteresis regime has the potential to help designers build burners with lower turndown ratios, allowing operation at lower loads. This has significant implications for boiler, oven, and gas turbine designs as energy becomes more expensive and the demands of flexible operating loads becomes more important as a design parameter. Only by understanding the cases of low fuel velocity and relatively "simple" co-flow can more complex burner analysis be performed. Any comprehensive theory on flame stability will have to include the sometimes unexpected behaviors that can occur in hysteresis flames in co-flow.

6. Bibliography

[1] Scholefield, D.A. and Garside, J.E., 1949, Third Symposium on Combustion, Flame, and Explosion Phenomenon, pp.102-110.

[2] Vanquickenborne, L. and van Tieggelen , A., Combustion and Flame, 10, p. 59, 1966

[3] Eickhof, H., Lenze, B., and Leuckel, W., "Experimental Investigation of the Stabilization Mechanism of Jet Diffusion Flames", Twentieth Symposium (International) on Combustion / The Combustion Institute, 1984, pp. 311-318

[4] Kalghatgi, G., "Lift-off Heights and Visible Lengths of Vertical Turbulent Jet Diffusion Flames in Still Air", Combustion Science & Technology, 1984, Vol. 41, pp. 17-29.

[5] Tieszen, S.R., Stamps, D.W., and O'Hern, T.J., 1996, "A Heuristic Model of Turbulent Mixing Applied to Blowout of Turbulent Jet Diffusion Flames," Combustion and Flame, 106, pp. 442-466.

[6] Brown, C.D., Watson, K.A., and Lyons, K.M., 1999, "Studies on Lifted Jet Flames in Coflow: The Stabilization Mechanism in the Near- and Far-Fields", Flow Turbulence and Combustion, 62, pp .249-273.

[7] Watson, K.A., Lyons, K.M., Donbar, J.M., and Carter, C.D., "Scalar and velocity field measurements in a lifted methane-air diffusion flame", Combustion and Flame, 117:257-271, 1999.

[8] Montgomery, C.J., Kaplan, C.R., and Oran, E.S., "The effect of co-flow velocity on a lifted methane-air jet diffusion flame", Twenty-Seventh Symposium (International) on Combustion / The Combustion Institute, 1998, pp.1175-1182.

[9] Peters, N. and Williams, F.A., AIAA Journal, 21 (3), 423, 1983

[10] Broadwell, J.E., Dahm, W.J.A, and Mungal, M.G., Twentieth Symposium (International) on Combustion / The Combustion Institute, 1984, pp. 303-310

[11] Miake-Lye, R.C. and Hammer, J.A., Twenty-Second Symposium (International) on Combustion / The Combustion Institute, 1988, pp. 817-824.

[12] Dahm, W.J.A. and Dibble, R.W., 1988, Twenty-Second Symposium (International) on Combustion / The Combustion Institute, pp. 801-808.

[13] Pitts, W.M., "Large scale turbulent structures and the stabilization of lifted turbulent jet diffusion flames", Twenty-Third Symposium (International) on Combustion, The Combustion Institute, 1990, pp. 661-668.

[14] Savas, O. and Gollahalli, S.R., "Flow structure in near-nozzle region of gas jet flames", AIAA Journal, Vol 24, No. 7, July 1986.

[15] Gollahalli, S.R., Savas, O., Huang, R.F., and Rodriguez Azara, J.L., 1986, Twenty-first Symposium (International) on Combustion, The Combustion Institute pp. 1463-1471

[16] Lin, C.K., Jeng, M.S, and Chao, Y.C., 1993, "The Stabilization Mechanism of the Lifted Jet Diffusion Flame in the Hysteresis Region," Exp. Fluids 14, pp. 353 – 365.

[17] Demare, D. and Baillot, F., 2001, "The Role of Secondary Instabilities in the Stabilization of a Non-premixed Lifted Jet Flame", Phys. Fluids, 13, 9, pp. 2662 – 2670.

[18] Muniz, L. and Mungal, M.G., 1997, "Instantaneous Flame-Stabilization Velocities in Lifted-Jet Diffusion Flames," Combustion and Flame 111, pp.16-31.

[19] Su, L.K., Han, D., and Mungal, M.G., "Experimental Results on the Stabilization of Lifted Jet Diffusion Flames", Center for Turbulence Research, Annual Research Briefs 2000, pp. 79-89.

[20] Han, D. and Mungal, M.G., "Direct Measurement of Entrainment in Reacting/Non-Reacting Turbulent Jets", Combustion and Flame 124:370-386, 2001

[21] Watson, K.A., Lyons, K.M., Donbar, J.M., and Carter, C.D., "On scalar dissipation and partially premixed flame propagation", Combustion Science & Technology, 175: 649-664, 2003.

[22] Upatnieks, A., Driscoll, J.F., Rasmussen, C. C. and Ceccio, S.L., 2004, "Liftoff on Turbulent Jet Flames-Assessment of Edge Flame and Other Concepts Using Cinema-PIV", Combustion and Flame, 138, pp.259-272.

[23] Lyons, K.M. and Watson, K.A., 2001, "Visualizing Diffusion Flame Formation in the Wake of Partially Premixed Combustion", ASME Journal of Energy Resources Technology, 123 (3): 221-227.

[24] Savas, O. and Gollahalli, S.R., "Stability of lifted laminar round gas-jet flames", Journal of Fluid Mechanics, vol. 165, pp.297-318, 1986.

[25] Chung, S.H. and Lee, B.J., 1991, "On the Characteristics of Laminar Lifted Flames in a Nonpremixed Jet," Combustion and Flame, 86, pp. 62-72.

[26] Lee, B.J., Kim, J.S., and Chung, S.H., 1994, Twenty-Fifth Symposium (International) on Combustion / The Combustion Institute, pp. 1175-1181.

[27] Lee, B.J., Cha, M.S., and Chung, S.H., 1997, "Characteristics of Laminar Lifted Flames in a Partially Premixed Jet," Combustion Science and Technology, 127, pp. 55- 70.

[28] Lee, B.J. and Chung, S.H., 1997, "Stabilization of Lifted Tribrachial Flames in a Laminar Nonpremixed Jet," Combustion and Flame, 109, pp. 163-183.

[29] Ko, Y.S. and Chung, S.H., 1999, "Propagation of Unsteady Tribrachial Flames in Laminar Non-premixed Jets," Combustion and Flame, 118, pp. 151-163.

[30] Lee, B.J. and Chung, S.H., 2001, "Characteristics of Reattachment and Blowout of Laminar Lifted Flames in Partially Premixed Propane", Combustion and Flame, 127, pp. 2194-2204.

[31] Clark, M., Transport Modeling for Environmental Engineers and Scientists, 1996

[32] Yimer, I., Campbell, I., Jiang, L-Y., "Estimation of the Turbulent Schmidt Number from Experimental Profiles of Axial Velocity and Concentration for High Reynolds-Number Jet Flows", Canadian Aeronautics and Space Journal, Vol 48, No. 3, 2002

[33] Ghosal, S. and Vervisch, L., 2001, "Stability Diagram for Lift-Off and Blowout of a Round Jet Laminar Diffusion Flame," Combustion and Flame, 123 , pp. 646-655.

[34] Boulanger, J., Vervisch, L., Reveillon, J., and Ghosal, S., "Effects of heat release in laminar diffusion flames lifted on rould jets", Combustion and Flame, 134 (355-368), 2003

[35] Lee, J., Won, S.H., Jin, S.H., and Chung, S.H., 2003, "Lifted Flames in Laminar Jets of Propane in Co-flow Air", Combustion and Flame, 135: 449-462**.**

[36] Kuo, Principles of Combustion, 1st edition

[37] D.B. Spalding, Combustion and Mass Transfer, 1st edition, 1979

[38] H. Schlichting, Boundary Layer Theory, 6th edition, 1968

[39] Bird, R.B, Stewart, W.E, and Lightfoot, E.N., Transport Phenomena, 2nd edition, 2002

[40] NIST Standard Reference Database 69 - March 2003 Release: *NIST Chemistry WebBook,* http://webbook.nist.gov/chemistry/name-ser.html, U.S. Department of Commerce

[41] Chen, R-H., Kothawala, A., Chaos, M. and Chew, L.P., "Schmidt, Number Effects on Laminar Jet Diffusion Flame Lift-off", Combustion and Flame to be published 2005.